



HAL
open science

Method for integration of lattice structures in design for additive manufacturing

Abdul Hadi Azman

► **To cite this version:**

Abdul Hadi Azman. Method for integration of lattice structures in design for additive manufacturing. Materials. Université Grenoble Alpes, 2017. English. NNT : 2017GREAI004 . tel-01688758

HAL Id: tel-01688758

<https://theses.hal.science/tel-01688758>

Submitted on 19 Jan 2018

HAL is a multi-disciplinary open access archive for the deposit and dissemination of scientific research documents, whether they are published or not. The documents may come from teaching and research institutions in France or abroad, or from public or private research centers.

L'archive ouverte pluridisciplinaire **HAL**, est destinée au dépôt et à la diffusion de documents scientifiques de niveau recherche, publiés ou non, émanant des établissements d'enseignement et de recherche français ou étrangers, des laboratoires publics ou privés.

THÈSE

Pour obtenir le grade de

DOCTEUR DE LA COMMUNAUTÉ UNIVERSITÉ GRENOBLE ALPES

Spécialité : **GI : Génie Industriel : conception et production**

Arrêté ministériel : 25 Mai 2016

Présentée par

Abdul Hadi AZMAN

Thèse dirigée par **François VILLENEUVE**
et codirigée par **Frédéric VIGNAT**

préparée au sein du **Laboratoire G-SCOP**
et de l'**École Doctorale I-MEP2**

Method for integration of lattice structures in design for additive manufacturing

Méthode pour l'intégration des structures treillis dans la conception pour la fabrication additive

Thèse soutenue publiquement le **24 Février 2017**,
devant le jury composé de :

Daniel COUTELLIER

Professeur des universités, Université de Valenciennes et du Hainaut Cambrésis,
Président

Jérôme PAILHES

Maître de Conférences HDR, ENSAM, Campus de Bordeaux-Talence,
Rapporteur

Lionel ROUCOULES

Professeur des universités, ENSAM, Campus d'Aix en Provence, Rapporteur

Eric MAIRE

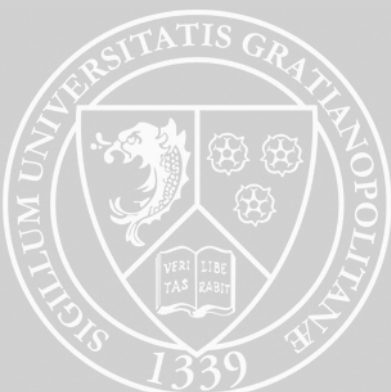
Directeur de Recherche CNRS HDR, rattaché à l'INSA de Lyon, Examineur

Frédéric VIGNAT

Maître de Conférences HDR, Grenoble-INP, Co-Directeur de thèse

François VILLENEUVE

Professeur, Université Grenoble Alpes, Directeur de thèse



None of us got to where we are
alone.

Harvey Mackay

Acknowledgement

This dissertation is the result of the work that has been conducted during years of research with the G-SCOP laboratory, and under the Univ. Grenoble Alpes, France. In various ways, it has involved several persons and organisations that I am most eager to acknowledge.

First and foremost, I would like to thank my supervisors. To François Villeneuve for his trust and confidence in me which goes a long way to my master degree year, for his constructive comments, directions, and the continuous moral support. To Frédéric Vignat for his availabilities, helpful and relevant comments, as well as fruitful discussion and corrections.

Secondly, I would like to express the gratitude to the National University of Malaysia (UKM) and the Ministry of Higher Education Malaysia (MOHE) for the funding of the research. I would also like to thank the Product-Process Design (CPP) and Additive Manufacturing team for their direct and indirect participation and investment in this work, for their kindness and valuable guidelines.

My sincere thanks also go to the jury members who have agreed to evaluate this dissertation. I am honoured and thankful to Jérôme Pailhes and Lionel Roucoules for their interest in this work and by agreeing to be the reporters. I also thank Daniel Coutellier and Eric Maire for their acceptance to be my viva examiner.

I express my appreciation to the staffs, my colleagues and friends at the G-SCOP Laboratory who participated and contributed in one way or another. In particular, to Marie-Joséphé, Fadila, Souad, Myriam, Kevin, Jean-Yves, Sébastien, Christelle, Hoang, Jing Tao, Rachad, and Olga. Thank you for your support, for the various exchanges, convivialities and your help during these years.

Finally, I would like to convey my heartfelt appreciation to my families. To my mother Zainoha Zakaria and my father, Azman Hassan for their prayers, encouragement and blessing. From 1993 to 1997, it was my parents who both completed at the same time their PhDs at the University of Loughborough, UK, now exactly twenty years on, 2013-2017, me and my wife repeat the same accomplishment by both doing our PhDs at the same time in Grenoble. They have been an inspiration to me in completing my PhD. I would like thank my

mother-in-law Aishah for her support and wisdom, and to my grandparents for the wait. But most importantly, to my wife, Asma' and our sons, Talhah and Suhayb, not only for their patience and endless support, but also for their love and their sharing of every moment along this memorable journey. To my brothers, sisters, friends and their families whom I can't possibly mention all their names, thank you very much. It has been a long and challenging journey, but with many memorable memories.

Now this is not the end. It is not even the beginning of the end. But it is, perhaps, the end of the beginning.

Winston Churchill

*Abdul Hadi Azman
Grenoble, February 2017*

Contents

List of Figures	v
List of Tables	vii
Definition of used terms	viii
Acronyms	x
General introduction	1
1 Literature review	7
1.1 Importance of lattice structures	8
1.1.1 Industrial requirements in the twenty-first century . . .	8
1.1.2 The need for lattice structures	8
1.2 Introduction on lattice structures	9
1.3 Manufacturing lattice structures	12
1.3.1 Manufacturing stochastic and prismatic structures . . .	12
1.3.2 Conventional lattice structure manufacturing methods	13
1.3.3 Metallic Additive Manufacturing	14
1.3.4 Conclusion	18
1.4 Lattice structure properties	19
1.4.1 Mechanical properties	21
1.4.2 Conclusion	25
1.5 Lattice structure design methods	25
1.5.1 Design for additive manufacturing	25
1.5.2 Design for additive manufacturing methodology propo- sitions	26
1.5.3 Conclusion	29
1.6 CAD file formats for additive manufacturing	29
1.6.1 CAD tools to create lattice structures	29
1.6.2 Analysis of current CAD file formats	30
1.6.3 Conclusion	34
1.7 Literature review conclusion	35
2 CAD tools in additive manufacturing	37
2.1 Evaluating current CAD tools performances in the context of design for additive manufacturing	38
2.1.1 Human Machine Interface	40
2.1.2 CAD software utility	42
2.1.3 CAD file format	44
2.1.4 RAM usage	46

2.1.5	Conclusion	48
2.2	Evaluating current CAE tools performances in the context of design for additive manufacturing	48
2.2.1	FEA computation file size	49
2.2.2	FEA time duration	50
2.2.3	Conclusion	51
2.3	Conclusion	52
3	Lattice structure design strategy	53
3.1	Definitions of used terms	55
3.2	Proposed lattice structure design method	56
3.2.1	Concept to link lattice structure, solid material and equivalent material	56
3.2.2	Step-by-step of the proposed method	61
3.2.3	Application example of the proposed lattice structure design method	62
3.3	A methodology for the creation of equivalent lattice structure materials	69
3.3.1	FEA simulation and variables	69
3.3.2	Simulation execution	74
3.3.3	Stress concentration	75
3.3.4	Results	77
3.3.5	Analysis	83
3.4	Results verification	87
3.4.1	Comparison with results from other articles	87
3.4.2	Comparison with case study results	90
3.4.3	Conclusion	98
3.5	Summary	99
4	Definition and creation of the skeleton model of the lattice structures	101
4.1	Lattice structure configurations	103
4.1.1	Pattern	104
4.1.2	Relative density	104
4.1.3	Progressivity	106
4.1.4	Conformality	106
4.1.5	Design space	108
4.1.6	Joint shape	109
4.2	Creation of skeleton model	109
4.2.1	Skeleton model concept	109
4.2.2	Skeleton model algorithm	111

Contents

4.3	Visualisation	119
4.4	Manufacturing	121
4.5	Summary	123
	General conclusion	124
	Bibliography	127
A	Detailed FEA simulation results for the lattice structures	133
B	Skeleton model points, lines, sections and joints lists	136

List of Figures

1	Example of an octet-truss lattice structure manufactured with additive manufacturing	1
2	An overview of the motivations, problematic, research questions and contributions of the PhD	6
1.1	Architected materials according to (Ashby, 2013)	9
1.2	Stochastic, periodic, prismatic, and lattice structures	11
1.3	An octet-truss lattice structure 3D model in CAD	16
1.4	Inside an EBM machine (Lu et al., 2009)	16
1.5	Difference between a designed lattice structure strut in CAD, its numerical equivalent cylinder, geometrical equivalent cylinder and the manufactured strut with additive manufacturing (Suard, 2015)	18
1.6	Young’s Modulus-density space materials diagram (Ashby, 2013)	20
1.7	Three main lattice structure design variable influence according to (Ashby, 2006)	21
1.8	Stiffness experiment of octet-truss (stretching-dominated) and kelvin foam (bending-dominated). The octet-truss lattice structure demonstrates markedly superior specific stiffness compared with the open-cell foam (Kelvin foam) (Zheng et al., 2014)	24
1.9	Design strategy categories for additive manufacturing according to (Tang et al., 2014)	26
1.10	Square bracket design proposed using a new design method for additive manufacturing (Vayre et al., 2012a)	27
1.11	Steps for design-optimization of a lattice structure (Zhang et al., 2015)	28
1.12	Integrated multi-level and multi-discipline design process (Tang et al., 2014)	28
2.1	The roles of each criterion in evaluating CAD tools for additive manufacturing	38
2.2	Circular lattice structure bars	39
2.3	Different lattice structure dimensions	40
2.4	Creating a basic 1 cm \times 1 cm \times 1 cm octet truss lattice structure with circular section bars	41
2.5	First and second repetition from elementary structure to obtain a 5 cm \times 5 cm \times 5 cm size octet truss lattice structure	42

List of Figures

2.6	Cubic lattice structure repetition duration	43
2.7	Octet-truss lattice structure repetition duration	44
2.8	Cubic lattice structure file size	45
2.9	Octet-truss lattice structure file size	46
2.10	Cubic lattice structure RAM consumption	47
2.11	Octet-truss RAM consumption	47
2.12	FEA simulation on an octet-truss lattice structure	49
2.13	Octet-truss lattice structure FEA computations file size	50
2.14	Octet-truss lattice structure FEA time duration	51
2.15	Summary of evaluation, problems, conclusions and solutions of chapter two	52
3.1	Which type of lattice structure to choose? Cubic or hexa-truss lattice structure? Which densities are needed?	54
3.2	Bounding box(blue) and lattice structure (yellow)	55
3.3	Lattice structure design method based on the use of equivalent material	56
3.4	The relation between lattice structure, solid material and equiv- alent material	57
3.5	Step-by-step of the new design method to design lattice struc- tures	60
3.6	Design space	63
3.7	Solid material and boundary conditions	64
3.8	Displacements and Von Mises stress results of the FEA	64
3.9	Relative Young's modulus in function of relative density	65
3.10	Relative Young's modulus in function of relative density for octet-truss lattice structure at 0° angle position	66
3.11	Relative strength in function of relative density for octet-truss lattice structure at 0° angle position	67
3.12	FEA on equivalent material with relative density at 13%	67
3.13	Lattice structure CAD model	68
3.14	Compression and shear test on a hexa-truss lattice structure	70
3.15	Isometric view of 5 × 5 × 5 elementary units. From left to right : octet-truss, cubic, hexa-truss and open-cell lattice structure	70
3.16	Side view of each elementary unit. From left to right : octet- truss, cubic, hexa-truss and open-cell elementary unit	71
3.17	Cubic lattice structure at 0° and 45° angle	71
3.18	Side view of open-cell foam lattice structures with 11.9%, 25.3% and 36.9% relative densities	72

List of Figures

3.19	5 × 5 × 5 unit octet-truss lattice structures with different length and sections of struts but same densities	72
3.20	High density hexa-truss lattice structure	73
3.21	Stress concentration in sharp edges of an octet-truss lattice structure	76
3.22	Stress concentration in sharp edges of an cubic lattice structure	76
3.23	Stress concentration in sharp edges of an hexa-truss lattice structure	77
3.24	Stress concentration in sharp edges of an open-cell foam lattice structure	77
3.25	Octet-truss lattice structure compression test at 0° and 45° angle	78
3.26	Octet-truss lattice structure shear test at 0° and 45° angle . . .	78
3.27	Relative strength in function of relative density for octet-truss lattice structure at 0° and 45° angle	79
3.28	Cubic lattice structure compression at 0° and 45° angle	79
3.29	Cubic lattice structure shear test at 0° and 45° angle	80
3.30	Relative strength in function of relative density for cubic lattice structure at 0° and 45° angle	80
3.31	Hexa-truss lattice structure compression test at 0° and 45° angle	81
3.32	Hexa-truss lattice structure shear test at 0° and 45° angle . . .	81
3.33	Relative strength in function of relative density for hexa-truss lattice structure at 0° and 45° angle	82
3.34	Open-cell foam lattice structure compression test at 0° and 45° angle	82
3.35	Open-cell foam lattice structure shear test at 0° and 45° angle	83
3.36	Relative strength in function of relative density for open-cell foam lattice structure at 0° and 45° angle	83
3.37	Comparison of relative Young's modulus in function of relative density at 0° angle	84
3.38	Comparison of relative Young's modulus in function of relative density at 45° angle	85
3.39	Comparison of relative shear modulus in function of relative density at 0° angle	85
3.40	Comparison of relative shear modulus in function of relative density at 45° angle	86
3.41	Relative Young's modulus in function of relative density for octet-truss lattice structure, in comparison with Suard's results	87
3.42	Experimental compression test of octet-truss lattice structure conducted by (Suard, 2015)	88
3.43	FEA on diamond lattice structure by (Neff, 2015)	88

List of Figures

3.44	Relative Young's modulus in function of relative density for diamond lattice structure, in comparison with Neff's results . . .	89
3.45	Relative strength in function of relative density for bending and stretching-dominated lattice structures, in comparison with Ashby's results	89
3.46	FEA on the L shaped lattice structure (left) and equivalent material (right)	91
3.47	FEA on the C shaped lattice structure (left) and equivalent material (right)	91
3.48	Displacements of the L shape part: Lattice structure (left) and equivalent material (right)	92
3.49	Von Mises stress of the L shape part: Lattice structure (left) and equivalent material (right)	93
3.50	Displacements of the C shape part: Lattice structure (left) and equivalent material (right)	95
3.51	Von Mises stress of the C shape part: Lattice structure (left) and equivalent material (right)	97
3.52	General view of the proposed lattice structures design method	99
4.1	Chapter 4	102
4.2	Lattice structure configurations	103
4.3	First order relative density as a function of the true relative density for the cubic lattice structure. The red line represents the isovalue	105
4.4	First order relative density as a function of the true relative density for the octet-truss lattice structure.	105
4.5	Different types of conformal lattice structures	107
4.6	Example of a cubic lattice structure with an upper planar and curved surface of the design space	108
4.7	Connection between extremity struts and design space	109
4.8	Cubic lattice structure with rounded joint edges	109
4.9	Skeleton model: Lattice structure defined by points, lines and sections	111
4.10	Class, functions, input and output information of the algorithm	111
4.11	Elementary structure repetition to obtain 3 x 3 x 3 unit lattice structure	113
4.12	Overlapping points and lines after elementary structure repetition	113
4.13	Step one case one and two	114
4.14	Step two	115
4.15	Step three case one and two	115

List of Figures

4.16	Constant scaled 3 x 3 x 3 unit cubit lattice structure with a pitch dimension of 2	116
4.17	Progressive scaled 3 x 3 x 3 unit cubit lattice structure	117
4.18	Method one	117
4.19	Method two	118
4.20	Method to obtain non-conformal extremity struts	119
4.21	Example of a cubic, octet-truss and hexa-truss lattice structure created with points and lines visualised in a viewer (Paraview)	120
4.22	Visualisation of lattice structure built by geometric primitive lines and cylinders	121
4.23	Slicing lattice structure lines into layers and adding section to sliced lines	122
4.24	Adding section to sliced lines	123
4.25	Proposal of a new CAD file format for additive manufacturing taking into aspect CAD, CAE and CAM requirements	126
B.1	Lattice structure generator user interface created to create lattice structures	146
B.2	Proposal of lattice structure generator user interface to create lattice structures	146

List of Tables

1.1	Definition of elementary and lattice structure used in this PhD	11
1.2	Octet-truss (Ashby, 2006), tetrakaidecahedron (Zhu et al., 1997) and open-cell foam elementary structures	12
1.3	Investment casting (Mun et al., 2015)Expanded metal sheet (Kooistra and Wadley, 2007), metallic wire assembly (Queheillalt and Wadley, 2005) and snap fit (Dong et al., 2015) method process to manufacture lattice structures.	13
1.4	Synthesis: Advantages and disadvantages of additive manufacturing and conventional lattice structure manufacturing techniques	19
1.5	Types of deformation for lattice structures according to (Suard, 2015)	22
1.6	Influence of stretching and bending-dominated structures on mechanical properties according to (Ashby, 2006)	23
1.7	Obj file format key information	33
1.8	Synthesis : CAD File Formats Comparison	35
2.1	Average time to generate 1st and 2nd repetition	43
2.2	Lattice structure CAD file sizes	45
2.3	RAM consumption	46
2.4	Octet-truss lattice structure FEA computations file size	50
2.5	Octet-truss lattice structure FEA time duration	51
3.1	Material properties of the octet-truss lattice structure equivalent material	90
3.2	Percentage difference between the displacement of the lattice structure and the equivalent material (L shape part)	92
3.3	Percentage difference between the Von Mises stress of the lattice structure and the equivalent material (L shape part)	94
3.4	Percentage difference between the displacement of the lattice structure and the equivalent material (C shape part)	96
3.5	Percentage difference between the Von Mises stress of the lattice structure and the equivalent material C shape part)	97
4.1	Number of points and lines for cubic, octet-truss, hexa-truss and open-cell foam elementary structure	104
4.2	Constant and gradient lattice structures	107

List of Tables

4.3	Elementary octet-truss structure: Point, line, section and connection list	110
4.4	Elementary cubic structure: Point and line list	112
A.1	Relative Young's modulus and relative strength for cubic lattice structure compression and shear test at 0° and 45° angle .	133
A.2	Relative Young's modulus and relative strength for octet-truss lattice structure compression and shear test at 0° and 45° angle	134
A.3	Relative Young's modulus and relative strength for hexa-truss lattice structure compression and shear test at 0° and 45° angle	134
A.4	Relative Young's modulus and relative strength for open-cell lattice structure compression and shear test at 0° and 45° angle	135
B.1	Elementary octet-truss structure: Point and line list	136
B.2	Elementary hexa-truss structure: Point and line list	137
B.3	Elementary open-cell foam structure: Point and line list	138
B.4	3 x 3 x 3 unit cubic lattice structure with with a pitch size of one	139
B.5	Scaled 3 x 3 x 3 unit cubic lattice structure with a pitch size of 2	140
B.6	Scaled 3 x 3 x 3 unit cubic lattice structure with gradient elementary structures	141
B.7	Conformal cubic lattice structure with non-parallel upper and lower boundaries	142
B.8	Conformal cubic lattice structure with parallel upper and lower boundaries	143
B.9	Output point and line list	144
B.10	Output section and join shape list	145

Definition of used terms

Definitions adopted by researchers are often not uniform, so some key terms are explained to establish positions taken in the PhD research.

Architected material

Architected material is a combination of a monolithic material with space to generate a new structure which has the equivalent of a new monolithic material.

Cellular structure

Cellular material is another name for architected materials. Cellular structures can be categorized into two types: stochastic (foams) and periodic structures.

Stochastic foams

Cellular materials which cannot be characterized by a single unit cell area are referred to as stochastic foams.

Periodic structure

Cellular materials characterized by a unit cell that can be translated through the structure are referred to as periodic materials

Prismatic structure

Periodic materials which the unit cells are translated in two dimensions. These are known as prismatic cellular materials

Lattice structure

Periodic materials which have three-dimensional periodicity, which means that its unit cells are translated in three axis. These structures are frequently referred to as lattice or micro-truss materials

Curling

Curling is the effect of high distortion on the extremities of the planes in parts manufactured by additive manufacturing.

Acronyms

Acronyms

AM	Additive manufacturing
AMF	Additive Manufacturing File
ALM	Additive Layer Manufacturing
B-Rep	Boundary representation
CAD	Computer-aided-design
CAM	Computer-aided-manufacturing
CAE	Computer-aided engineering
EBM	Electron beam melting
FEM	Finite element method
FF	Freeform fabrication
IGES	Initial Graphics Exchange Specification
PRS	Powder Recovery System
RAM	Random-access memory
RM	Rapid Manufacturing
RP	Rapid Prototyping
SLS	Selective Laser Sintering
STL	STereoLithography
STEP	Standard for the Exchange of Product model data
VRML	Virtual Reality Modelling Language
3D	Three-dimensional

General introduction

Introduction

Additive manufacturing is a recent development in manufacturing. It is now possible to manufacture metallic lattice structures easily with additive manufacturing. Lattice structure is a type of architected material and can be defined as “*a combination of two or more materials, or of material and space, assembled in a way as to have the attributes not offered by any one material alone*”(Ashby, 2013). Lattice structures can be used to produce high strength low mass parts. It brings many advantages, for example produce lighter aeroplanes and consequently improve fuel savings. However, the breakthrough in lattice structure manufacturing capability is yet to be followed by a breakthrough in lattice structure design methods and CAD tools. Currently only traditional design methods are available for additive manufacturing design strategies, which do not consider the requirements of lattice structure applications. Thus, despite its advantages, lattice structures are still not widely used. This work focuses on lattice structure design methods and creation in CAD tools to facilitate wide use of lattice structures in products. Figure 1 is an example of an octet-truss lattice structure manufactured with the Electron Beam Melting (EBM) technology.

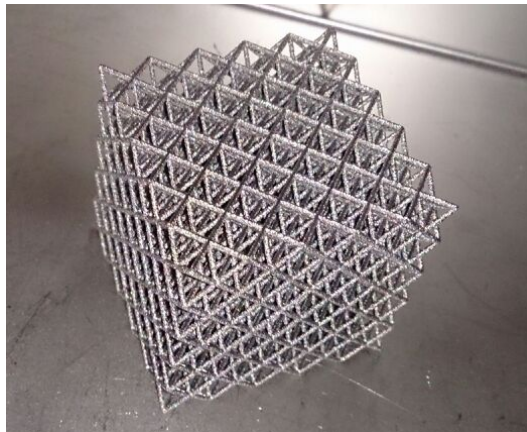


Figure 1: Example of an octet-truss lattice structure manufactured with additive manufacturing

Motivation

In a fast moving world, where technology improves and advances rapidly, nothing stays still. Today's industrial designers seek to optimize product designs to best meet the requirements of clients and markets. The bar has been set higher and higher to fulfil the ever demanding economical, environmental and society needs. Hence, the emphasize on research and development to improve performances and gains in every possible way has become essential. It has become important for engineers to design and manufacture high performance lightweight products. For example, lighter parts in the aerospace and automotive industries can contribute to huge amounts of savings in fuel consumption. This is a very important factor for companies in reducing costs. This PhD aims to help engineers to integrate lattice structures in part designs and produce lightweight products.

Problematic

It is now possible to manufacture high strength low mass parts using lattice structures manufactured with additive manufacturing. However, even though lattice structures can now be manufactured easily with additive manufacturing, they are currently not widely used in part designs. New capabilities in manufacturing technology creates new requirements for design strategies. This progress in manufacturing is yet to be followed by new innovations and improvements in lattice structure design methods and computer-aided-design (CAD) tools. Current design strategies and CAD tools are not tailored for additive manufacturing. Designers currently do not have the required information to correctly integrate lattice structures in part designs and also do not have the necessary tools for easy lattice structure creation and manipulation in CAD software. This constitutes a major stumbling block for the wide use of lattice structures in part designs. It is important to know the conditions and factors that influence lattice structure design decisions and its applications.

Research question

From this first observation regarding metallic additive manufacturing and current lattice structure design methods and CAD tools, the main questions that arise are :

- What are the advantages of integrating lattice structures in part designs?
- Why are lattice structures so little used in part designs?
- What are the informations necessary to help designers to design parts containing lattice structures?
- How can lattice structures be created quickly and easily in CAD?

These questions will be thoroughly answered in the literature review and the following chapters.

Objective

The principal aim of this PhD is to facilitate and improve the integration of lattice structures in additive manufacturing parts. This improvement will be in two areas, first in the design strategy of the lattice structures and secondly the creation, visualisation and slicing in CAD and CAM environment respectively.

Lattice structure design strategy For the design strategy, the goal is to help designers to have the necessary information to choose the correct lattice structure pattern and density based on the part's requirements. This will contribute towards better integration of lattice structures in additive manufacturing part designs and make it easier to conduct finite-element-analysis (FEA).

Create, visualise and slice lattice structure After choosing the configurations of the lattice structures, the next goal is to help designers to create the lattice structures easily and quickly in CAD software and also to make it easier to visualise and slice in CAD and CAM environment. Improvements in CAD tools to design lattice structures are needed and will greatly improve the additive manufacturing numerical chain.

Research strategy

To answer the research questions and achieve the desired objectives, the PhD strategy has been outlined as follows. The following explains the work done for each stage of the Phd strategy.

Chapter 1: Literature review The aim of this literature review is to study what had previously been published in this field of research. This chapter investigates the importance of lattice structures, lattice structure manufacturing techniques, lattice structure mechanical properties, lattice design methods and current CAD file formats for additive manufacturing.

Chapter 2: CAD tools in additive manufacturing In this second chapter, the aim is to evaluate the performances of current CAD and CAE tools to determine whether they are adequate enough for the needs of additive manufacturing. Experiments were conducted in CATIA V5, observations and analysis were made on the time taken to create lattice structure models, RAM consumption during the operations, time taken to execute finite-element-analysis and CAD and FEA computation file sizes.

Chapter 3: Lattice structure design strategy In this chapter, the aim is to propose a new lattice structure design method. This new design method will serve as a guideline for engineers to choose the correct lattice structure pattern and density. A methodology to define equivalent lattice structure materials is needed to eradicate the creation of lattice structure with surfaces and volumes.

Chapter 4: Definition and creation of the skeleton model of the lattice structure In this chapter, the goal is to visualise and slice lattice structures in CAD and CAM respectively. First, lattice structure configurations were determined. Next the aim is to study the informations needed to represent and create lattice structures in CAD. Finally, the visualisation and slicing of the lattice structures are explored.

Contribution

There are three main contributions in this PhD. A new lattice structure design strategy is presented. This serves as a guideline for designers to integrate lattice structures in additive manufactured parts. With this guideline, designers will have at their disposal a guideline to choose lattice structure patterns and densities. This will help the integration of lattice structures additive manufactured parts.

The second contribution is a methodology to create equivalent lattice structure materials. This solid material equivalence replaces the need to create lattice structures in CAD and finite-element-analysis, which are both

time consuming. This will save time in CAD 3D model creation and finite-element-analysis in CAE software.

The third contribution is the proposal to define lattice structures with points, lines, sections and joints instead of surfaces and volumes. The points, lines, sections and joints information are referred to as the skeleton model. Lattice structure geometrical configurations were determined and an algorithm for the creation of a skeleton model for these configurations were presented. A method is presented to visualise and slice lattice structures from the skeleton model. This proposal is a starting point for future works to create a new CAD file format, CAD and CAM tools suitable for lattice structures and additive manufacturing.

Overview

Figure 2 illustrates an overview of this PhD thesis. Starting with the motivation of the work, problematic, research questions and contributions of this research. Chapter two evaluates current CAD tools performances to design lattice structures. A new lattice structure design method is presented in chapter three and in chapter four we propose a new methodology for the creation and representation of 3D lattice structure models.

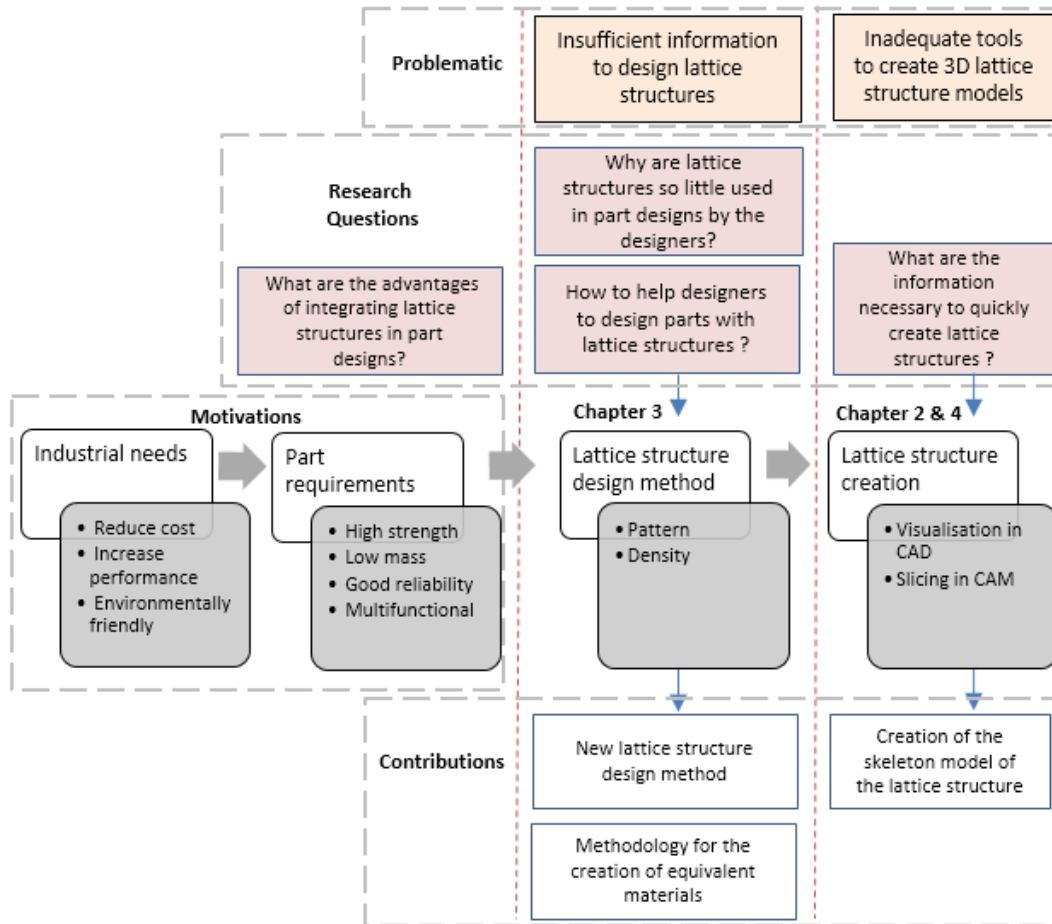


Figure 2: An overview of the motivations, problematic, research questions and contributions of the PhD

Literature review

Contents

1.1	Importance of lattice structures	8
1.1.1	Industrial requirements in the twenty-first century . .	8
1.1.2	The need for lattice structures	8
1.2	Introduction on lattice structures	9
1.3	Manufacturing lattice structures	12
1.3.1	Manufacturing stochastic and prismatic structures . .	12
1.3.2	Conventional lattice structure manufacturing methods	13
1.3.3	Metallic Additive Manufacturing	14
1.3.4	Conclusion	18
1.4	Lattice structure properties	19
1.4.1	Mechanical properties	21
1.4.2	Conclusion	25
1.5	Lattice structure design methods	25
1.5.1	Design for additive manufacturing	25
1.5.2	Design for additive manufacturing methodology propo- sitions	26
1.5.3	Conclusion	29
1.6	CAD file formats for additive manufacturing	29
1.6.1	CAD tools to create lattice structures	29
1.6.2	Analysis of current CAD file formats	30
1.6.3	Conclusion	34
1.7	Literature review conclusion	35

This literature review will be the basis and starting point for this research. This review was conducted by studying what had previously been published regarding lattice structures, specifically concerning the importance of lattice structures, lattice structure properties, lattice structure design methods, lattice structure applications in products, manufacturing of lattice structures and CAD file formats for additive manufacturing. The objective is to find the problems encountered by designers to integrate lattice structures in part designs and the benefits of lattice structure application.

1.1 Importance of lattice structures

1.1.1 Industrial requirements in the twenty-first century

As the world becomes more competitive, industries are looking at every viable prospect to stay relevant and be ahead of the competition. Economical and environmental needs are forcing companies to reduce cost, increase performance gains, and reduce wastes. New solutions have to be invented to gain every possible improvement. As the need for energy conservation increases, the need for lightweight parts increases too (Manfredi et al., 2014). The benefits of weight reduction are significant. In the aerospace industry, where the need to reduce weight is important, companies are trying to manufacture lighter aeroplanes. Reduction in the weight of an aeroplane can contribute to vast amount of savings in fuel expenses. In the automotive industry, reducing a cars weight contributes to fuel economy and lower CO₂ emissions (Beyer, 2014). Studies have shown that a 10% reduction in weight can save around 6-8% in fuel consumption.

1.1.2 The need for lattice structures

It is important to produce parts which are lightweight but have good mechanical properties. Lattice structure is a good solution to achieve this objective. High strength low mass property is a key advantage of lattice structure (Chu et al., 2008). Lattice structures can be used to achieve excellent performance and multi functionality while reducing weight. This concept of architected material comes from the desire to put material only where it is needed (Tang et al., 2014). The research field regarding lattice structures has received increased attention due to their advantages over stochastic structures in producing lightweight and high strength parts (Ashby et al., 2000).

The free-form capability of additive manufacturing enables engineers to manufacture lattice structures. This ability to manufacture lightweight structures entices engineers in the aerospace industry to use lattice structures manufactured with additive manufacturing (Wong and Hernandez, 2012). In the aerospace industry, lightweight parts are needed to improve their performances. Weight reduction is really important in the aviation industry, where a reduction of one kilogram in an aeroplane can help fuel savings of up to 3000 USD per year (Fall, 2013). Hence the importance of lattice structures in producing lightweight structures to reduce cost. The cost factor is important in the automotive industry, thus low-cost titanium powders are needed to expand its use in this domain (Froes and Dutta, 2014). Lattice structures are also important in biomedical engineering, where it is suitable for cell attachment and growth on implants (Darwish and Aslam, 2016; Ponder et al., 2008). The main players of additive manufacturing are from the aerospace and medical industries, while other industries such as automotive are beginning to exploit the use of titanium alloys.

1.2 Introduction on lattice structures

History and background Lattice structure is a type of architected material, which is a combination of a monolithic material and space to generate a new structure which has the equivalent mechanical properties of a new monolithic material (Ashby, 2013).

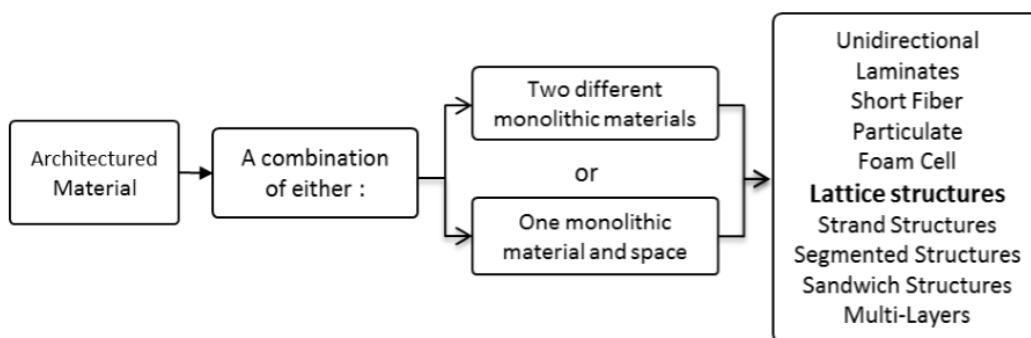


Figure 1.1: Architected materials according to (Ashby, 2013)

Figure 1.1 illustrates the two combinations and categories of architected material. Architected materials are also known as cellular structures. The word “cell” originates from a latin word called “cella”, which means a small compartement or an enclosed space (Gibson and Ashby, 1999). Clusters

of cells creates a cellular structure. Most common cellular structures in everyday life are wood, cork and sponges. These structures have existed for ages and human beings have benefited from their various uses. For example, cork has been used in wine bottles since the Roman age. Engineers are now capable of making cellular structures. Structures such as honey-comb like structures have emerged to create lightweight structures.

Lattice structures in nature There are also many materials in nature which contain lattice structure designs. These materials play a role in lightweight structures. Natural tubular structures often have honey-comb like or foam like core, which supports denser outer cylindrical shell and increases the resistance of the shell to local buckling failure (Gibson, 2005). These materials can be a reference for the configurations of lattice structures in creating lightweight high strength materials. For example, hexagonal lattice structures have some similarities with cellular structures of wood. The stiffness and strength of a species of wood depends on its density and the direction of the load applied on it. Its stiffness and strength is higher if the direction of the load applied is the same as the direction of the wood, compared to if it was applied across it. Another example is the structure of trabecular bone. The structure of the bone is adapted to the loads applied to it. It grows in response to the magnitude and direction of the load applied (Gibson, 2005).

Stochastic and periodic structures Architected materials can be divided into two categories, stochastic and periodic structures. Materials characterized by a unit cell that can be translated through the structure are referred to as periodic materials (Wadley, 2002). Whereas cellular materials which cannot be characterized by a single unit cell area are referred to as stochastic foams.

Prismatic and lattice structures It exists two types of periodic cellular structures. First, periodic materials where the unit cells are translated in two dimensions are known as prismatic cellular materials (Wadley, 2002). An example of a prismatic cellular material is the honeycomb structure, which has very good properties for a high stiffness and low mass structure (Rochus et al., 2007). The second type, are periodic materials which have three-dimensional periodicity. This means that its unit cells are translated along three axis. These structures are frequently referred to as lattice materials (Wadley, 2002). Therefore, a lattice structure is an example of a cellular structure.

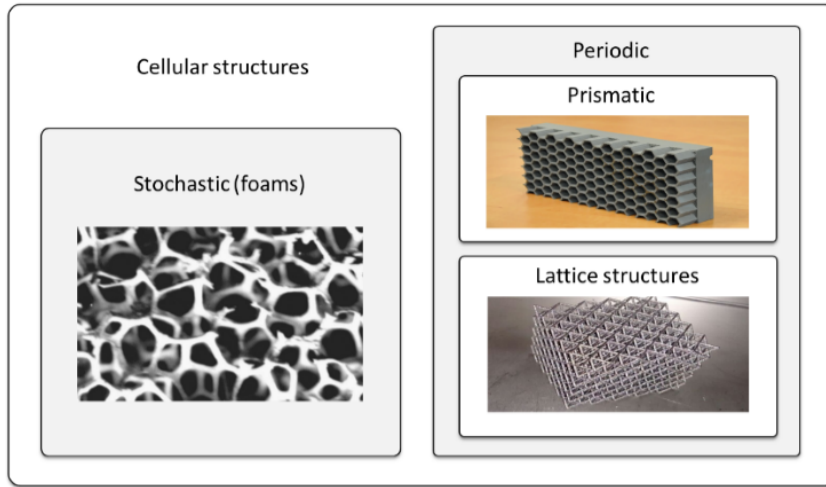


Figure 1.2: Stochastic, periodic, prismatic, and lattice structures

In this work, the terms described above are used to identify specific structures and avoid ambiguity. The Venn diagram in figure 1.2 shows the difference between stochastic, periodic, prismatic and lattice structures. In this work, we consider lattice structures as periodic cellular structures. Table 1.1 illustrates the definition of the terms used in this PhD for elementary and lattice structures.

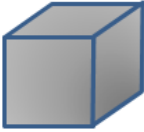
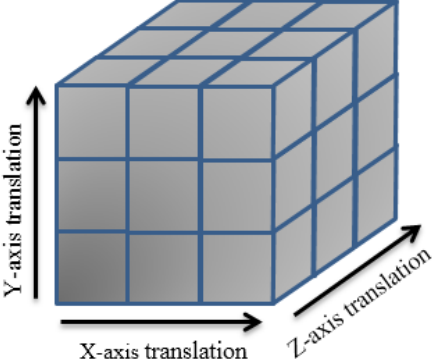
Elementary Structure	Lattice structure
	

Table 1.1: Definition of elementary and lattice structure used in this PhD

Lattice structure patterns There are many types of lattice structure patterns. A lattice structure pattern depends on the pattern of its elementary structure, as shown in table 1.1. Common lattice structure patterns are octet-truss, cubic, tetrakaidecahedron, and open-cell foam lattice structures. Table 1.2 illustrates an octet-truss elementary structure containing an octahedral core surrounded by tetrahedral units, tetrakaidecahedron structure and open-cell foam structure. Open-cell foam structures imitate stochastic structures by placing struts connected at the joints. These joints have low connectivity with other joints.

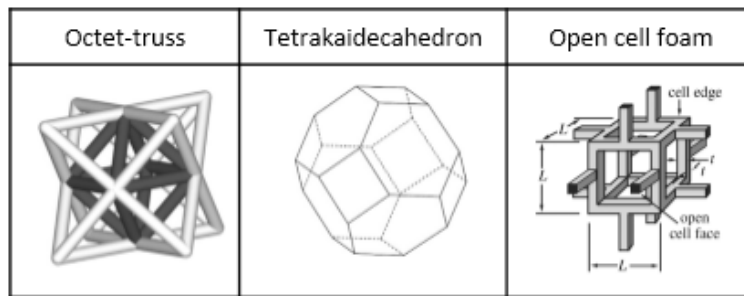


Table 1.2: Octet-truss (Ashby, 2006), tetrakaidecahedron (Zhu et al., 1997) and open-cell foam elementary structures

1.3 Manufacturing lattice structures

Cellular structures in nature have been used by humans since thousands of years. Now, new techniques have emerged to manufacture these structures. We examine the processes that can be used to manufacture cellular and lattice structures.

1.3.1 Manufacturing stochastic and prismatic structures

The first processes capable of manufacturing cellular structures were mainly for stochastic and prismatic structures. Manufacturing lattice structures used to be more costly compared to manufacturing stochastic metal foams. This resulted in wide use of metal foams and honey-combs in structures.

The manufacturing of metallic cellular structures emerged as an important new field of metallurgy, various techniques have emerged to manufac-

ture these structures. These techniques can be either from liquid or solid state. For example in liquid state process, gas injection is used to create these structures, whereas in solid state processes, foaming agents are used to manufacture cellular metals.

1.3.2 Conventional lattice structure manufacturing methods

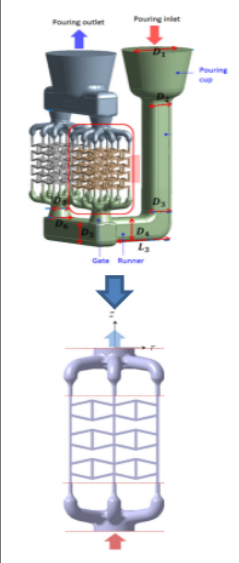
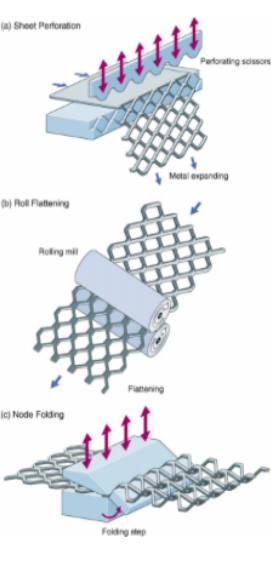
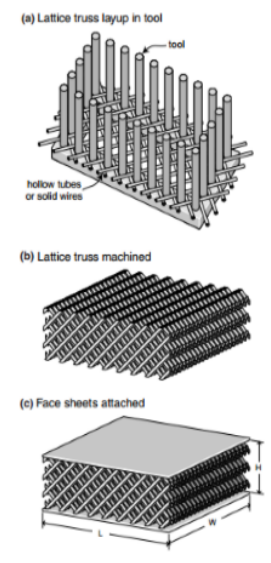
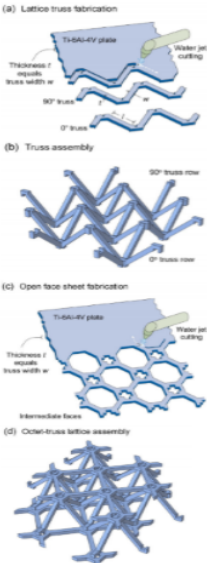
Investment casting	Expanded metal sheet	Metallic wire assembly	Snap fit method
			

Table 1.3: Investment casting (Mun et al., 2015) Expanded metal sheet (Kooistra and Wadley, 2007), metallic wire assembly (Queheillalt and Wadley, 2005) and snap fit (Dong et al., 2015) method process to manufacture lattice structures.

In this section, we review conventional manufacturing techniques to produce lattice structures and its limitations. There are four different techniques, investment casting, expanded metal sheets, metallic wire assembly (Moongkhamklang et al., 2008) and snap fit method. Table 1.3 illustrates each manufacturing technique. For the investment casting technique, first the pattern assembly is dipped in ceramic slurry to obtain a ceramic shell coating. The next step is the drying and dewaxing of the pattern assembly. The final step is the shell cracking to obtain the final product. Expanded

metal sheets process consists in three main operations which are slitting, flattening and folding the metal sheets. In the metallic wire assembly process, first stainless steel solid wires and hollow tubes are assembled using tooling to align the cylinders in collinear layers. Orientation alternates for each layer to form the lattice's structure. Finally the structure is bonded using a brazing technique. In the snap-fitting method (Dong et al., 2015; Finnegan et al., 2007), metal sheets were cut with water jet according to the truss pattern. Then the rows of the trusses were aligned and snap-fit attached to the structure to form the octet-truss lattice structure. Finally the lattice structure is brazed for bonding of the structure.

Disadvantages of conventional lattice structure manufacturing techniques Each of the conventional manufacturing method explained in the previous paragraph has its own limitations. For example, the metallic wire assembly process has limitations in terms of the lattice structure pattern able to be manufactured. The operation to form the lattice pattern is complicated and is not capable of manufacturing complex lattice structures patterns. Whereas the expanded metal sheet process produces large amounts of waste and the metal has to be perforated and punched (Suard, 2015), which limits the number of metals that can be processed. As for investment casting, the need to infiltrate and flow into the tortuous structure also limits the process for alloys which has high fluidity (Wadley et al., 2003). Investment casting is able to manufacture aerospace-quality titanium alloy lattice structures (Li et al., 2008) and complex shapes, however it is not cost-effective and needs new methods to detect and repair the casting defects which are often present in this process (Wang et al., 2003).

1.3.3 Metallic Additive Manufacturing

Additive manufacturing is defined by the American Society for Testing Materials (ASTM) as “ a process of joining materials to make object from 3D model data, usually layer upon layer, as opposed to subtractive manufacturing methodologies ” (Standard, 2012). In the last ten to twenty years, many new metallic additive manufacturing technologies have been developed. It is now possible to manufacture metallic end products with additive manufacturing (Vayre et al., 2012b).

History The first breakthrough in additive manufacturing was in 1987, when Carl Deckard, a university of Texas researcher succeeded in developing layered manufacturing and printed 3D models using a laser light to fuse layer

by layer metal powders to create a prototype. The first patent for 3D objects by CAD was awarded to Charles Hull, who was widely regarded as the father of the rapid prototyping industry.

Classification There are many types of additive manufacturing technologies. These can be categorized into two categories, either layer-based or direct deposition (Vayre et al., 2012b). Examples of layer-based additive manufacturing are selective laser sintering (SLS), selective laser melting (SLM) and electron beam melting (EBM). The two types of energy sources used to melt the metallic powders for additive manufacturing machines are laser and electron beam. The techniques which fully melt the particles are SLM and EBM. Whereas the processes which partially melt the particles are SLS and direct metal laser sintering (DMLS). Only EBM and SLM are capable of manufacturing metallic lattice structures. In this Phd, we focus on the lattice structures manufactured with EBM.

EBM technology Additive manufacturing is a manufacturing process based on a layer-by-layer approach. It is the opposite to subtractive manufacturing. Parts are manufactured by melting successive layers of materials rather than removing them, as is the case of subtractive manufacturing. Additive manufacturing is capable of manufacturing free-form parts. Thus suitable for lattice structure manufacturing.

During the manufacturing process, each layer of the part is melted to the exact geometry of the 3D CAD model. During this process, the machine builds a series of layers with each one on top of the previous one. Additive manufacturing requires a 3D CAD model of each part, for example the octet-truss lattice structure in figure 1.3. The 3D CAD model is then sliced into slices in one direction (Brackett et al., 2011) by a pre-processing additive manufacturing software. Fine metallic powders are melted to form the exact geometrical form of the part.

The system for an electron-beam-melting (EBM) machine consists of a vacuum chamber, work piece, powder container, and the powder melting system, as shown in figure 1.4. An EBM machine uses high voltage and an incandescent cathode to generate an electron beam which melts the powder. This takes place in a high vacuum chamber to avoid oxidation of the metal powder and parts (Wong and Hernandez, 2012). The machine has to be placed in a closed-door room to avoid oxidation of metallic powder and dust mixing with the powder.

After the manufacturing process, the part is then taken out from the machine to remove the unmelted metallic powder. This process is conducted

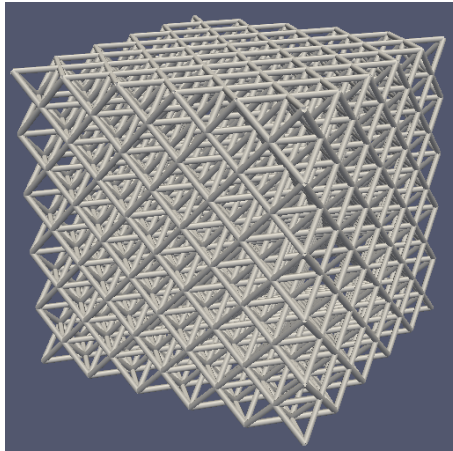


Figure 1.3: An octet-truss lattice structure 3D model in CAD

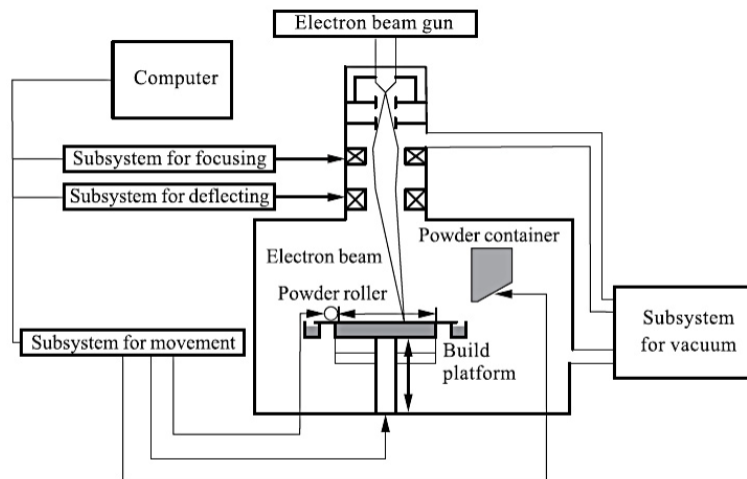


Figure 1.4: Inside an EBM machine (Lu et al., 2009)

using the powder recovery system (PRS). The PRS machine blows away all the unmelted powder which will then be collected, filtered and reused in the additive manufacturing machine for the next manufacturing cycle.

When positioning the parts in the build, supports are added. These supports are added in the pre-processing software dedicated to additive manufacturing. They are important to help support the molten parts and also to evacuate heat from the part.

Advantages of additive manufacturing Compared to conventional manufacturing processes, additive Manufacturing has many advantages. For example, the ability to manufacture complex forms and shapes (Vayre et al., 2012a). This capability gives a whole new freedom for designers when designing the parts. Thus helping engineers to produce hollow parts and improve the functionality of components. For example, engineers can now design and manufacture topology optimised parts and lattice structures.

Additive manufacturing is no longer limited to plastic parts and is capable of producing technical components and not just prototypes (Reinhart and Teufelhart, 2011). Engineers can directly manufacture metallic end products. This saves time and eradicates the need to use a mould.

Additive manufacturing enables the use of titanium alloys and cobalt chromium instead of conventional materials. Studies have proved that the titanium parts manufactured with additive manufacturing have mechanical properties which are good or better than the conventionally manufactured titanium alloys (Dutta and Froes, 2015).

Tests in the most difficult conditions have been done on additive manufactured parts. Cooper et al. tested hydraulic manifolds against real conditions found in the demanding world of motorsports application. Parts produced by additive manufacturing show that this technology is reliable in consistently producing accurate dimensions and also in meeting the mechanical criterias needed (Cooper et al., 2012). This study proved the robust capabilities and consistency of components manufactured with additive manufacturing. Therefore, it will provide users the confidence to use this technology to provide mechanical and geometrical properties that match those of traditional manufacturing processes. Studies have shown that titanium alloy parts manufactured with additive manufacturing have mechanical properties which are as good or better than those manufactured with conventional manufacturing processes (Froes and Dutta, 2014).

Constraints and limits of additive manufacturing In the previous paragraphs, many advantages of additive manufacturing have been explained. However, it does bring it's own constraints and disadvantages too. Supports are needed to dissipate heat during the building process and also to avoid overhanging surfaces from collapsing (Vayre et al., 2012a,b). There is also the need to remove un-melted powder from the build after the process and a potential need for post surface-treatment if needed for functional surfaces (Cooper et al., 2012). These problems has resulted in many new research. New discoveries have to be made to solve these problems. In terms of cost and environmental friendliness, there is not yet reliable research to conclude that

additive manufacturing is better than traditional manufacturing processes. It is a new process that will come alongside the others.

Manufacturability of lattice structures These manufacturability constraints have to be taken into account when designing lattice structure. Manufacturability of lattice structures have to be integrated during the design process to avoid problems (Zhang et al., 2015). For example, the effects of curling, the need of supports and the capability of removing unmelted metallic powders with the PRS have to be considered in the design process of lattice structures. The difference between the struts of the lattice structure CAD models and those of the manufactured structures poses a problem, especially for structures with thin struts. Figure 1.5 illustrates the diameter difference between the struts designed in CAD and those manufactured with additive manufacturing. A mechanical equivalent diameter of lattice structure struts manufactured with additive manufacturing was proposed by (Suard, 2015).

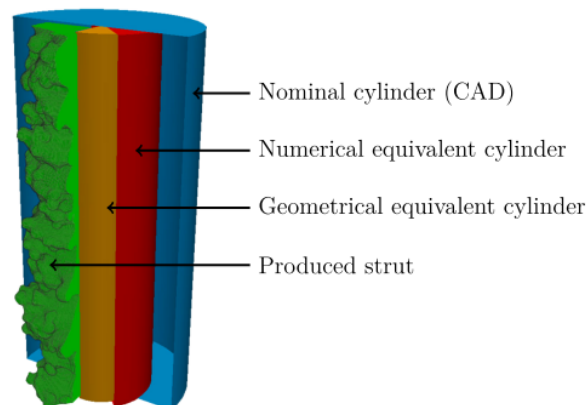


Figure 1.5: Difference between a designed lattice structure strut in CAD, its numerical equivalent cylinder, geometrical equivalent cylinder and the manufactured strut with additive manufacturing (Suard, 2015)

Table 1.4 summarises the advantages and disadvantages of additive manufacturing and conventional lattice structure manufacturing techniques explained in this section.

1.3.4 Conclusion

Existing lattice structure manufacturing processes such as investment casting, expanded sheet metal, metallic wire assembly and snap-fit method have

	Advantages	Disadvantages
Additive Manufacturing	Ability to manufacture complex forms and hollow parts Enables the use of titanium alloys and cobalt instead of conventional materials Equivalent or better mechanical properties than with conventional manufacturing processes	The need of supports to dissipate heat and avoid overhanging surfaces collapsing The need to remove unmelted powder after the building process Potential need for post surface-treatment
Conventional techniques	Not addressed	Complicated operations Produces large amount of waste Limits the number of metals that can be processed Limits to alloys with high fluidity Not cost-effective Needs new methods to detect and repair casting defect

Table 1.4: Synthesis: Advantages and disadvantages of additive manufacturing and conventional lattice structure manufacturing techniques

limitations. For the last ten years, additive manufacturing has become a viable answer to manufacture lattice structures and is gaining popularity as the primary manufacturing process for lattice structures ahead of conventional methods (Rashed et al., 2016). With additive manufacturing, many types of lattice structures can be manufactured easily and reliably. Hence, contributing to the possible wide use of lattice structures.

However, additive manufacturing has its manufacturing constraints too, such as curling, the need for support and the need to blow away the unmelted metallic powder. These manufacturability constraint factors have to be considered and integrated in new lattice structure design strategy propositions.

1.4 Lattice structure properties

Introduction In material science, material properties can be shown in many possible diagrams. However, they all have one thing in common, which is that they have parts of the diagram filled with materials, and parts which have holes and are empty (Ashby, 2013). For example, figure 1.6 shows the big holes in the top left and bottom right corner in the Young's modulus-density space. This means that it does not exist a monolithic material which has high elastic modulus and low density.

Monolithic materials are not able to fill the whole space in material science and are not sufficient to fulfil all required properties, hence creating the need of architected material. With architected material, it is possible to produce parts with high stiffness-to-density ratio and fill these holes of the

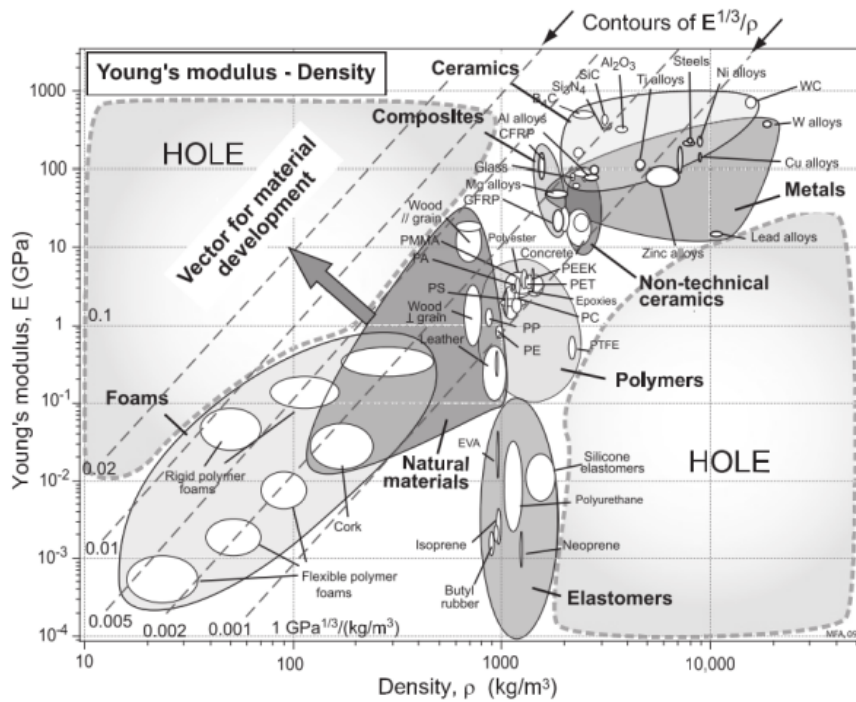


Figure 1.6: Young’s Modulus-density space materials diagram (Ashby, 2013)

diagram. These materials such as foams and lattice structures must be seen as a single material in its own right, with its own properties. If a cellular material outperforms an existing material in the material property diagram, then the material property space has been extended (Ashby, 2013). The possibility to fill the big holes left in this Young’s modulus-density diagram with lattice structure is very interesting.

History Cellular structures have been known for generations, but it was only in the last 30 years that an understanding of materials with a cellular-like structure has emerged. Previously, manufacturing lattice structures were limited by the process available during that period. It now exists techniques to manufacture lattice structures easily. This has impacted the research in lattice structure properties. Previously, the majority of cellular material research publications were related to the cellular structures which were able to be manufactured at that time. Thus, the majority of research papers published were about material properties of stochastic and prismatic materials only. It was then possible to manufacture these types of structures easily and reliably by manufacturing processes such as foaming solidification (Wadley,

2002).

There were however already some manufacturing processes which were capable of manufacturing lattice structures, but these processes were expensive, complicated and had many limitations. Making it not cost effective and not suitable. This increased cost outweighed the improvements gained in weight reduction of the parts manufactured. Manufacturing stochastic metals were more cheaper than manufacturing periodic lattice structures (Wadley, 2002). The high cost and complexity of titanium investment casting process and limitations of other conventional process to manufacture lattice structures resulted in very limited mechanical property information for titanium-based lattice structures as a function of their relative density (Dong et al., 2015).

1.4.1 Mechanical properties

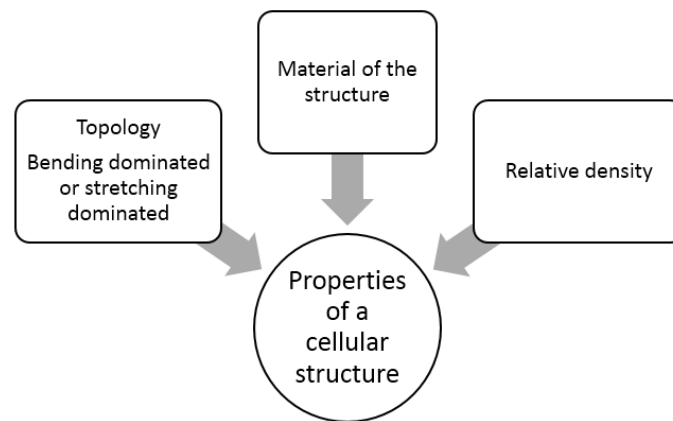


Figure 1.7: Three main lattice structure design variable influence according to (Ashby, 2006)

Influences of a structure's property There are three main factors which influence the properties of a structure, the material of the structure, its cell topology, and its relative density (Ashby, 2006). This is shown in figure 1.7. The material of which the lattice structure is made of influences the structure's mechanical, thermal and electrical properties. Whereas the elementary structure pattern or topology influences the bending-dominated or stretching-dominated property of the structure. The relative density depends on the struts size and length. The relative Young's modulus of a bending-dominated structure scales with the square of the relative density. The scaling law of strength can be derived as:

$$\frac{E}{E_s} \propto \left(\frac{\rho}{\rho_s}\right)^2 \quad (1.1)$$

Prismatic structures have single properties which are only in one direction of the part. Whereas lattice structures can have multifunctional properties and along each X, Y and Z axis of the part. Another interesting possibility is to create a lattice structure which has different mechanical properties for each direction of the part, depending on the requirements of the part in each direction.

Stretching and bending-dominated structures To help differentiate the lattice structure mechanical properties and its applications, these structures can be categorized in two different deformation categories: bending-dominated and stretching-dominated structures. Stretching-dominated is useful to produce high stiffness and low weight parts, for example cubic and octet-truss lattice structures. On the other hand, by orienting the lattice structures struts in a certain pattern to obtain a bending dominated structure, it is also possible to manufacture parts suitable for energy absorption (Evans et al., 2001). The design pattern of a lattice structure influences its mechanical property. This information (Suard, 2015) is summarized in table 1.5 for each lattice structure pattern.

Features	Cubic	Octet-truss	Tetrakaidecahedron	Open-cell foam
Type of deformation	Stretching dominated	Stretching dominated	Bending dominated	Bending dominated
Application	For high stiffness low mass parts	For high stiffness low mass parts	For high energy absorption parts	For high energy absorption parts

Table 1.5: Types of deformation for lattice structures according to (Suard, 2015)

The difference between stochastic and periodic structure mechanical properties influences their applications. Stochastic foams are bending-dominated structures, thus are well equipped for energy absorption. Table 1.6 shows the influence of stretching and bending-dominated structures in mechanical properties.

The experiment in figure 1.8 shows that stretching-dominated structures offer greater stiffness and strength per unit weight than those in which the

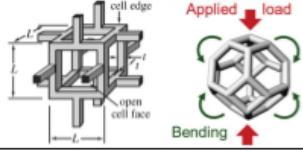
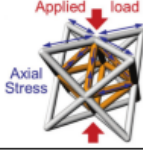
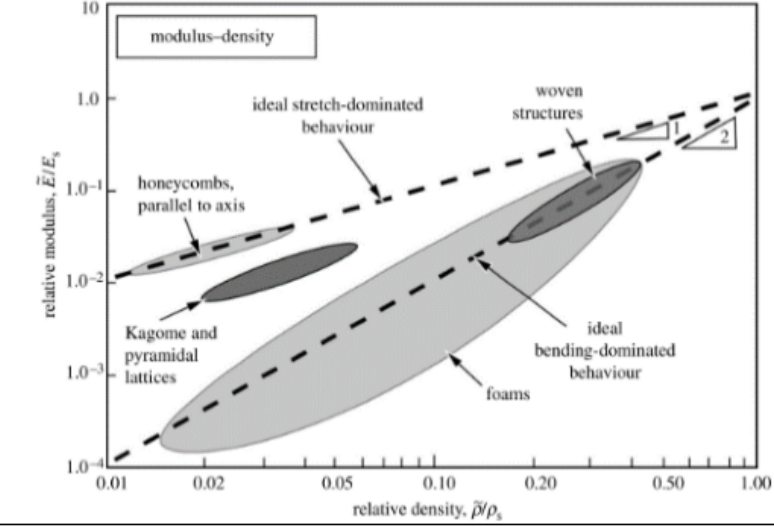
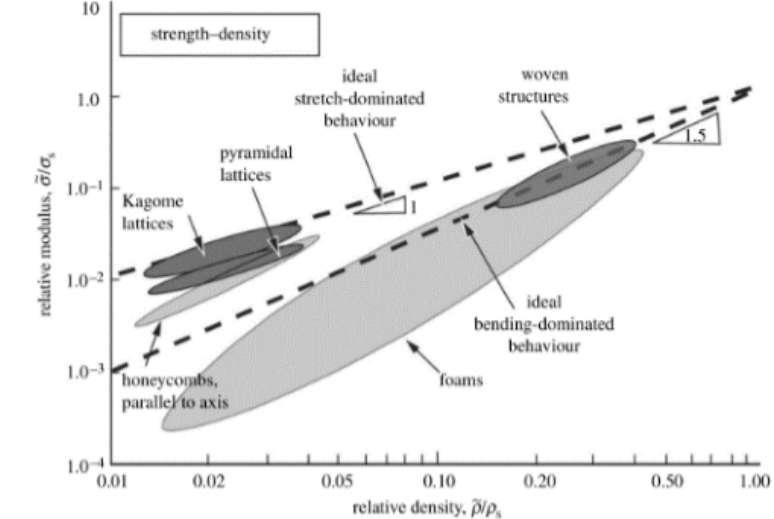
Mechanical properties	Bending-dominated	Stretching-dominated
Examples of elementary patterns	1) Open-cell, 2) Tetrakaidekahedron 	1) Octet-truss 
Relative Young's modulus-relative density graph	 <p>modulus-density</p> <p>relative modulus, \bar{E}/E_s</p> <p>relative density, $\bar{\rho}/\rho_s$</p> <p>ideal stretch-dominated behaviour</p> <p>honeycombs, parallel to axis</p> <p>Kagome and pyramidal lattices</p> <p>foams</p> <p>ideal bending-dominated behaviour</p> <p>woven structures</p>	
Relative stiffness-relative density	 <p>strength-density</p> <p>relative modulus, $\bar{\sigma}/\sigma_s$</p> <p>relative density, $\bar{\rho}/\rho_s$</p> <p>ideal stretch-dominated behaviour</p> <p>pyramidal lattices</p> <p>Kagome lattices</p> <p>honeycombs, parallel to axis</p> <p>foams</p> <p>ideal bending-dominated behaviour</p> <p>woven structures</p>	

Table 1.6: Influence of stretching and bending-dominated structures on mechanical properties according to (Ashby, 2006)

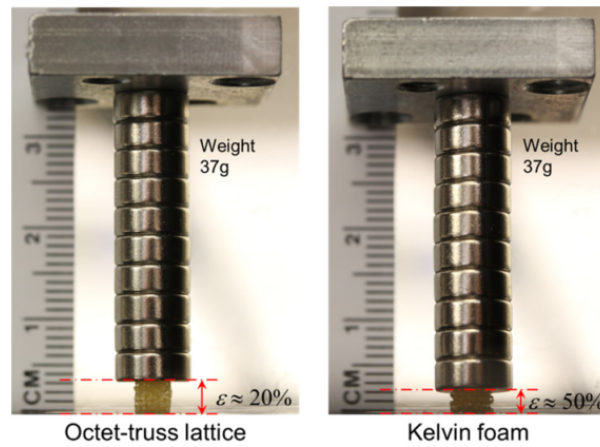


Figure 1.8: Stiffness experiment of octet-truss (stretching-dominated) and kelvin foam (bending-dominated). The octet-truss lattice structure demonstrates markedly superior specific stiffness compared with the open-cell foam (Kelvin foam) (Zheng et al., 2014)

dominant mode of deformation is bending (Deshpande et al., 2001). In this experiment, a compression test was conducted to compare and study the stiffness of an octet-truss lattice structure and a Kelvin foam. An octet-truss is a stretching-dominated structure, whereas a Kelvin foam is a bending-dominated structure.

Therefore, to maximize stiffness and strength, the structure must be stretching-dominated. This information provides an initial basis for the study of lattice structure mechanical properties. However, it must be further detailed and research is needed to find out for all lattice structure configurations. At the moment it does not yet exist a cellular structure database which contains elastic constants, yield criteria and failure mode of different lattice structure patterns (Zhang et al., 2015).

1.4.2 Conclusion

Many comprehensive researches and papers regarding cellular structure properties have already been published (Wadley, 2006; Ashby et al., 2000; Ashby, 2006; Wolcott, 1990). However, research regarding lattice structure properties are yet to be fully explored and studied. Previous material science papers published regarding cellular structures depended predominantly on their manufacturability, which explains why many research previously conducted were mainly on foams and prismatic structures only. For example mechanical properties of the honeycomb structure and metal foams.

Manufacturing process to manufacture lattice structure existed, but was expensive and thus outweighed its weight improvements, consequently making it not extensively used in mechanical parts. Hence not many publications were published on lattice structure properties and many are yet unexplored. The main publications were regarding the main structures such as the octet-truss lattice structure. However, the innovation of additive manufacturing technology changes all this. Technological advances in additive manufacturing has provided opportunities to use lattice structures in part designs. Thus, creating the need to study lattice structure properties. This vacuum of information is one of the reason that prevents designers from using lattice structure in part designs. Lattice structure configurations and properties have to be studied in order to integrate it correctly in part designs.

1.5 Lattice structure design methods

In this section, the aim is to explain about lattice structure design methods and additive manufacturing from a design perspective.

1.5.1 Design for additive manufacturing

Additive manufacturing has brought unprecedented freedom for engineers to manufacture parts with complex forms. However, current design methods do not take full advantages of additive manufacturing capabilities. Hence the need for a new design method with the consideration of lattice structures design for additive manufacturing parts. In this section, we take a look at current design methods proposed for additive manufacturing.

Additive manufacturing has many new advantages compared to conventional manufacturing processes and therefore creates new opportunities in manufacturing. These advantages will only be fully utilized and optimized to its maximum if the whole process in creating the parts is specifically tailored for additive manufacturing. The challenge is now on designers to be

innovative in the design process to reach the maximum potential of additive manufacturing capabilities. Improvements in the design strategy and CAD tools are needed in order to take full advantage of these capabilities (Rosen, 2007).

Current design strategies are not tailored to optimize additive manufacturing (Vayre et al., 2012a). The advantages of additive manufacturing will only be reached and optimized to its maximum if the design method is specifically tailored for its use. It may require a change in the numerical chain so that additive manufacturing can be used at its full potential by designers. Designers have to find new design strategies to achieve this objective (Cooper et al., 2012). To fully optimise the potential of additive manufacturing geometrical freedom, it is important to progress in design guidelines for additive manufacturing (Kranz et al., 2015). There is currently a lack of design methods to help engineers design lattice structure parts for additive manufacturing.

1.5.2 Design for additive manufacturing methodology propositions

Design methods for additive manufacturing can be divided into many categories. First in terms of the scale size of the parts, and second its purpose in different disciplines. Figure 1.9 summarizes these categories of design strategy proposals for additive manufacturing according to (Tang et al., 2014). In this PhD, the scope of the research focuses on the design strategy of meso-level structures. Macro-level structure design proposals concentrates on the use of topology optimization of the form of the parts, whereas meso-level structures focuses lattice structure designs.

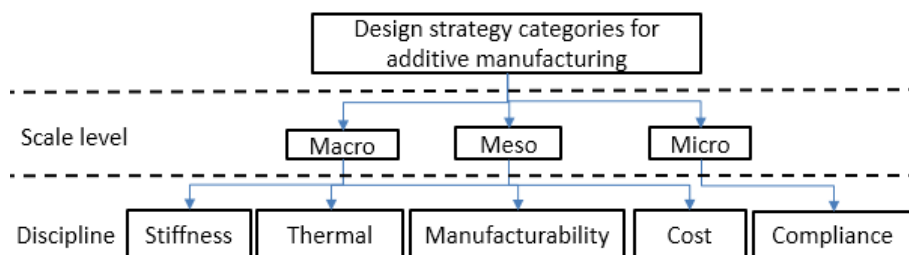


Figure 1.9: Design strategy categories for additive manufacturing according to (Tang et al., 2014)

A new design method has been proposed by (Vayre et al., 2012a) to improve the additive manufacturing design process. It consists of four steps.

The first step is to analyse the specifications of the part, then to propose single or several rough shapes. Third to optimize the shapes and define certain parameters. Lastly the design is validated. Figure 1.10 illustrates this design strategy. This proposition has taken into account the advantages of additive manufacturing to design lightweight structures. However, this proposition can be further improve as it does not take advantage of the use of lattice structures in the method.

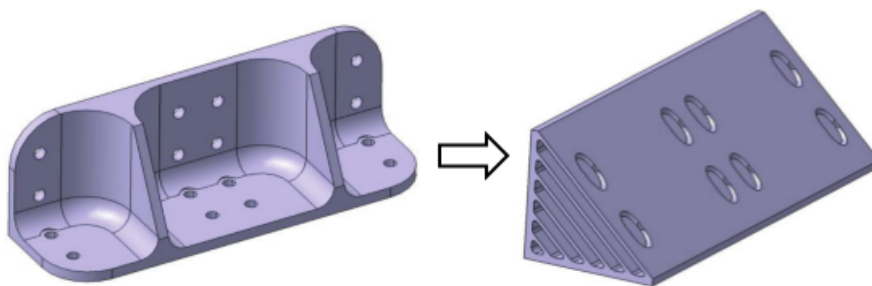


Figure 1.10: Square bracket design proposed using a new design method for additive manufacturing (Vayre et al., 2012a)

Other proposition includes, topology optimization on lattice structure struts to modify its densities (Zhang et al., 2015). This idea integrates cellular structure construction, topology optimization and material model calibration. Using scaling laws, the topology optimization of the cellular structure is applied just as it is usually applied on a continuous solid object. Figure 1.11 illustrates the steps in this proposition. This design-optimization method permits engineers to conduct topology optimization on the lattice structures just as they are done for solid objects. Explicit lattice structures are then constructed by mapping the continuous characterization parameters to individual cells.

A new design method has been proposed which integrates multi-level and multi-discipline design methods into a single process, as shown in figure 1.12. Tang et al. notes that current design methods have two limitations. First, most design methods are focused on a single level scale and second, that there are few design methods that integrate multi-functions in a single part (Tang et al., 2014). They proposed a framework incorporating multifunction and multilevel design method in a single part. Their method integrates the use of traditional topology optimization into multi discipline optimization framework and the use of the homogenization theory to convert the result of topology optimization into meso-lattice structures (Tang et al., 2014).

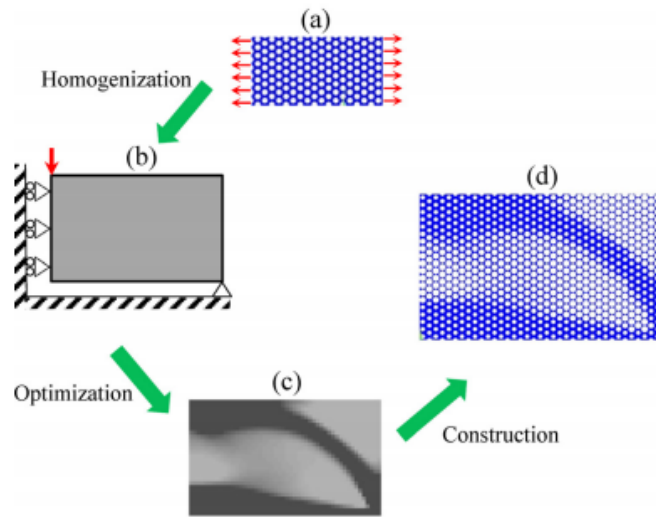


Figure 1.11: Steps for design-optimization of a lattice structure (Zhang et al., 2015)

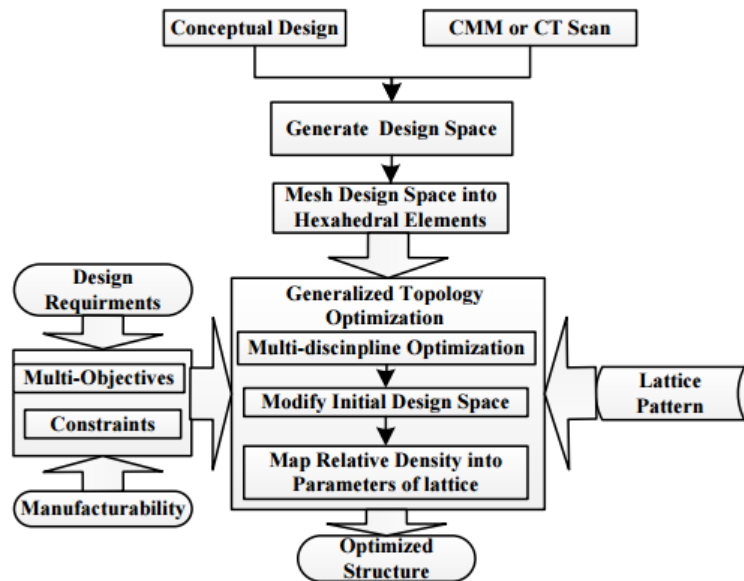


Figure 1.12: Integrated multi-level and multi-discipline design process (Tang et al., 2014)

1.5.3 Conclusion

Current design methods are not tailored to optimize additive manufacturing requirements. Some research have tried to explore and find a solution to this problem. For example, new design for additive manufacturing methodology proposition and the optimization of lattice structures. These propositions are a start and have to be explored further in order to make it more reliable to be used in additive manufacturing. The integration of lattice structures is not yet clear. Currently it does not exist a lattice structure pattern selection method to select suitable lattice structure patterns for each purpose. New lattice structure design strategies are needed to maximise its use in part designs.

1.6 CAD file formats for additive manufacturing

Additive manufacturing application has increased tremendously in the twenty-first century. Applications and research in additive manufacturing have increased and are now applied in many domains. Many new technologies and improvements have been made. However, the breakthrough in manufacturing has not yet been followed by a breakthrough in CAD.

1.6.1 CAD tools to create lattice structures

New CAD tools are needed in order to take full advantage of additive manufacturing capabilities. Many researchers said they see the lack of capable CAD tools as a limit for their research and for the utilization of additive manufacturing technologies (Rosen, 2007). It may require a change in the numerical chain so that additive manufacturing can be used at its full potential by designers (Vayre et al., 2012a). CAD software must be tailored to meet additive manufacturing needs (Campbell et al., 2012). Additive manufacturing requires 3D CAD models of each part, which are then sliced into slices in one direction in a CAM software to generate cross section profiles (Brackett et al., 2011). These cross section profiles are exported directly to the additive manufacturing machine to be manufactured layer-by-layer. Most commercially available CAD programs use parametric B-Rep systems, thus making it challenging to produce digital models for additive manufacturing. These are suited to modeling forms and shapes associated with conventional manufacturing processes such as extrusions, but less suitable for complex geometries associated with additive manufacturing (Thompson

et al., 2016). Traditional CAD systems require an interface that can develop complex structures and store their data and properties (Thompson et al., 2016).

1.6.2 Analysis of current CAD file formats

STL STL has been the de facto format for the last two decades (Hiller and Lipson, 2009). STL is a very simple format and has only triangular facets and is potential for defining faces with any number of edges (McMains et al., 2002). This is the general format for STL :

```
solid name
facet normal  $n_i$   $n_j$   $n_k$ 
  outer loop
    vertex  $v1_x$   $v1_y$   $v1_z$ 
    vertex  $v2_x$   $v2_y$   $v2_z$ 
    vertex  $v3_x$   $v3_y$   $v3_z$ 
  endloop
endfacet
endsolid name
```

The STL file format has many disadvantages. For example, it is not good enough to handle multiple and graded materials (Hiller and Lipson, 2009). It also does not contain information on surface colors. This problem is specific to rapid printing machines which possess the capability to print 3D coloured objects. There are four main deficiencies in the STL file format:

1. Redundancy in the file format.
2. Lack of a complete geometric description. Exact shape reconstruction is impossible.
3. No well-defined approximation method.
4. Lack of technological information.

Consequently, these four deficiencies give the following implications respectively:

1. Large STL file formats which slows down fabrication
2. Produce a lack of coherence between facets and a risk for creating mismatching vertices and incorrect topology. Consequently, object distortions may be produce.

There is redundancy in the file format because the normal can be determined in two different ways (Al-Ahmari and Moiduddin, 2014). The first is by calculating the vertices which are ordered in a counter-clockwise round

the facet, and the other is by referring to the normal specified in the STL format. Which makes one of them redundant. Unless in cases where the facet is very small and calculations based on the vertex positions are usually inaccurate. Lack of coherence between facets is also another problem. There is no information except for the vertices' positions. Which means that it is necessary to search for matching vertices if the model is to be recreated. This is potentially time consuming and prone to creating incorrect topology. These problems of the STL format are well known. But it is still used and no real alternative has been able to replace STL. The solution to this problem is still an open question, the obvious solution is to replace it with a proper data exchange format. But this has not yet been achieved due to the well-known problems of introducing a new format. There are a few extension to the STL file format aimed at overcoming these problems. Three approaches have been discussed to improve data communication for free-form fabrication, by the use of approximation control parameters, the development and use of STL extensions and with STEP based methods. These extension proposals show that small work and extensions can improve largely the STL format. However, this study also shows that even with extensions and improvements, it is still necessary to replace the STL file format for the use in additive manufacturing.

STEP The Standard for the Exchange of Product Model Data (STEP) is a comprehensive ISO standard (ISO 10303) that describes how to represent and exchange digital geometry and product information (Iyer et al., 2001). It provides information for the complete product life-cycle, such as manufacturing, design, maintenance, utilization and disposal (Bhandarkar et al., 2000). STEP is a solid model representation which is unnecessarily complex for the needs of the additive manufacturing community. The main reason for the development of formats such as IGES and STEP was to have a neutral CAD file format which was application independent (Iyer et al., 2001). Thus it is supported by all CAD systems. STEP was created as a successor to the IGES file format (McHenry and Bajcsy, 2008).

It is subdivided into a head and data section. The head section consists of a fixed structure, whereas the data section contains the application data to a given Express schema. The entities to be captured and exchanged in STEP are defined in schemas written in an information modellings language called EXPRESS.

The ISO 10303 has parts which contains Applications Protocol (Aps). Examples of Aps which exist currently area :

- AP 202 Associative draughting (1996)

- AP 203 Configuration-controlled design (1994)
- AP 207 Sheet metal die planning and design (1999)
- AP 224 Mechanical product definition for process planning using machining features (1999)
- AP 225 Building elements using explicit shape representation (1999)

The most common AP use is the application protocol AP 203, Configuration-controlled design. It is used for transferring product shape models, assembly structure, and configuration control information.

IGES The Initial Graphics Exchange Specification (IGES) file format was published by the National Bureau of Standards in 1980. It was designed to store information of 2D and 3D parts. It can be regarded as “The first modern electronic data exchange tool” (Bhandarkar et al., 2000). It was popular, but not enough to satisfy all the requirements of engineers and researchers, which eventually lead to the development of the STEP file format. The IGES file format is a neutral format which permits the transfer of data between CAD and engineering systems. The IGES file format does not provide data other than drawing or 3D modeling, thus it is not suitable for CAM needs, and also does not provide any life-cycle related information like the STEP file format (Bhandarkar et al., 2000). The IGES file format has some problems, such as that it does not have a formal data model, causing ambiguities. Its structure of 80 characters also makes it very verbose and very difficult to understand. This makes it very difficult to identify and correct mistakes and errors (Bhandarkar et al., 2000; McHenry and Bajcsy, 2008). Since IGES does not have a formal data model, few problems have surfaced for CAD vendors which have developed their own extension to the file format. Such as the loss of information and inconsistency with other CAD systems. Thus making it unacceptable for engineering use (Bhandarkar et al., 2000).

AMF The proposed Additive Manufacturing Format (AMF) looks to be a very good prospect to replace STL files as the de facto format for additive manufacturing. However, this has not been the case because it is not open-source and the capabilities of AMF to define material colors and types of materials are not really needed or used by most additive manufacturing machines. AMF is defined by curved triangles of the surface of a part. Acceptance of this file format for use in additive manufacturing in the end depends on its endorsement by both the CAD suppliers and additive manufacturing manufacturers (Al-Ahmari and Moiduddin, 2014).

PLY The Polygon file format, or also known as Stanford triangle format is a pure-mesh based format. It uses polygon meshes and can include information about texture and color but does not define materials or microstructure volumetrically. It was intended to store and view data from 3D scanners. Its purpose was to be flexible and act as a portable 3D file format (McHenry and Bajcsy, 2008). The Ply file format has both binary and ASCII versions. For the binary version, it includes information to make it machine independent. It is popular due to its simplicity and flexibility (McHenry and Bajcsy, 2008). Users can define key types to make extensions. Ply supports geometry in the form of vertices, edges, faces, vertex colours, textures and materials (McHenry and Bajcsy, 2008).

OBJ OBJ is a mesh based format, which is compact and widely accepted in the 3D modeling community. It can map textures easily but lacks the ability to define materials or microstructure volumetrically. The Obj file format is a simple, text based file format (McHenry and Bajcsy, 2008). It was developed by Wavefront technologies.

The Obj file format consists of line of keys and various values. It supports geometry informations such as vertices, edges, faces, parametric surfaces, vertex, textures, material properties, and groups (McHenry and Bajcsy, 2008). It is widely adopted by other CAD systems and can be imported and exported by a number of them (McHenry and Bajcsy, 2008). Below is an example of an Obj file format keys and values:

```
v 0.0 0.0 0.0
v 0.0 1.0 0.0
v 1.0 0.0 0.0
f 1 2 3
```

Table 1.7 shows the key informations :

Key	Description
#	Comment
v	Vertex
l	Line
f	Face
vt	Texture Coordinate
vn	Normal
g	Group
...	...

Table 1.7: Obj file format key information

VRML Virtual Reality Modeling Language (VRML) is a mesh-based file format which was intended to allow 3D content to be viewed over the web (Nadeau et al., 1998). It includes information about 3D surface, colour, and also information that is irrelevant for additive manufacturing. For example, transparency, animations, lights, sounds, and embedded navigation URLs. VRML does not support defining multiple materials within a given mesh or arbitrary microstructure.

Synthesis on CAD file formats In table 1.8, we compare each CAD file format, its advantages and disadvantages.

1.6.3 Conclusion

Additive manufacturing is a new technology which has its own numerical chain. To fulfil its potential, each stage of the numerical chain has to be tailored according to additive manufacturing requirements. Hence a need to study each phase in the numerical chain to see whether improvements are needed.

From the analysis of various CAD file formats, we conclude that there is currently not a file format which is fully optimized for additive manufacturing. Each file format which exists today were created for other uses and technologies in the past. Recent work have been conducted to create new CAD file formats for additive manufacturing, or modify existing ones to correspond to the need of additive manufacturing, but these are yet to replace STL as the de facto CAD file format in additive manufacturing. New CAD tools are needed to overcome the these limitations. Thus the need to study and create a new CAD file format for additive manufacturing which takes into consideration the requirements of each phase in the numerical chain. It will require a change in the numerical chain so that designers can use lattice structures and additive manufacturing at its maximum potential (Vayre et al., 2012a).

File Format	Type	Original purpose	Advantage	Disadvantage
IGES (1980)	Geometry : Vertices,lines polylines,arcs, curves, parametric surface, CSG, b-rep, Open source	To exchange data between CAD systems Store 2D and 3D models	Neutral CAD file format	No formal information model Incomplete exchange due to changes by CAD systems Life-cycle support information only for design applications 80-column format is not easily human understandable Difficulty to correct errors
STL (1988)	Triangulated Open source	Stereo lithography machines	Easy conversion Wide range input output Simple slicing algorithm Sequential memory access	Large file size Truncation errors Incompleteness Inconsistency Incorrect normal and intersections Degerate facets
OBJ (1992)	Geometry; vertices Open source	For Wavefront 'Technologies' advanced animation package	Simple Compact Wide accepted in 3D modelling community	Not able to define materials
STEP (1993)	Triangulated boundary Faceted boundary General surface B-rep solid Open source	Describe life cycle product data independant from any system To success IGES	Resoures available to transfer slide data Integrated resouces contains all needed to define contours and patterns Use exact geometry and NURBS curves Contains geometry and materials information Possible to include process information	Unnecessarily complex for the needs of additive manufacturing
PLY (mid 1990s)	Geometry : Vertices,edges, faces,vertex, colours,textures, materials	Store 3D data from scanners	Simplicity Flexibility Allows user defined types	Does not define materials or microstructure volumetrically
VRML (1997)	Open source	Represent 3D interactive vector graphics for the internet	Includes information of surface and colours	Unnecessary information for AM: transparency,animations, lights, sounds, URLS Impossible to define multiple materials
AMF (2011)	Curve triangles Open source	AM machines	Resolution independent	Contains unnecessary information for metallic AM

Table 1.8: Synthesis : CAD File Formats Comparison

1.7 Literature review conclusion

With the progress in additive manufacturing as a reliable process to manufacture lattice structures, it should have been the catalyst in the wide use of these structures in products. However, this is not yet the case as there is still a large vacuum of information regarding lattice structure mechanical properties, lattice structure design strategies and CAD file format and software for additive manufacturing. Hence lattice structures are currently not

broadly used in mechanical parts even though it has many advantages, such as producing high strength low mass structures.

Therefore, in order to reach the great potential of additive manufacturing and to facilitate wide use of lattice structures in products, improvements and research must be made in these four aspects :

- Lattice structure mechanical properties
- Lattice structures design strategies
- CAD and CAE tools for lattice structures
- CAD file formats for additive manufacturing

These four aspects are investigated in the following chapters to achieve the PhD objective.

CHAPTER 2

CAD tools in additive manufacturing

Contents

2.1	Evaluating current CAD tools performances in the context of design for additive manufacturing	38
2.1.1	Human Machine Interface	40
2.1.2	CAD software utility	42
2.1.3	CAD file format	44
2.1.4	RAM usage	46
2.1.5	Conclusion	48
2.2	Evaluating current CAE tools performances in the context of design for additive manufacturing	48
2.2.1	FEA computation file size	49
2.2.2	FEA time duration	50
2.2.3	Conclusion	51
2.3	Conclusion	52

2.1 Evaluating current CAD tools performances in the context of design for additive manufacturing

Lattice structure is an important element in the design of additive manufacturing parts. Therefore, there is a need to design parts containing lattice structures efficiently and conveniently using CAD tools. This chapter aims to evaluate the current CAD tool's performances in the context of design to create lattice structure 3D models.

The criteria chosen to evaluate these performances are:

- The total number of operations the operator has to perform to design the basic lattice structure pattern.
- The total time the operator needs to design a lattice structure
- The time taken by the CAD software to apply and generate a repetition function.
- The CAD file sizes
- The RAM usage in CAE and CAM software.

These criteria are used to evaluate the performances of current CAD tools in terms of human machine interface, and data exchange between CAD, CAE and CAM for additive manufacturing, as shown in figure 2.1.

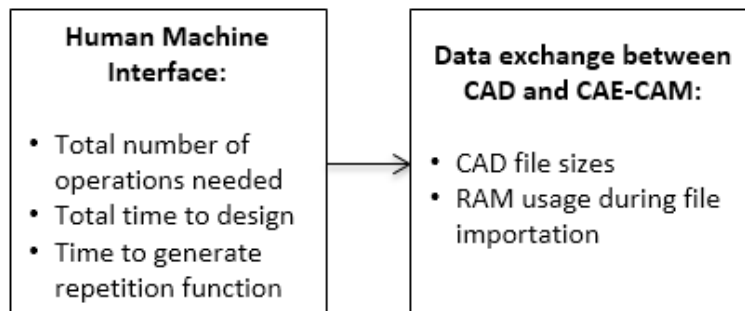


Figure 2.1: The roles of each criterion in evaluating CAD tools for additive manufacturing

The computer used to carry out this experiment has the following specifications:

1. Windows 7 Professional 64 bits
2. Intel® Processor Core i7-3540M CPU @ 3.00 GHz

3. 8 GB RAM
4. 500 GB hard disc

Three variables have been chosen for the design of the experiment:

1. Dimensions and volumes of the parts
2. Lattice structure patterns
3. Sections of the bars of the lattice structures

Two lattice structure patterns were chosen to see how the software handles the design of simple lattice structures such as cubic lattice structures and also more complicated lattice structure patterns such as an octet-truss lattice structure:

1. Octet-truss lattice structures
2. Cubic lattice structures

The bars of the lattice structures were designed with two different sections to see if it makes any differences in term of software and operator:

1. Square section
2. Circular section

Figure 2.2 shows an example of a struts circular section.

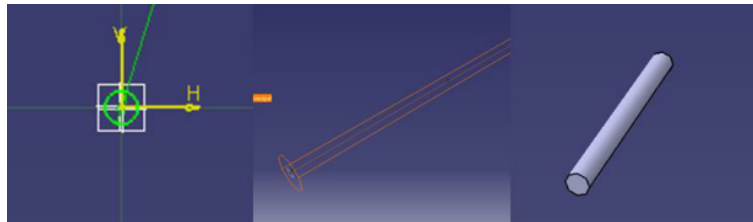


Figure 2.2: Circular lattice structure bars

Four part dimensions were chosen to see how the software adapts for different sizes of parts. These volumes were chosen to see the gradual effects of volume sizes on the performance of the CAD software. The maximum dimension chosen is $20\text{ cm} \times 20\text{ cm} \times 20\text{ cm}$, which is approximately the maximum dimension that can be built in current additive manufacturing machines. The four dimensions and volumes are (see figure 2.3) :

1. $5\text{cm} \times 5\text{cm} \times 5\text{cm}$ (volume : 125cm^3)
2. $10\text{cm} \times 10\text{cm} \times 10\text{cm}$ (volume : 1000cm^3)
3. $15\text{cm} \times 15\text{cm} \times 15\text{cm}$ (volume : 3375cm^3)
4. $20\text{cm} \times 20\text{cm} \times 20\text{cm}$ (volume: 8000cm^3)

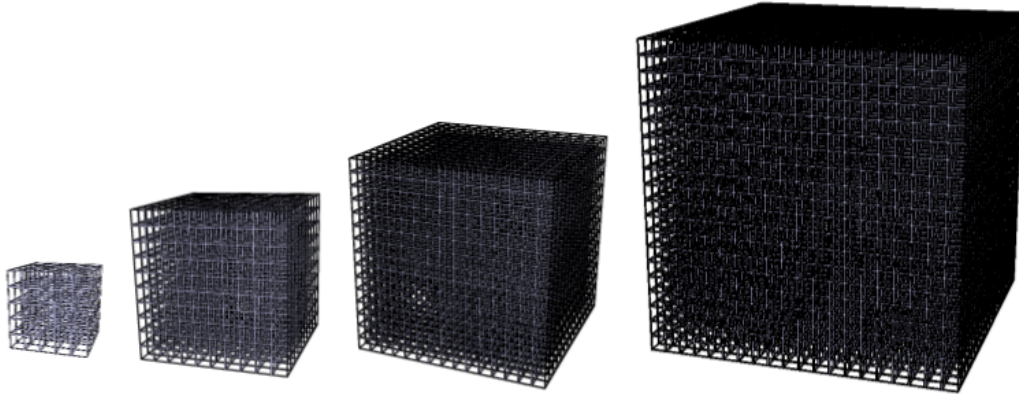


Figure 2.3: Different lattice structure dimensions

2.1.1 Human Machine Interface

The objective of this section is to observe the challenges experienced by the user when designing lattice structures in a CAD software. The software used in this experiment is CATIA. It uses the same B-REP models to describe the geometry and as other commercially available CAD software. Therefore the results with CATIA will be comparable and representative of other CAD software such as Solidworks and Creo.

A total of 19 different parts with the different variables have been designed in the CAD software. Each operation and difficulty was observed and noted. Figure 2.4 is an example of some of the steps to design a $1\text{ cm} \times 1\text{ cm} \times 1\text{ cm}$ octet-truss elementary structure.

Making up this elementary structure in a classical CAD environment requires no less than 91 operations. Some of these are illustrated in figure 2.4.

1. Create a new plane
2. Draw a circle in the sketch to form the section of the bar
3. Extrude the circle to form the bar
4. Create a new plane to draw the circle section bars
5. Repeat function to generate symmetrical bars
6. Create a new plane
7. Apply the repeat function to generate symmetrical bars
8. Create a new plane
9. Apply the extrude function to generate a new bar
10. Create a new plane
11. Apply the extrude function to create a new bar

12. Repeat function to generate symmetrical bars

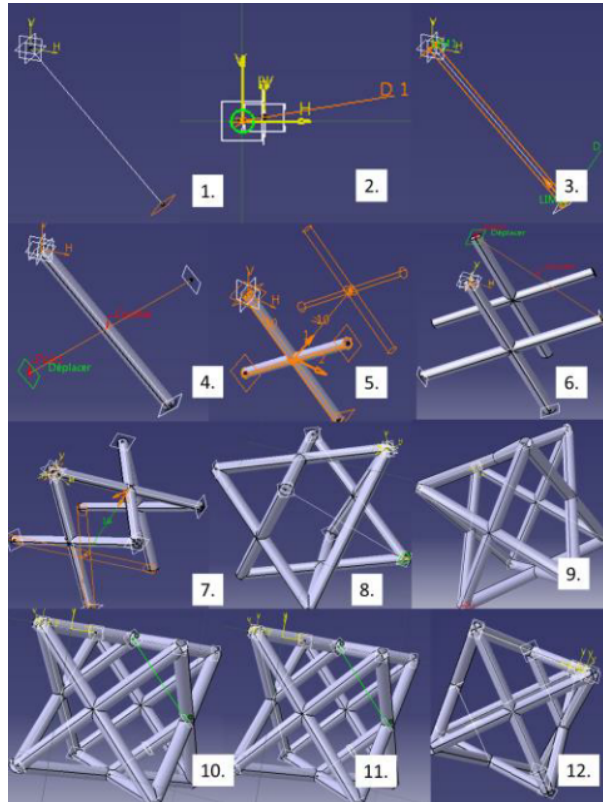


Figure 2.4: Creating a basic $1\text{ cm} \times 1\text{ cm} \times 1\text{ cm}$ octet truss lattice structure with circular section bars

These are just some of the operations done to create the elementary feature. Making the $1\text{ cm} \times 1\text{ cm} \times 1\text{ cm}$ lattice structure requires 91 operations, consisting of:

- 35 operations to create a sketch
- 21 extruding operations
- 3 rectangular repetition operations
- 25 operations to define a new plane
- 7 operations to define a new point

The total time that I needed to create this $10\text{ mm} \times 10\text{ mm} \times 10\text{ mm}$ octet-truss lattice structure is 1 hour and 35 minutes. As described in this section, the basic $10\text{ mm} \times 10\text{ mm} \times 10\text{ mm}$ lattice structure had to be

designed manually step by step and must be represented graphically to obtain the lattice structure pattern in the CAD software. The method is time consuming because the lattice structures have to be represented and designed from scratch. There are no special functions to automatically generate the desired lattice structures in the current CAD software.

To create a $50\text{ mm} \times 50\text{ mm} \times 50\text{ mm}$ lattice structure, the next step is to apply:

1. The rectangular repetition function along the XY plane with a spacing of 1 cm and 5 instances to obtain a $5\text{ cm} \times 5\text{ cm}$ part dimension.
2. The rectangular repetition function along XZ plane to obtain a $5\text{ cm} \times 5\text{ cm} \times 5\text{ cm}$ structure.

The same repetition procedure was done to obtain other dimensions and volumes. For example, $10\text{ cm} \times 10\text{ cm} \times 10\text{ cm}$, $15\text{ cm} \times 15\text{ cm} \times 15\text{ cm}$, and $20\text{ cm} \times 20\text{ cm} \times 20\text{ cm}$ lattice structures. Figure 2.5 shows these two steps of rectangular repetition to obtain the final desired volume.

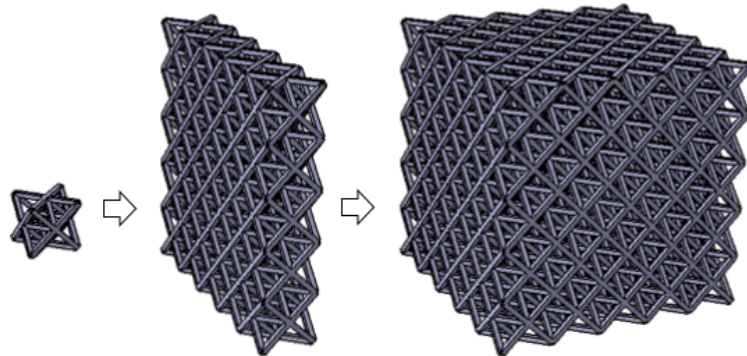


Figure 2.5: First and second repetition from elementary structure to obtain a $5\text{ cm} \times 5\text{ cm} \times 5\text{ cm}$ size octet truss lattice structure

2.1.2 CAD software utility

The performance of the CAD software when processing certain operations was examined. The objective is to observe the performance of the software in doing these operations for the eight cases studied. The time taken to apply the first and second repetitions of the basic lattice structure was used as a criterion to evaluate this performance. Each of the first and second rectangular repetition operation was repeated three times during the study

to obtain an average time and more reliable results. Table 2.1 and figure 2.6 and figure 2.7 show the time taken by the CAD software to accomplish these operations for each part.

Bars Section Forms		Square		Circular	
Repetition		1st	2nd	1st	2nd
Lattice Structure	Size (cm)	Average Time (s)	Average Time (s)	Average Time (s)	Average Time (s)
Square	5x5x5	4	16	25	55
	10x10x10	20	24	48	138
	15x15x15	48	90	149	490
	20x20x20	126	297	262	1181
Octet Truss	5x5x5	24	77	35	107
	10x10x10	104	1843	88	1066
	15x15x15	293	N/A	402	N/A
	20x20x20	770	N/A	842	N/A

Table 2.1: Average time to generate 1st and 2nd repetition

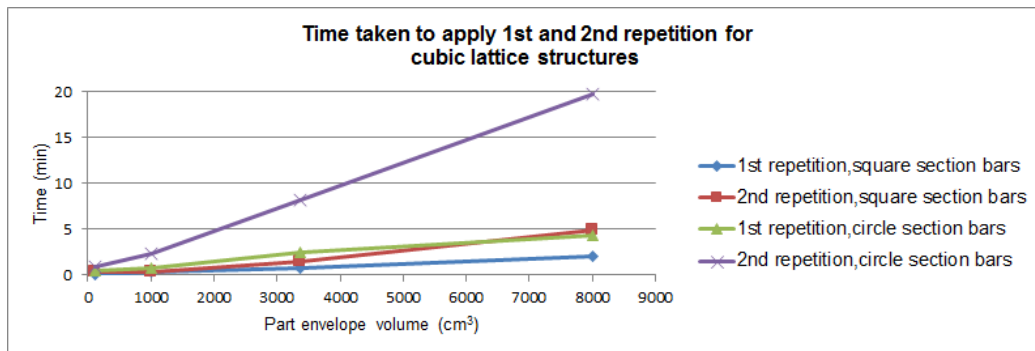


Figure 2.6: Cubic lattice structure repetition duration

The time that the CAD software needs to generate and execute the repetition function increases linearly with the volume of the parts. Thus the operations become time consuming for large volume parts. An octet-truss lattice structure takes two to ten times more time than a cubic lattice structure when applying the repetition function due to the higher number of surface areas compared to square lattice structures.

When applying the second repetition function for the parts starting from 15 cm × 15 cm × 15 cm dimensions, the software could no longer execute

the repetition function successfully, even after more than three hours of waiting time. The RAM used by the CAD software reached 2.292 GB and the software did not respond and had to be restarted. The CAD software and the computer were not capable of generating the second repetition function for an octet-truss lattice structure over $15\text{ cm} \times 15\text{ cm} \times 15\text{ cm}$ volume.

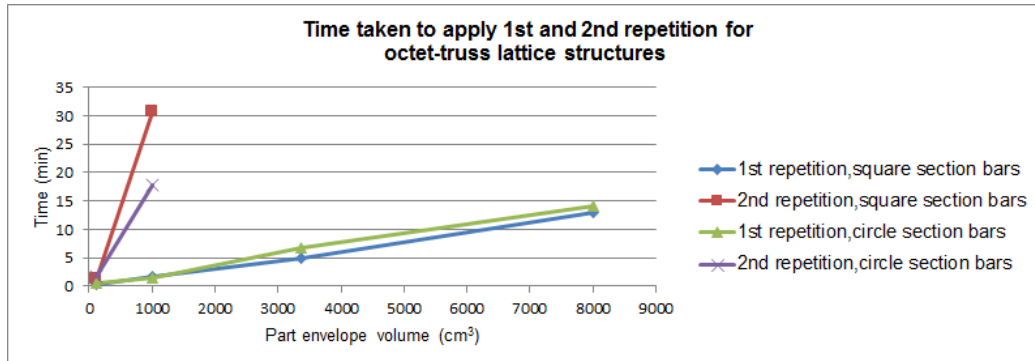


Figure 2.7: Octet-truss lattice structure repetition duration

2.1.3 CAD file format

The second result examined is the size of the CAD files for each part when exported to different CAD file formats. The objective is to find out the effects of the type and size of lattice structures on file sizes and whether current file formats are suitable for the requirements of additive manufacturing. The parts were exported and saved in the CAD software to different file formats such as IGES, STL and STEP. These are common file formats used to import parts in CAM and CAE software.

		Section Forms	File Size (MB)					
		Size (cm)	Square Section Bars			Circular Section Bars		
			IGES	STL	STEP	IGES	STL	STEP
Lattice Structure Type	Square Lattice Structure	1x1x1	0.06	0.03	0.04	0.17	0.12	0.08
		5x5x5	3.79	1.89	2.20	6.30	5.51	3.27
		10x10x10	27.94	14.07	17.13	44.12	23.60	38.21
		15x15x15	91.67	46.37	57.57	142.96	122.66	77.14
		20x20x20	214.21	108.61			283.41	181.69
	Octet Truss	1x1x1	0.4	0.2	0.2	0.5	0.4	0.3
		5x5x5	29.9	14.9	20.4	42.3	36.4	23.4
		10x10x10	228.1	114.0	161.9		280.4	67.0
		15x15x15						
		20x20x20						

Table 2.2: Lattice structure CAD file sizes

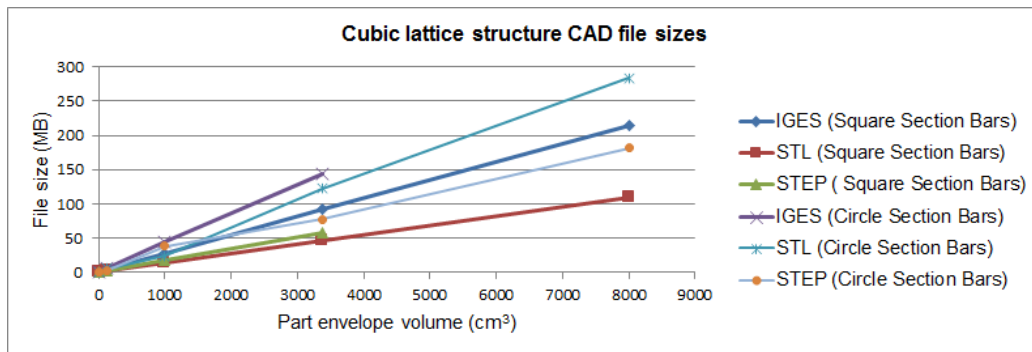


Figure 2.8: Cubic lattice structure file size

Table 2.2 and figures 2.8 and 2.9 show the CAD file sizes of the lattice structures for different configurations. Each file format has different file sizes for the same part volume. This is because each format is written in a different way. The files sizes depend on how the information of the part is interpreted and written. Each file format saves the information differently. The IGES, STL and STEP format generated large file sizes for lattice structures parts. For example, a STL file for 10 cm x 10 cm x 10 cm octet truss reached 280.4 MB. This shows that current file formats generate large file sizes and are not suitable to store information of lattice structure parts. For example, STL format generates and stores information on triangular meshes of the surface area of the part. Therefore, when the parts contain large surface areas, the file increases heavily. Currently, there has yet to be a file format which can

describe lattice structure patterns and dimensions with a minimum set of information. For example, describing the basic elementary structure and repetition should suffice.

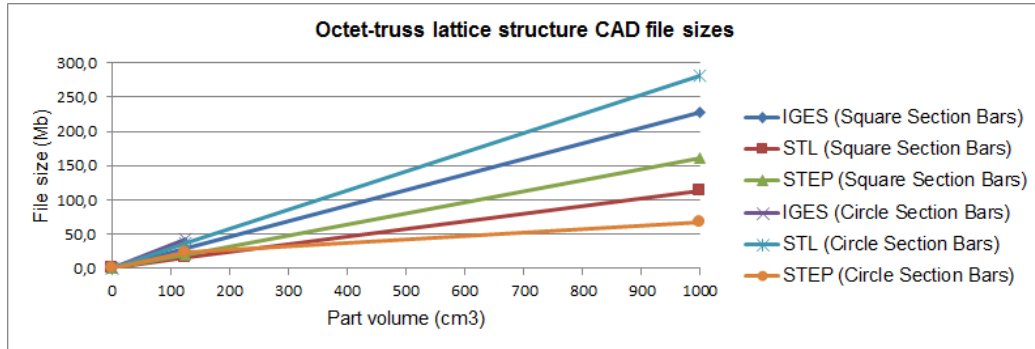


Figure 2.9: Octet-truss lattice structure file size

2.1.4 RAM usage

The RAM used by the computer to import and load the files in CAD, CAM and CAE software was examined and noted. The objective is to find out whether the files generated could be loaded in CAE and CAM software or if errors occurred. ANSYS and MAGICS were chosen as the CAE and CAM software respectively in this experiment. The results are shown in table 2.3 and figures 2.10 and 2.11

Section Forms		RAM consumption (MB)						
		Square Section Bars			Circle Section Bars			
	Size (mm)	CATIA	MAGICS	ANSYS	CATIA	MAGICS	ANSYS	
Lattice Structure Type	Square Lattice Structure	1x1x1	260.4	47.9	411.5	260.9	103.6	150.5
		5x5x5	265.7	50.3	430.5	273.5	108.6	196.7
		10x10x10	323.1	70.8	498.4	329.6	132.4	739.5
		15x15x15	498.0	117.2		513.0	199.8	2347.9
		20x20x20	830.4	209.6		816.8	389.7	
	Octet Truss	1x1x1	219.4	54.8	148.0	250.8	135.5	147.7
		5x5x5	305.5	78.8	487.4	300.1	162.1	542.4
		10x10x10	882.5	218.3		712.6	404.4	
		15x15x15						
		20x20x20						

Table 2.3: RAM consumption

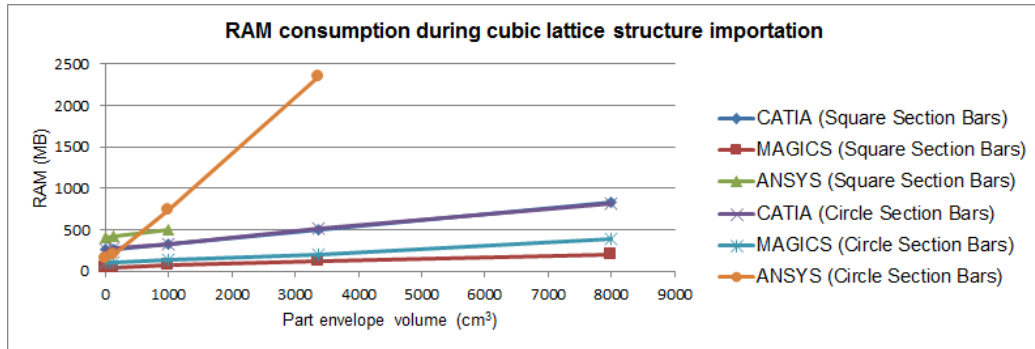


Figure 2.10: Cubic lattice structure RAM consumption

Five STL files of the parts could not be loaded in ANSYS. When loading the parts into the software, the computer indicated nearly 4 GB of RAM was used by the software. It eventually failed to load the parts into the software. This showed that for large-sized STL files and lattice structure parts, the CAE software is not capable of processing the information and even loading the parts into the software. Large surface areas of the parts contributed to high quantity of information to be processed by the software.

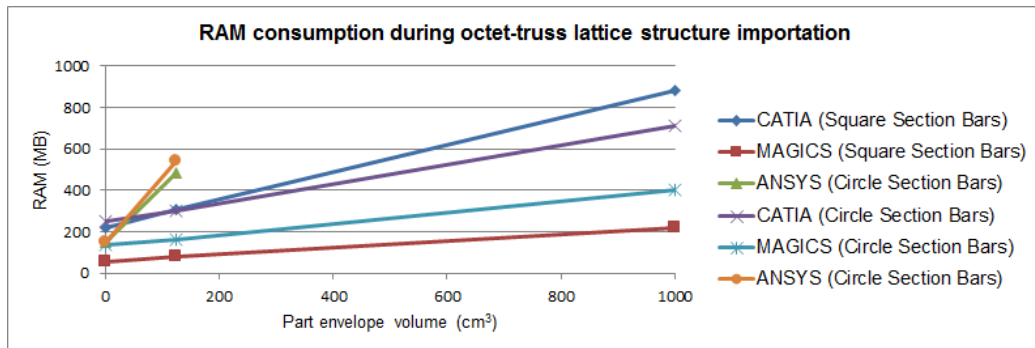


Figure 2.11: Octet-truss RAM consumption

From this case study, it is evident that current CAD software and file formats are not competent to design and store lattice structure parts efficiently and is not suited to exchange data with CAE and CAM software. The results obtained show that it is difficult to design lattice structure CAD models, as the process is very time consuming and generates large file sizes. This thus leads to high RAM consumption, making it very heavy for the software and computer to handle. For large volumes, the parts prove to be too heavy for

the computer to manipulate in CAD, CAE and CAM software. This is due to the large number of surface areas of the lattice structure that the software has to process. In certain cases, the software was unable to achieve the desired operation. The patterns of the cellular structures had to be drawn one by one and then the repetition function was used until the desired structure was achieved. These problems made it impractical for users to design usual cellular structures quickly and efficiently, consequently making the process time consuming.

2.1.5 Conclusion

New requirements in part designs for additive manufacturing result in new needs for computer-aided-design. Current CAD software are not tailored for these new requirements. Actual CAD, CAE and CAM tools and file formats are insufficient to fulfil these new needs for additive manufacturing and has to be replaced. Product designs, CAD, CAE and CAM requirements are taken into consideration for the creation of a new CAD file format. A new research has to be carried out in order to determine the most robust and efficient method to design lattice structures in CAD software.

2.2 Evaluating current CAE tools performances in the context of design for additive manufacturing

In this section, a case study was done to evaluate current CAE tools performances to perform finite-element-analysis (FEA) on lattice structures. The objective is to evaluate whether the performances of current CAE tools are adequate to perform these tasks efficiently and conveniently on lattice structures using volumic FEA. Two case studies were conducted. In the first one, the FEA computation file size was measured and analysed. In the second one, the time to execute an FEA on the lattice structures was taken. The results were analysed and conclusions were made.

In this experiment, the lattice structure pattern chosen is the octet-truss lattice structure, while the variable of the experiment is the different dimensions of the structure. Figure 2.12 shows the force applied. It is a compression test with -500N applied in the Z-axis. Each elementary octet-truss structure is $1\text{cm} \times 1\text{cm} \times 1\text{cm}$ in dimension. The dimensions and volumes of the structures are:

1. $2\text{cm} \times 2\text{cm} \times 2\text{cm}$ (volume : 8cm^3)

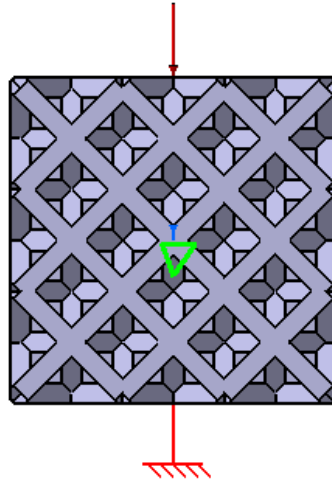


Figure 2.12: FEA simulation on an octet-truss lattice structure

2. $3\text{cm} \times 3\text{cm} \times 3\text{cm}$ (volume : 27cm^3)
3. $4\text{cm} \times 4\text{cm} \times 4\text{cm}$ (volume : 64cm^3)
4. $5\text{cm} \times 5\text{cm} \times 5\text{cm}$ (volume: 125cm^3)
5. $6\text{cm} \times 6\text{cm} \times 6\text{cm}$ (volume: 216cm^3)
6. $7\text{cm} \times 7\text{cm} \times 7\text{cm}$ (volume: 343cm^3)

2.2.1 FEA computation file size

After the analysis, the FEA computation files were saved. Each file size was noted and shown in table 2.4. The FEA computation file size increases tremendously when the volume of the parts increases. For the $7 \times 7 \times 7$ unit octet-truss lattice structure, the FEA computations file size reached 36.6 GB. This made the computer slow and consumed a lot of disk space. Figure 2.13 shows the significant increase in FEA computation file size compared to the increase in part volume.

Part envelope volume (cm ³)	Unit	FEA computations file size (GB)
8	2x2x2	0.3
27	3x3x3	1.3
64	4x4x4	3.7
125	5x5x5	7.4
216	6x6x6	19.3
343	7x7x7	36.6

Table 2.4: Octet-truss lattice structure FEA computations file size

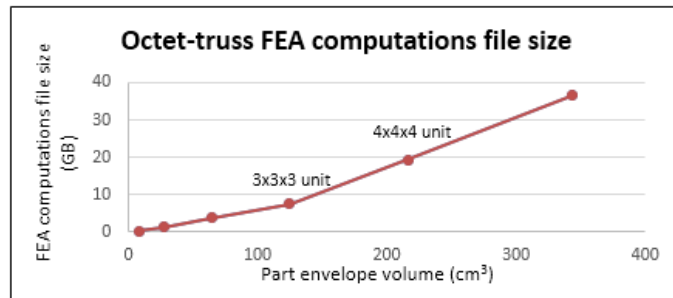


Figure 2.13: Octet-truss lattice structure FEA computations file size

2.2.2 FEA time duration

As soon as the FEA analysis was executed, the stopwatch started and the time duration was taken. The results are shown in table 2.5. The FEA duration increased significantly when the part envelope increased. For the $7 \times 7 \times 7$ unit octet-truss lattice structure, the time to execute the analysis was really long, 2 hours and 14 minutes. This proves to be very time consuming for the users to execute FEA on an octet-truss lattice structures. Figure 2.14 shows that the FEA analysis time increases significantly when the lattice structure's volume increases.

Part envelope volume (cm ³)	Unit	FEA time (min)
8	2x2x2	0.3
27	3x3x3	1.4
64	4x4x4	5.9
125	5x5x5	26.1
216	6x6x6	70.4
343	7x7x7	134.0

Table 2.5: Octet-truss lattice structure FEA time duration

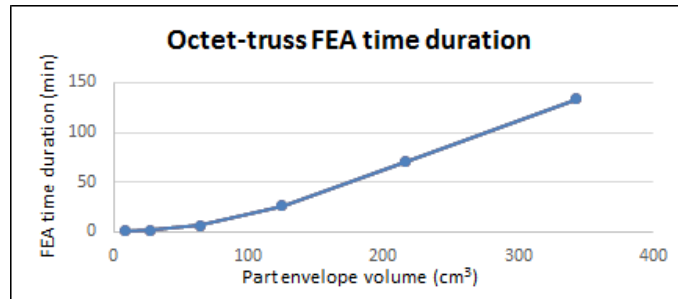


Figure 2.14: Octet-truss lattice structure FEA time duration

2.2.3 Conclusion

The CAE software consumes a significant amount of time to execute the analysis and it creates very large FEA computation file sizes. If lattice structures are to be the norm in lightweight high strength additive manufactured parts, this is a problem that must be solved. Engineers and designers require tools that are powerful enough to conduct FEA on lattice structures easily and quickly. Current CAE software analyses parts based on the surface volume of the part. Thus for parts such as lattice structures which have a large amount of surfaces, this generates a problem for the software to execute FEA analysis. New methods and tools must be constructed to find a solution to this problem.

2.3 Conclusion

From this research, we conclude that current CAD software are not practical for users to design lattice structures efficiently for additive manufacturing parts and that current CAE software are not up to scratch in terms of performance to execute finite-element analysis on lattice structure parts.

There are two ways to overcome this problem. The first would be to create a new CAD application to quickly design a lattice structure in the CAD software, or the other would be to represent the lattice structure with a solid volume without the need to create the lattice structure CAD model with struts. This would be possible by creating a new CAD file format which interprets information of the part as lattice structures and by creating a new equivalent material, thus making it easier to design and conduct FEA. Figure 2.15 is a summary of the problems, conclusions and solutions presented in this chapter.

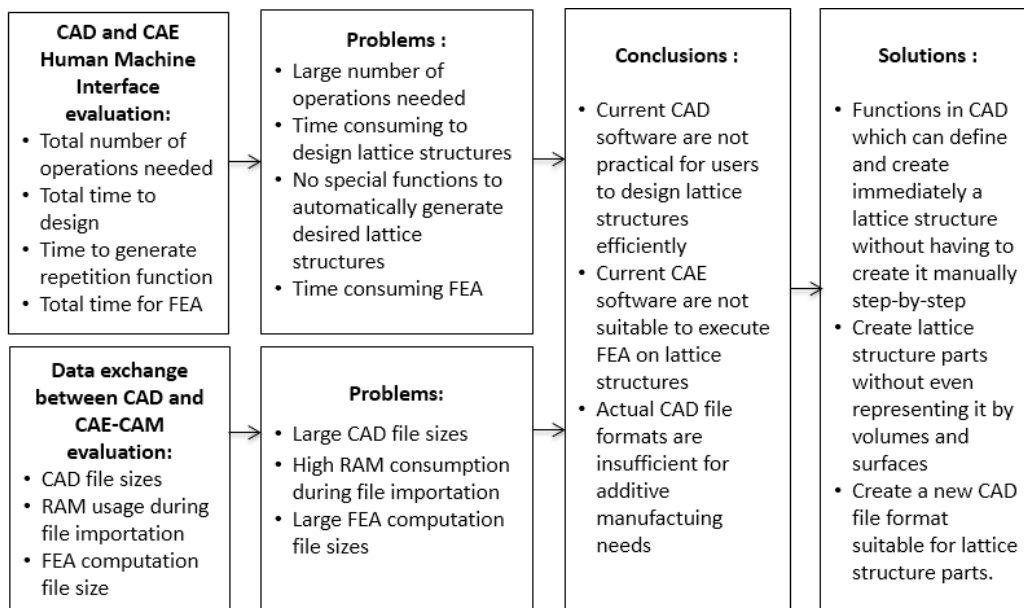


Figure 2.15: Summary of evaluation, problems, conclusions and solutions of chapter two

CHAPTER 3

Lattice structure design strategy

Contents

3.1	Definitions of used terms	55
3.2	Proposed lattice structure design method	56
3.2.1	Concept to link lattice structure, solid material and equivalent material	56
3.2.2	Step-by-step of the proposed method	61
3.2.3	Application example of the proposed lattice structure design method	62
3.3	A methodology for the creation of equivalent lattice structure materials	69
3.3.1	FEA simulation and variables	69
3.3.2	Simulation execution	74
3.3.3	Stress concentration	75
3.3.4	Results	77
3.3.5	Analysis	83
3.4	Results verification	87
3.4.1	Comparison with results from other articles	87
3.4.2	Comparison with case study results	90
3.4.3	Conclusion	98
3.5	Summary	99

In spite of the various benefits of lattice structures, engineers currently do not have the required information to integrate it easily and correctly in part design. They do not have the necessary information to choose the most suitable lattice structure configuration and they do not have the appropriate tools to evaluate the designed parts. We start this chapter by giving a real case example of this problem.

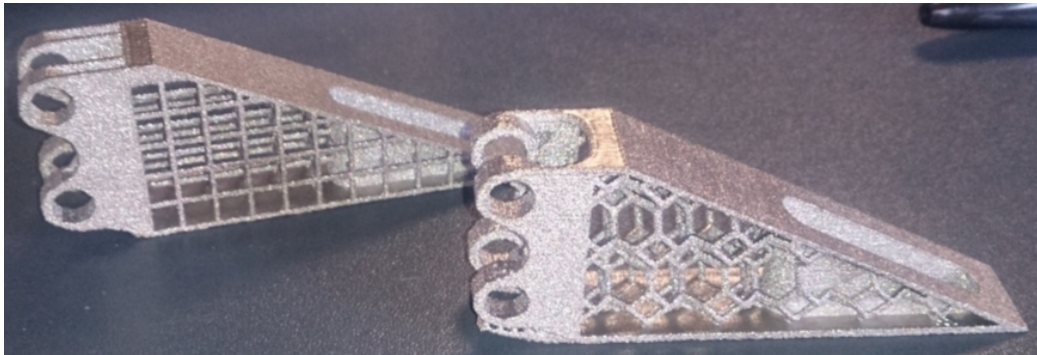


Figure 3.1: Which type of lattice structure to choose? Cubic or hexa-truss lattice structure? Which densities are needed?

The central volume of the part presented in figure 3.1 was initially solid. To reduce the weight of the part, the designers had wanted to integrate lattice structures in this central area of the part. What structure would thus be suitable: a cubic or hexa-truss lattice structure? The main questions that usually arise for the engineers in these situations are :

- How do I choose the most suitable lattice structure?
 - Which type of lattice structure patterns do I choose?
 - What lattice structure densities are needed?
- Does the selected lattice structure configuration validate the prescribed requirements?

Designers need a reliable guideline to help them choose the correct lattice structure pattern and density to fulfil the part's mechanical requirements. After describing the definitions of the used terms, we present the concept and the stages of the lattice structure design method. An application example of the proposed lattice structure design method is presented. Next, we show how to determine the characteristics of the equivalent material and we apply this approach for different lattice structures. The results obtained are compared

with a case study and theoretical and experimental results from the literature. Finally, an example to choose the lattice structure is presented.

3.1 Definitions of used terms

Definitions adopted by researchers are often not uniform, so the key terms in this chapter are explained to establish positions taken in this chapter and avoid ambiguity.

Design space Design space is the defined volume that limits the authorized area. It is defined in the part requirement. The lattice structure has to be designed within this volume.

Relative density The relative density is the ratio between the volume of material of the lattice structure and the volume of the bounding box. Equation 3.1 and figure 3.2 illustrate the relative density.

$$\text{Relative density} = \frac{\text{Lattice structure volume}}{\text{Bounding box}} \quad (3.1)$$

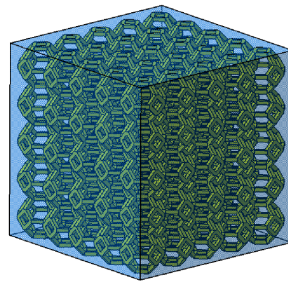


Figure 3.2: Bounding box(blue) and lattice structure (yellow)

Solid material The solid material is a volume corresponding to the bounding box of the lattice structure, filled with a dense material. The solid material has the mechanical properties of the material attributed.

Equivalent material The equivalent material is a volume corresponding to the bounding box of the lattice structure, filled with a dense material whose mechanical properties are similar to the mechanical properties of the lattice structure.

3.2 Proposed lattice structure design method

The aim of the guideline is to help designers have at their disposal the information needed to know which lattice structure configuration to use in their part designs. In chapter 2, we have concluded that large number of surfaces implied by the use of the lattice structures causes time consuming processes in CAD and CAE software. We also concluded that current CAD software are incapable of designing lattice structures easily and quickly. These factors influenced the decision in this proposed lattice structure design method to avoid altogether the need to create lattice structure CAD models based on volumes and surfaces and to do FEA on these elements.

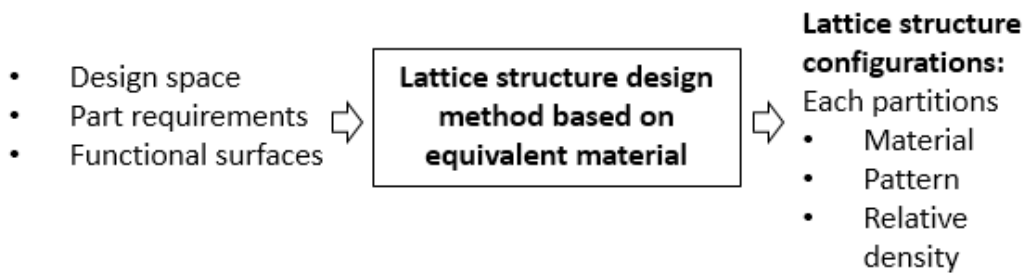


Figure 3.3: Lattice structure design method based on the use of equivalent material

Figure 3.3 shows an overview of this chapter. The input for the lattice structure design method is the design space, part requirements and functional surfaces. The design method is based on the use of equivalent material to choose the most suitable lattice structure which fulfils the parts requirements within the design space and respects the functional surfaces. With the use of equivalent material, the outcome of the design method are the choice of partitions and the material, pattern and relative density of each partition.

3.2.1 Concept to link lattice structure, solid material and equivalent material

The proposed idea in this new lattice structure design strategy is to replace and represent the lattice structure CAD model with an equivalent material. It is solid and does not contain any struts, thus has few surfaces only. With this lattice structure equivalent material, it will make it easier and quicker to conduct finite-element-analysis (FEA) due to the small number of surfaces involved. The main idea of the proposed method is to define the link between

a lattice structure, solid material and equivalent material. Two concepts are used to link the mechanical properties of a lattice structure and an equivalent material: the relative Young's modulus and the relative strength. The relative Young's modulus will be used to evaluate the strain of the lattice structure. The relative strength will evaluate the equivalent tensile stress (in our case Von Mises stress) of the lattice structure.

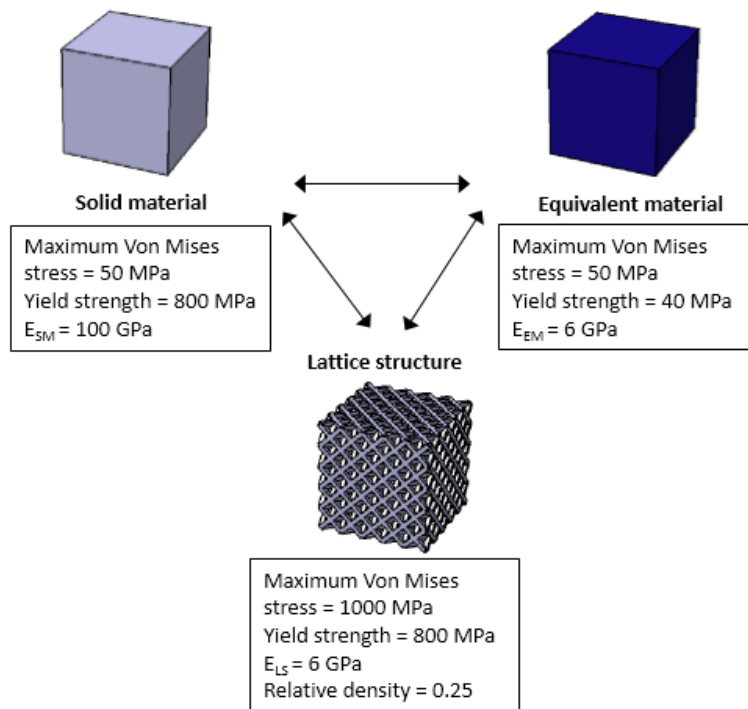


Figure 3.4: The relation between lattice structure, solid material and equivalent material

Figure 3.4 shows an example of the concept presented. Imagine a cubic design space that supports a defined mechanical loading. Let us suppose a solid material filling this space, consisting of a given material which the Young's modulus is 100 GPa and the yield strength is 800 MPa. Submitted to a defined mechanical loading, this solid material will have for example a maximum Von Mises stress of 50 MPa. This solid material will therefore be over dimensionned for the envisaged mechanical loading. If this solid material is replaced by a lattice structure with a relative density of 0.25, made of the same material as the solid material, the yield strength will be unchanged (800 MPa) but the equivalent Young's modulus of the lattice structure will be much lower (6 GPa). Subjected to the defined mechanical loading, the

maximum Von Mises stress in the lattice structure will be much higher (500 MPa). The equivalent material is a dense material which properties enables to easily predict the mechanical characteristic of the lattice structure. In our case, the equivalent material will have a Young's modulus equal to the equivalent Young's modulus of the lattice structure (6 GPa). It will also be necessary to attribute to the equivalent material a yield strength lower than the solid material to simulate the difference of strength between the solid material and the lattice structure. In this case, a yield strength of 40 MPa. The FEA conducted on the equivalent material will make it possible to quickly choose a suitable lattice structure.

To determine the corresponding characteristics of the equivalent material for different lattice structures and different materials, it is necessary to establish, for each type of lattice structure, a relation between the relative density of the lattice structure and the relative Young's modulus, and the relation between the relative density and the relative strength.

In the example presented in figure 3.4, the relative Young's modulus of the lattice structure is equal to 0.06 (6 GPa/100 GPa) and the relative strength is equal to 0.05 (50 MPa/1000 MPa). These two parameters make it possible to determine the equivalent material whose Young's modulus will be equal to $0.06 \times 100 \text{ GPa} = 6 \text{ GPa}$ and the yield strength will be equal to $0.05 \times 800 \text{ MPa} = 40 \text{ MPa}$. The proposed method does not consider any stress concentration. Section 3.3.3 of this chapter will analyse this hypothesis.

So we define the relative Young's modulus as the ratio between the Young's modulus of the lattice structure and the Young's modulus of the solid material. The Young's modulus of the equivalent material is the same as the Young's modulus of the lattice structure. For a given load, the relative strength is the ratio between the Von Mises stress of the solid material and the Von Mises stress of the lattice structure. Consequently, the relative strength is also the ratio between the yield strength of the equivalent material and the yield strength of the solid material. Equations 3.2 , 3.3 and 3.4 summarize these relations.

$$\text{Relative Young's modulus} = \frac{\text{Lattice structure Young's modulus}}{\text{Solid material Young's modulus}} \quad (3.2)$$

$$\text{Relative stress} = \frac{\text{Solid material Von Mises stress}}{\text{Lattice structure Von Mises stress}} \quad (3.3)$$

$$\text{Relative strength} = \frac{\text{Equivalent material yield strength}}{\text{Solid material yield strength}} \quad (3.4)$$

We also know that :

$$\text{Lattice structure Young's modulus} = \text{Equivalent material Young's modulus} \quad (3.5)$$

$$\text{Solid material yield strength} = \text{Lattice structure yield strength} \quad (3.6)$$

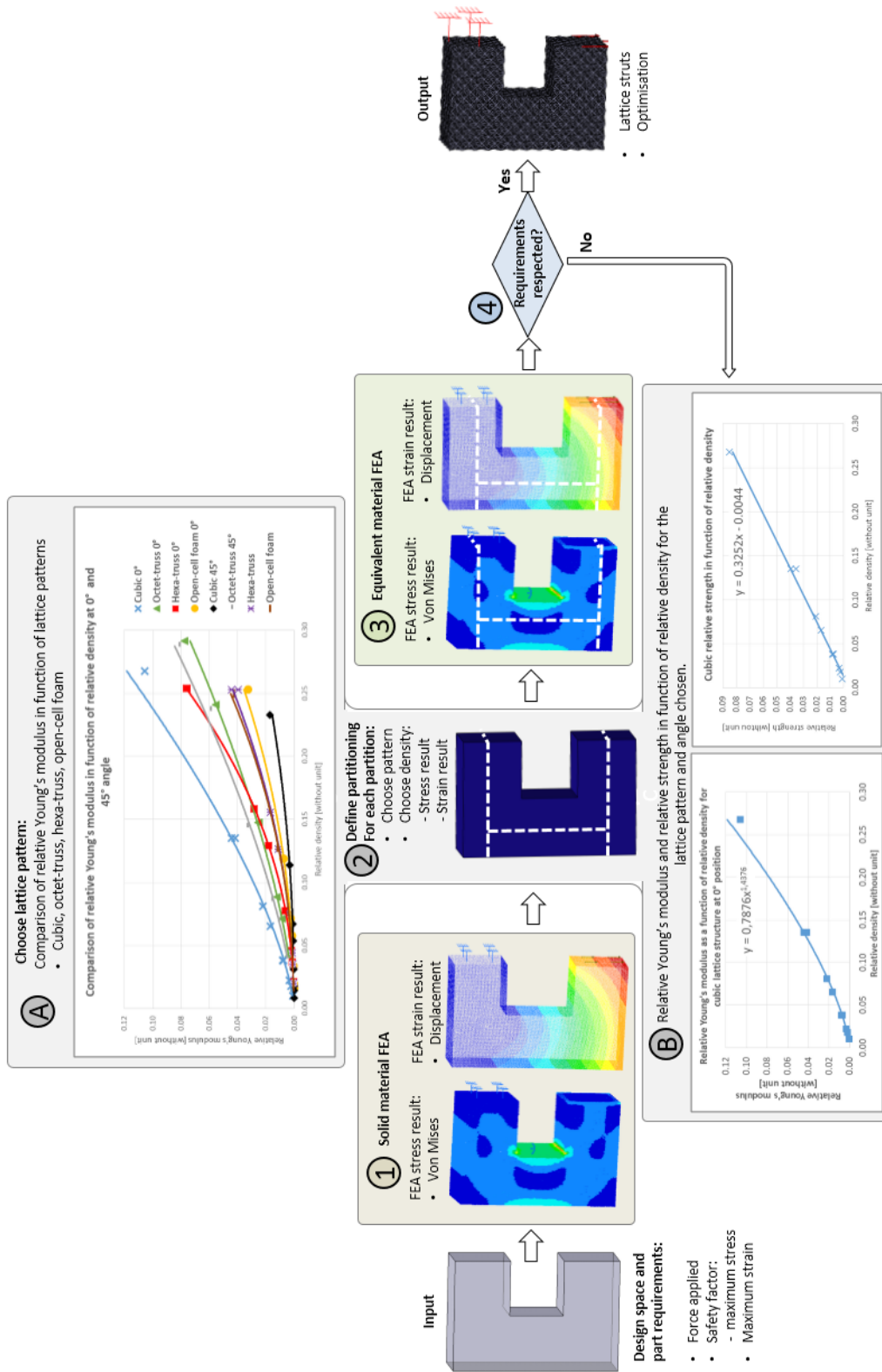


Figure 3.5: Step-by-step of the new design method to design lattice structures

3.2.2 Step-by-step of the proposed method

Figure 3.5 summarizes the different steps of the proposed method.

Input The input of the method are the design space and the part requirements, which in our case are the force applied, the safety factor, and the maximum strain. Safety factor is a term describing the load carrying capacity of a system beyond the expected or actual loads. This allows for emergency situations, unexpected loads or misuse. The safety factor used in this work is defined as:

$$\text{Safety factor} = \frac{\text{Maximum stress allowed}}{\text{Maximum stress applied}} \quad (3.7)$$

Step 1 In the first step, the designer creates a 3D CAD model with a solid material within the design space. Then the boundary conditions of the part are added and a FEA simulation is executed. The Von Mises stress distribution and the displacement distribution are the indicators to help choose the most suitable lattice structure pattern and relative density in step two.

Step 2 In the second step, the partitions have to be defined. The partitions are separations of the part into different zones. They are defined based on the displacement distribution and Von Mises stress distribution obtained from the step one results. Each partition can have different relative densities.

After the partitions are defined, the next stage consists of two parts: first to choose the most suitable lattice structure pattern for each partition, then to choose the relative density which fulfil the part's requirements for each partition.

To choose the most suitable lattice structure pattern and angle load, it is necessary to estimate the relative Young's modulus of each partition. This relative Young's modulus can be obtained by dividing the maximum displacement calculated in step one for a partition by the maximum strain defined in the requirements. Then, using the comparison of relative Young's modulus in function of different lattice structure pattern, a choice can be made (see figure 3.5 step 2 figure A).

Based on the maximum displacement and the maximum Von Mises stress of the FEA result in step one for each pattern, the relative density can be determined. It depends on the relative Young's modulus and the relative

strength of the partition. The relative strength of the partition can be obtained dividing the maximum Von Mises stress calculated in step one for a partition by the yield strength of the material divided by the safety factor defined in the requirements. The relative Young's modulus and the relative strength give two relative densities using the figure 3.5 (step 2 figure B). The relative density which fulfils both the relative Young's modulus and relative strength is chosen. Those parameters define the equivalent material used in step 3.

Step 3 In step three, a FEA is executed with the equivalent material defined in step two. For each partition, the maximum displacement and maximum Von Mises stress are determined. The displacement distribution and the Von Mises stress distribution are also obtained.

Step 4 From the FEA results obtained in step three, the maximum displacements and maximum Von Mises stress are verified in each partition to see if they comply with the parts requirements. To analyse the Von Mises stress distribution and to compare the values to the requirements, two ways are possible. Divide the values of every Von Mises stresses by the relative strength and compare them to the yield strength of the solid material, or compare every Von Mises stresses to the yield strength of the equivalent material.

If the verification in the partition does not comply with the requirements, then the partition is refined and improved. Steps two and three are repeated. This loop is repeated to optimize and verify the most suitable density in each partition.

Output The output from the design strategy aim to create a lattice structure CAD model based on the material, partitions, pattern and densities chosen. The following step is optimisation of the lattice struts to avoid stress concentrations, which will be for future works.

3.2.3 Application example of the proposed lattice structure design method

In this section, we present an example of the application of the proposed lattice structure design method. The example is conducted on a 'C' shaped part. This example is presented step-by-step according to the method presented in section 3.2.2.

Input A design space of a 'C' shaped form is given. The part's requirements are:

- Load = 10 000 N (See figure 3.7 for the load and boundary conditions)
- Maximum displacement = 6 mm
- Safety factor = 1.5
- Material : Ti-6Al-4V
- Design space : See figure 3.6

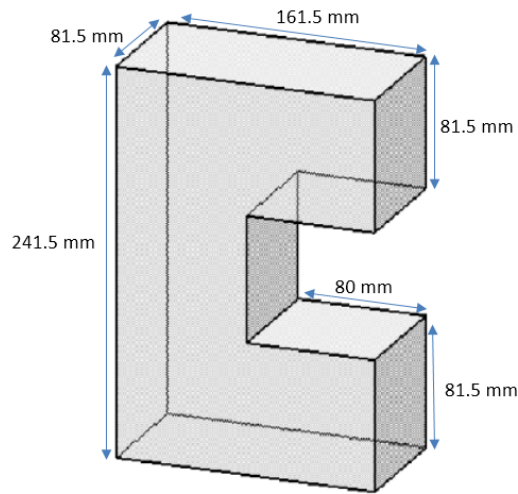


Figure 3.6: Design space

Step 1 The first step is to fill the design space with a solid material. Ti-6Al-4V is attributed as the material. Figure 3.7 shows the solid material and boundary conditions.

Here, we execute a FEA on the solid material and observe the displacements and Von Mises stress. Figure 3.8 shows the displacements and Von Mises stresses results of the FEA. The displacement and Von Mises stress results will be indicators to help choose the most suitable lattice structure pattern and relative density in step 2.

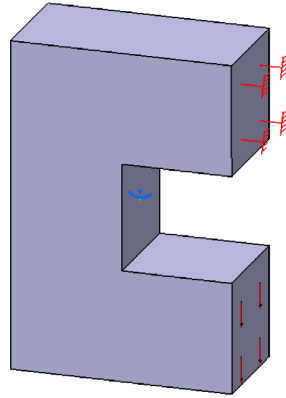


Figure 3.7: Solid material and boundary conditions

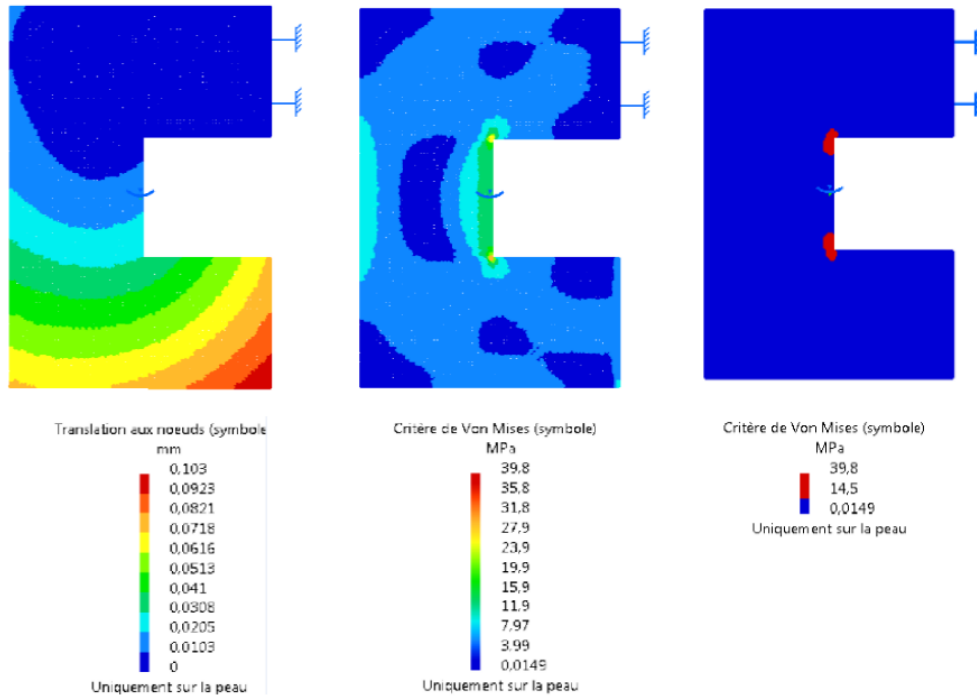


Figure 3.8: Displacements and Von Mises stress results of the FEA

Concerning the determination of the maximum Von Mises stress, the stress concentration due to the sharp edges are deducted from the value obtained from the FEA. Figure 3.8 gives the threshold value of the Von Mises stress after the deduction of the stress concentrations. The results

obtained from this FEA simulation are:

- Maximum displacement = 0.102 mm
- Maximum Von Mises stress = 14.5 MPa

Step 2 In the second step of this proposed lattice structure design method, first we define the partitions, then we choose the lattice structure pattern and its relative density. In this example, we decide to define a unique partition and to choose the same relative density through out the whole structure. The choice of the lattice structure pattern and relative density depends on the mechanical property of the lattice structure pattern (stretching or bending-dominated), its relative Young's modulus and relative strength. To choose the most suitable lattice structure pattern and angle load, it is necessary to estimate the relative Young's modulus of the partition. This relative Young's modulus can be obtained dividing the maximum displacement calculated in step one (0.102 mm) by the maximum strain defined in the requirements (6 mm). Then, using the comparison of relative young's modulus in function of different lattice structure pattern, a choice can be made (see figure 3.9). In that example, the relative Young's modulus is calculated with the equation 3.8.

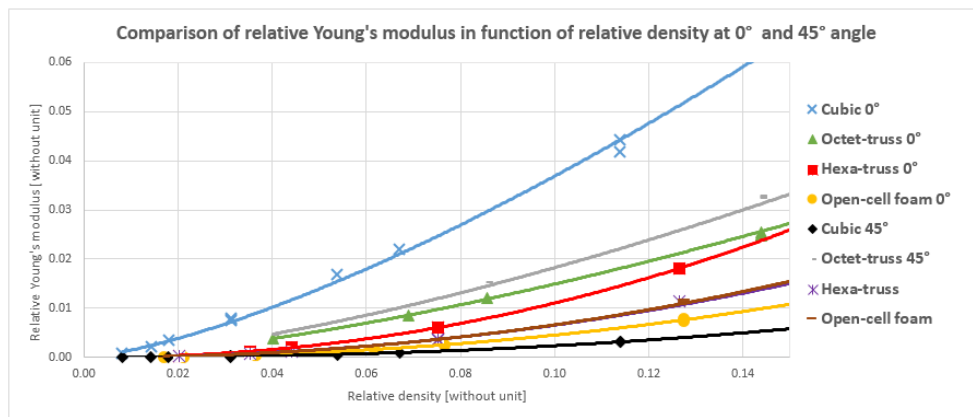


Figure 3.9: Relative Young's modulus in function of relative density

Based on figure 3.9, the octet-truss lattice structure at 0° position angle suits this case since it is stretching-dominated and considered isotropic in all directions. The relative Young's modulus in function of relative density for the octet-truss lattice structure at 0° position angle give the minimum relative density of the lattice structure.

$$\frac{\text{Maximum displacement calculated}}{\text{Maximum displacement allowed}} = \frac{0.102 \text{ mm}}{6 \text{ mm}} = 0.017 \quad (3.8)$$

From the relative Young's modulus in function of relative density graph in figure 3.10 at 0.017 relative Young's modulus, we obtain the corresponding relative density, which is 0.11.

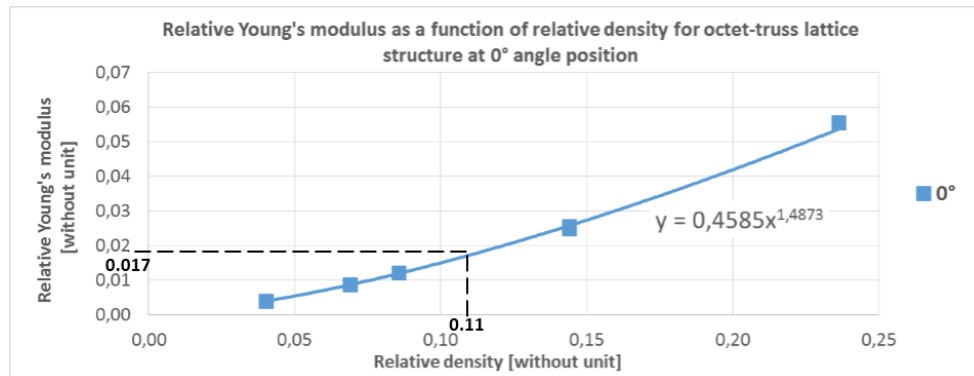


Figure 3.10: Relative Young's modulus in function of relative density for octet-truss lattice structure at 0° angle position

The maximum Von Mises stress result obtained in step 1 is 14.5 MPa. Equation 3.9 gives the maximum Von Mises stress considering the safety factor.

$$\text{Maximum Von Mises stress} \times \text{Safety factor} = 14.5 \text{ MPa} \times 1.5 = 21.75 \text{ MPa} \quad (3.9)$$

We obtain the following result :

$$\frac{\text{Maximum Von stress}}{\text{Solid material yield strength}} \times (\text{safety factor}) = \frac{21.75 \text{ MPa}}{910 \text{ MPa}} = 0.024 \quad (3.10)$$

From the relative strength in function of relative density graph in figure 3.11 at 0.024 relative strength, we obtain the corresponding relative density, which is 0.13.

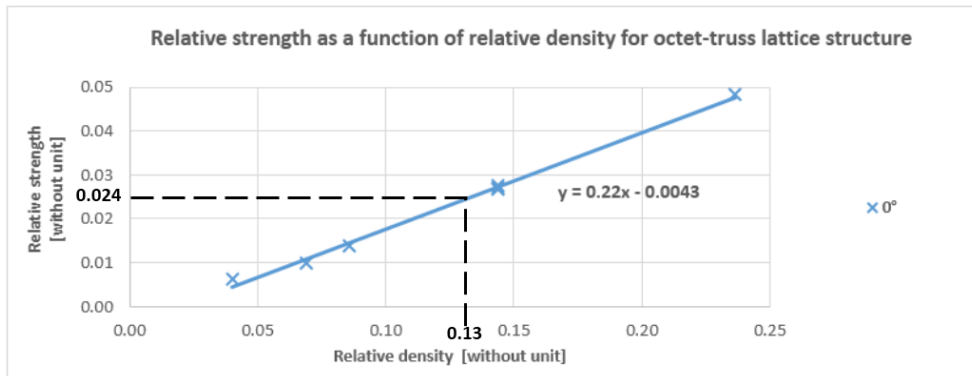


Figure 3.11: Relative strength in function of relative density for octet-truss lattice structure at 0° angle position

From both figures 3.10 and 3.11, the next step is to choose the highest relative density between the two. Therefore, in this example, the chosen relative density is 13%. Then, the equivalent material chosen is characterized by a relative strength of 0.024 and a relative Young's modulus of 0.022. The yield strength of the equivalent material is obtained by equation 3.4: $910 \text{ MPa} \times 0.024 = 21.84 \text{ MPa}$.

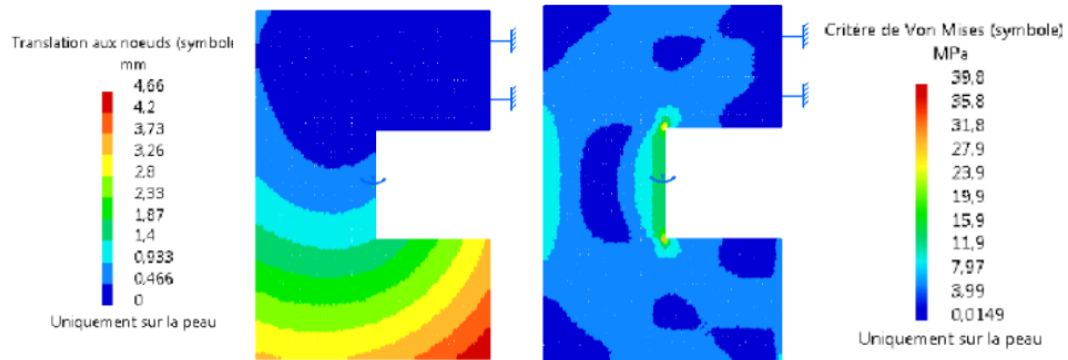


Figure 3.12: FEA on equivalent material with relative density at 13%

Step 3 In step three, a FEA is executed with the equivalent material chosen in step two. The maximum displacement and Von Mises stress are determined. The displacement distribution and the Von Mises stress distribution are also obtained. Figure 3.12 shows the result of FEA on the equivalent

material in terms of displacement and Von Mises stress. The FEA results with the equivalent material are:

- Maximum displacement = 4.7 mm

Step 4 The maximum displacement and maximum Von Mises stress obtained in step three are compared with the requirements of the part to validate the choice taken. If the displacement and Von Mises stress respect the maximum displacement and yield strength of the equivalent material allowed, the part is then validated. We compare the FEA values with the parts requirements :

- Maximum displacement (4.7 mm) lower than the maximum displacement allowed (6 mm)
- Maximum Von Mises stress multiplied by the safety factor ($14.5 \text{ MPa} \times 1.5 = 21.75 \text{ MPa}$) lower than equivalent material yield strength (21.84 MPa)

Both of these values are lower than the values allowed in the parts requirements. Therefore the lattice part is validated.

Output A lattice structure CAD model with the pattern and relative density chosen is created. Figure 3.13 shows the lattice structure CAD model created.

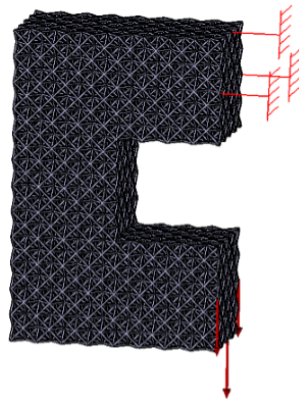


Figure 3.13: Lattice structure CAD model

3.3 A methodology for the creation of equivalent lattice structure materials

From the proposed lattice structure design method, research was needed to develop an equivalent material. In this section, we present the methodology to create the equivalent material and the FEA simulations conducted. The different variables, lattice patterns and simulations are described and the results are analysed.

From (Ashby, 2006), we know that the mechanical properties of a lattice structure depends on three factors, its material, lattice pattern and density. These three factors influence the displacement and Von Mises stress of a lattice structure. Thus, by executing FEA simulation on various lattice structure patterns and relative densities, we are able to determine the link between these configurations and their displacement and Von Mises stress. This knowledge helps us to know the mechanical properties of the lattice structure and enables the creation of equivalent materials.

As we explained in section 3.1, the proposed lattice structure design method needs knowledge on equivalent material. The creation of equivalent materials replaces the need to conduct FEA on lattice structures and reduces FEA time. Therefore, in this section, we propose a methodology to create these equivalent materials. The proposed methodology consists of executing FEA simulations for compression and shear tests on lattice structures to investigate the variation of relative Young's modulus, relative shear modulus and relative strength with different relative densities and patterns.

3.3.1 FEA simulation and variables

To obtain the relative Young's modulus, the relative shear modulus and relative strength, the FEA simulation was conducted in two different ways, a compression and shear loading test, as shown in figure 3.14.

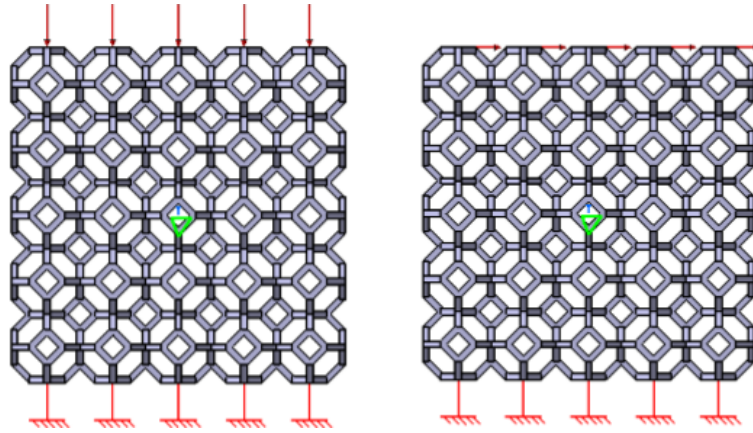


Figure 3.14: Compression and shear test on a hexa-truss lattice structure

Before conducting the simulations, the variables must first be determined. The variables depend on the objectives fixed. Thus the variables of the simulations are the lattice structure patterns, relative densities and the lattice structure position angle. The position angle is based on the angle of the lattice structure to the angle of the force applied.

Lattice structure pattern The first variable chosen is the lattice structure pattern. Four lattice structure pattern have been chosen, octet-truss lattice structure, cubic lattice structure, hexa-truss lattice structure and open-cell foam lattice structure. Figure 3.15 illustrates an example of each lattice structure pattern with a dimension of $5 \times 5 \times 5$ elementary units oriented at a 0° angle. Figure 3.16 shows each elementary unit of the lattice structure pattern. All the simulations were conducted on lattice structures with square strut sections.

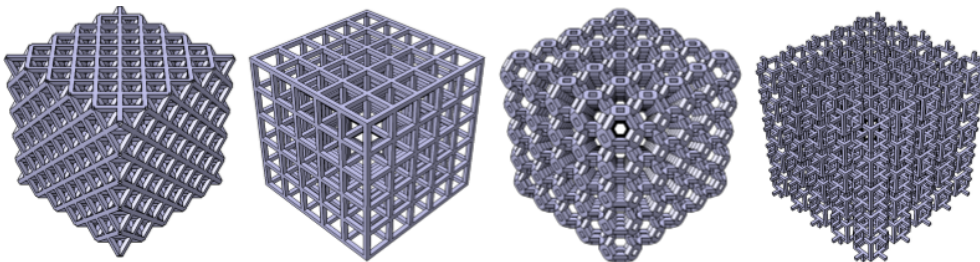


Figure 3.15: Isometric view of $5 \times 5 \times 5$ elementary units. From left to right : octet-truss, cubic, hexa-truss and open-cell lattice structure

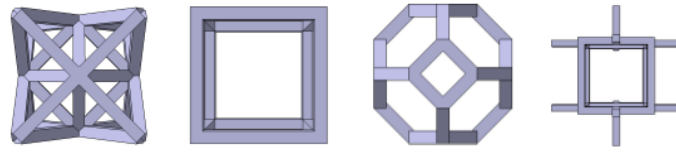


Figure 3.16: Side view of each elementary unit. From left to right : octet-truss, cubic, hexa-truss and open-cell elementary unit

Lattice structure position angle These lattice structures were tested in two different positional orientations relative to the loads applied to determine the mechanical properties in different directions. The angle of the force applied on the part replicates different lattice structure patterns. For example a cubic lattice structure becomes two different patterns if the force is applied at a 0° angle or a 45° angle. Therefore it is important to test the structures with stress from different angles. Figure 3.17 is an example of a cubic lattice structures which is oriented at 0° and 45° angles.

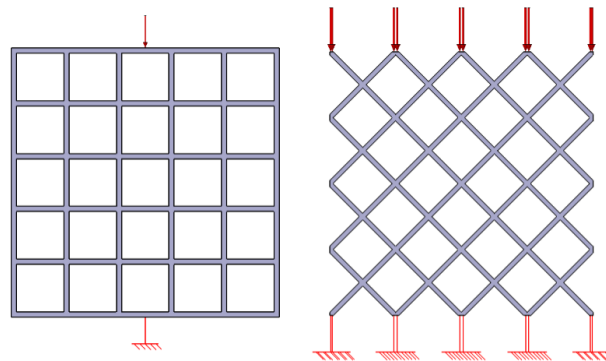


Figure 3.17: Cubic lattice structure at 0° and 45° angle

Lattice structure relative density The thickness of the square strut section and length dimensions of the struts are varied to obtain different lattice structure densities.

$$\text{Relative density} = \frac{\text{Lattice structure volume}}{\text{Lattice structure bounding box}} \quad (3.11)$$

The lengths of the elementary structures are 5 mm, 10 mm, 15 mm and 20 mm and the thickness of the square strut sections are 1 mm, 1.5 mm and 2 mm. Figure 3.18 shows an example of various relative densities for an

open-cell foam lattice structure. In this example, as the thickness is increased from 1 to 2 mm, the relative density of the open-cell foam lattice structure with a 5 mm elementary structure length increases from 11.9% to 36.9%.

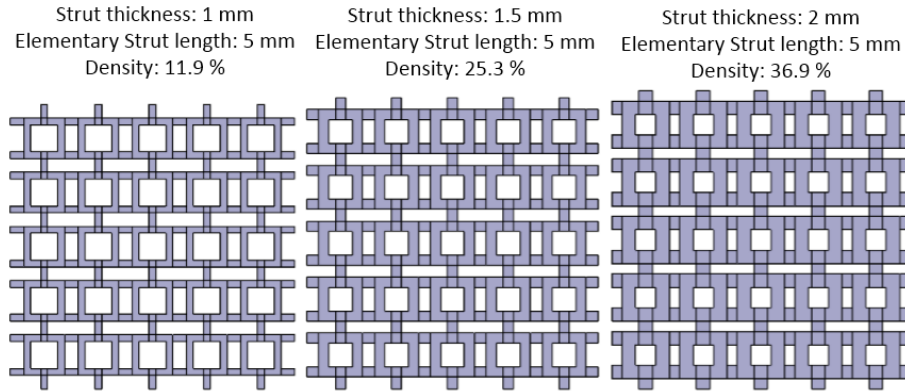


Figure 3.18: Side view of open-cell foam lattice structures with 11.9%, 25.3% and 36.9% relative densities

A lattice structure which has the same relative density can also have different thickness and different length of the struts, as shown in figure 3.19. In this example of an octet-truss lattice structure, the struts thickness varies from 1 mm to 2 mm, while its elementary structure length varies from 10 mm to 20 mm to obtain the same relative density of 14.8%.

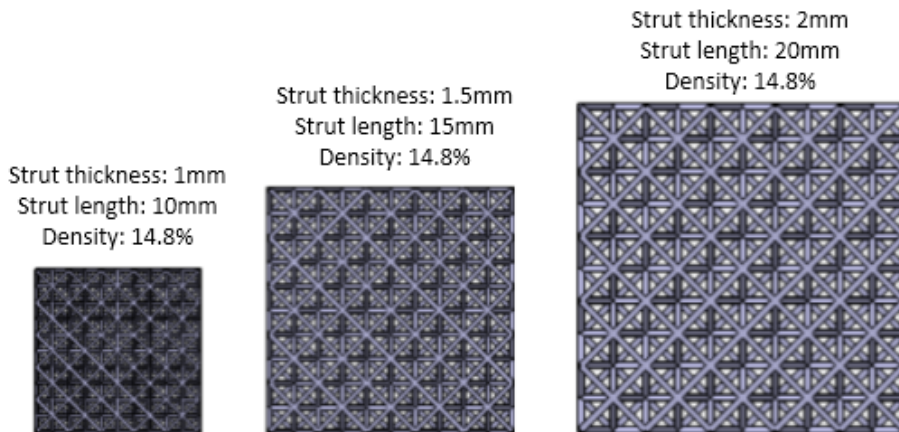


Figure 3.19: $5 \times 5 \times 5$ unit octet-truss lattice structures with different length and sections of struts but same densities

Manufacturing constraints and relative density range of validity

The relative density considered depends on the manufacturability constraint and the range of validity. For example, after the manufacturing process with the EBM machine, un-melted metallic powder have to be blown away to obtain the lattice structure. However, not all un-melted metallic powder can be blown away. For example, in cases where high density lattice structures are manufactured, it prevents the un-melted powder to be removed from the structures. That's why we focused in this experiment the relative density range to 25% (Suard, 2015). Figure 3.20 shows examples of two hexa-truss lattice structures which are not taken into account in the experiment because of its high density. At relative densities higher than 80%, the lattice structure can no longer be thought of as a lattice structure, but becomes a solid containing a distribution of small spherical holes.

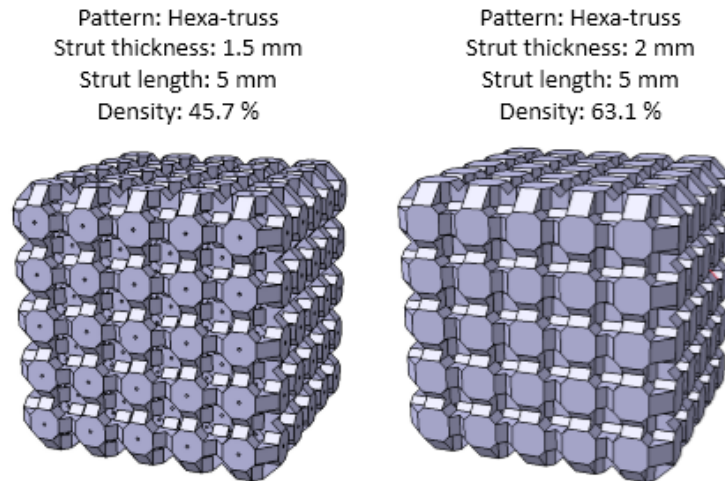


Figure 3.20: High density hexa-truss lattice structure

Lattice structure material In order to be universal for all types of materials, the results are explained in relative units. Therefore the results are independent of the materials used. Examples of the relative units involved are relative Young's modulus, relative shear modulus, relative Von Mises stress and relative density. Hence, it is sufficient to conduct the simulations with a single type of material. In this work, the material chosen in Ti-6Al-4V.

Summary of the experiment variables A total of 96 lattice structure CAD model were created with each of the variables chosen. Here is a summary of the variables chosen:

- Lattice structure pattern:
 - Cubic
 - Octet-truss
 - Hexa-truss
 - Open-cell foam
- Struts thickness (mm):
 - 1
 - 1.5
 - 2
- Elementary structure length (mm):
 - 5
 - 10
 - 15
 - 20
- Lattice angle position:
 - 0°
 - 45°

3.3.2 Simulation execution

In this section, we explain the execution of the simulation. The software chosen to do this simulation is CATIA V5. Each lattice CAD model was designed and imported in the generative structural analysis function in CATIA V5 to conduct finite-element-analysis. All the structures were of the same number of elementary units ($5 \times 5 \times 5$ units). The relative density of the parts were obtained by measuring the volume of the lattice structure, divided by its bounding box volume. For each simulation, the same value of force was applied (500 N). The mesh size has to be at least three times smaller than the thickness of the strut. A total of 192 FEA simulations were conducted with each variable for the compression and shear tests. Even though it would have been a faster simulation to conduct FEA beams instead of volumes, FEA beams has a limited range of application and is only valid for relative densities of up to 5% (Suard, 2015). FEA with volume is more precise than a beam simulation since it does not rely of beam assumptions (Suard, 2015). After executing the FEA, the results are then measured. The Von Mises stresses and displacements results were exported for each finite-element-analysis, consisting of each point coordinates' displacements and Von Mises stresses. Here is the step-by-step method to conduct the FEA and to obtain and analyse the data :

1. Define the boundary conditions
2. Define the mesh size
3. Execute the FEA simulation
4. Get the structure's displacement and Von Mises stress and export the result data for each element.
5. Calculate the Young's modulus of the structure by dividing the stress applied on the part by its strain (equation 3.14).

$$\text{Stress applied} = \frac{\text{Load applied}}{\text{Lattice structure envelope surface}} \quad (3.12)$$

$$\text{Strain} = \frac{\text{Displacement along direction of the force}}{\text{Initial length}} \quad (3.13)$$

$$\text{Lattice structure Young's modulus} = \frac{\text{Stress applied}}{\text{Strain}} \quad (3.14)$$

6. Divide the lattice structure's Young modulus by the Young's modulus of the material (Ti-6Al-4V in our case: 114GPa) to obtain the relative Young's modulus of the lattice structure (equation 3.15).

$$\text{Relative Young's modulus} = \frac{\text{Lattice structure Young's modulus}}{\text{Young's modulus of solid material}} \quad (3.15)$$

7. Eradicate the stress concentration results to get the realistic maximum Von Mises stress, which is at 99.5% instead of its maximum value. Section 3.3.3 explains this step in detail.
8. Calculate the relative strength by dividing stress applied on the structure with the Von Mises stress at 99.5% (equation 3.16).

$$\text{Relative strength} = \frac{\text{Stress applied}}{\text{Von Mises stress at 99.5\%}} \quad (3.16)$$

9. The results obtained are, relative Young's modulus, relative shear modulus and relative strength in function of the relative density.

3.3.3 Stress concentration

A stress concentration is an area of the mesh where the stress raises above the applied nominal stress. Since the section of the struts are square, this creates sharp 90° edges in the struts of the structure, therefore creating very small surface area and resulting in very high concentration of stress. Thus, the maximum Von Mises stress result can not be taken directly from the FEA data. Hence, to obtain a usable Von Mises stress result, a method

was made to eradicate the stress concentration results. In this method, a graph with the cumulative number of elements of the FEA mesh in function of the Von Mises stress value is made. For example, from the graph in figure 3.21, we can see that the Von Mises stress concentration exists for 0.5% of the FEA mesh elements. These are the areas of the sharp edges of the lattice struts, contributing very high Von Mises value for very little number of elements. Therefore, the result of the Von Mises stress of each FEA taken is the asymptote at 99.5% of the cumulative number of mesh elements. Figures 3.21, 3.22, 3.23 and 3.24 show the stress concentration for octet-truss, cubic, hexa-truss and open-cell foam lattice structures respectively and the Von Mises stress results.

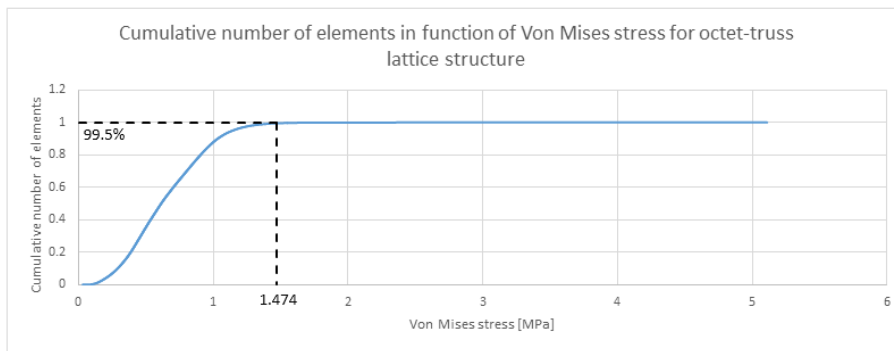


Figure 3.21: Stress concentration in sharp edges of an octet-truss lattice structure

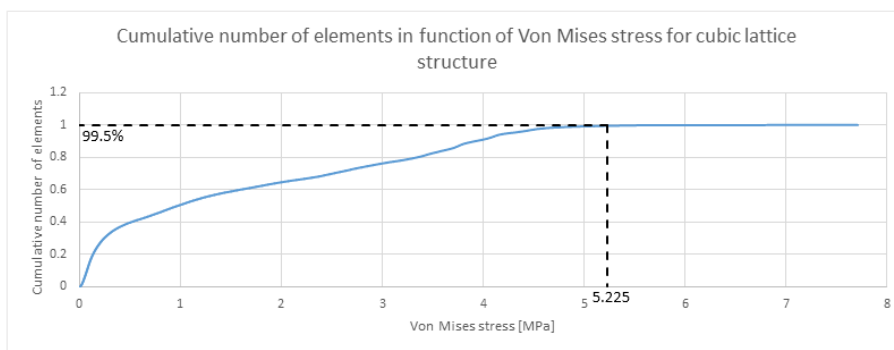


Figure 3.22: Stress concentration in sharp edges of an cubic lattice structure

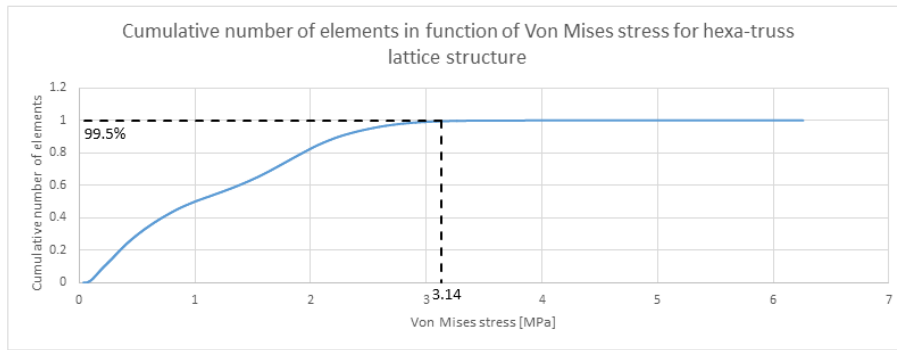


Figure 3.23: Stress concentration in sharp edges of an hexa-truss lattice structure

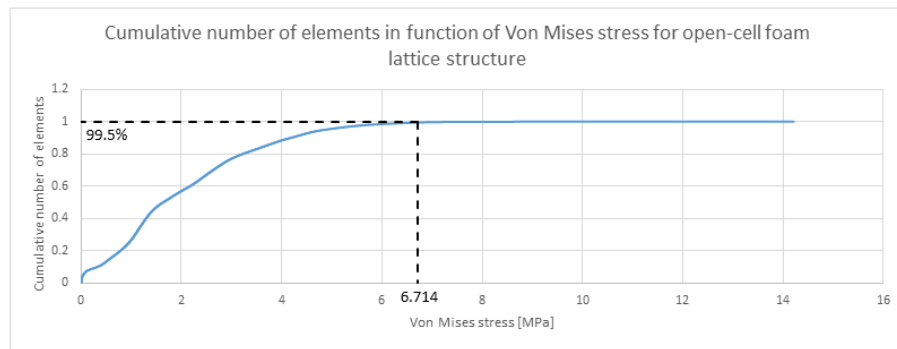


Figure 3.24: Stress concentration in sharp edges of an open-cell foam lattice structure

The research in this PhD limits to FEA of the elements unaffected by the stress concentration. The following procedures of adding rounded edges (see figure 4.8) and optimizing lattice struts in stress concentrated areas are not treated in this thesis. It will be a perspective of the research and for future works.

3.3.4 Results

In this section, results obtained are presented for each lattice structure. All the detailed results are presented in appendix A.

Octet-truss lattice structure Figure 3.25 and figure 3.26 show the relative Young's modulus and the relative shear modulus in function of relative

density for the octet-truss lattice structure. The octet truss lattice structure has approximately the same relative Young's modulus in the 0° and 45° directions. The octet truss lattice structure has the same relative shear modulus in the 0° and 45° directions.

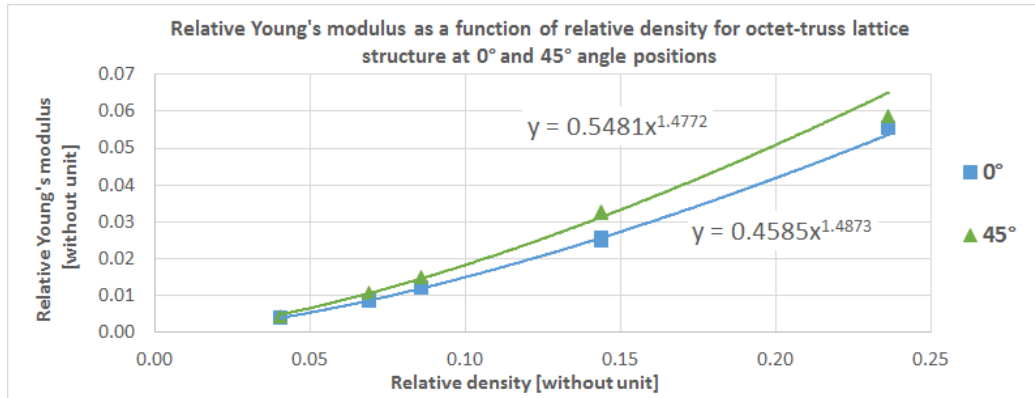


Figure 3.25: Octet-truss lattice structure compression test at 0° and 45° angle

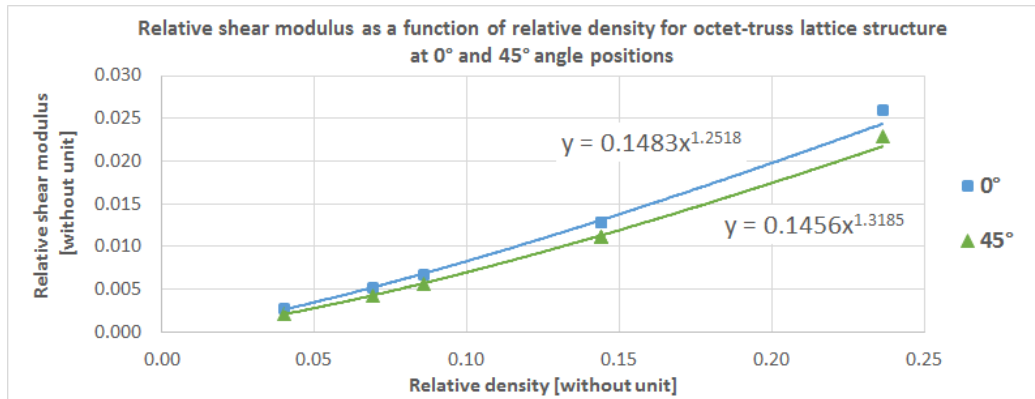


Figure 3.26: Octet-truss lattice structure shear test at 0° and 45° angle

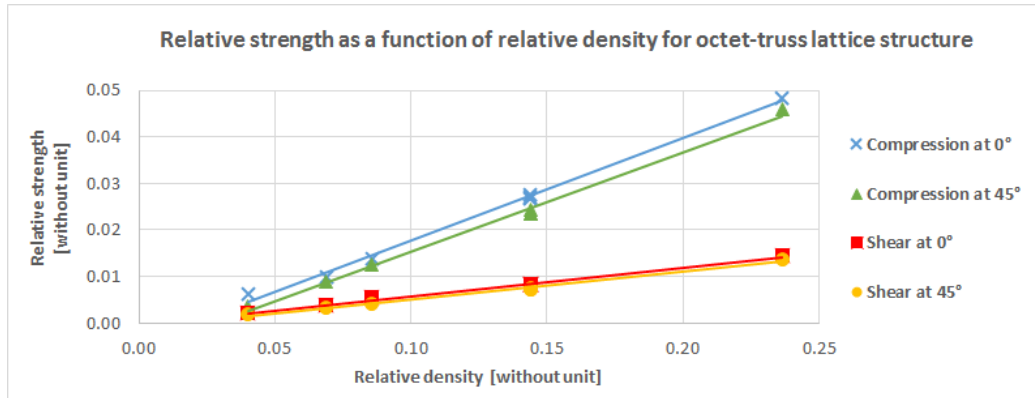


Figure 3.27: Relative strength in function of relative density for octet-truss lattice structure at 0° and 45° angle

Figure 3.27 shows the relative strength in function of the relative density of the octet-truss lattice structure. For the application of the lattice structure design method presented in 3.2.2, the relative strength from the compression test is used to define the equivalent material.

Cubic lattice structure Figures 3.28 and 3.29 show the relative Young’s modulus and the relative shear modulus in function of relative density for the cubic lattice structure. The cubic lattice structure’s relative Young’s modulus is significantly higher in the 0° direction compared to the 45° direction. The cubic lattice structure has the same relative shear modulus in 0° and 45° directions.

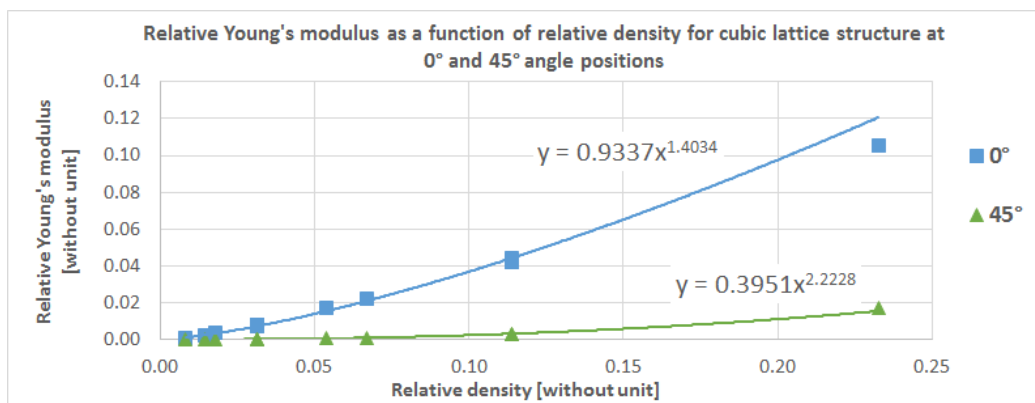


Figure 3.28: Cubic lattice structure compression at 0° and 45° angle

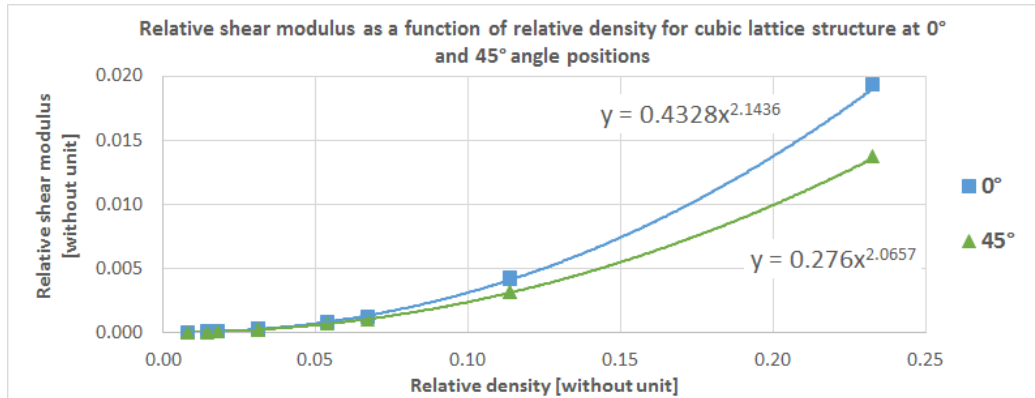


Figure 3.29: Cubic lattice structure shear test at 0° and 45° angle

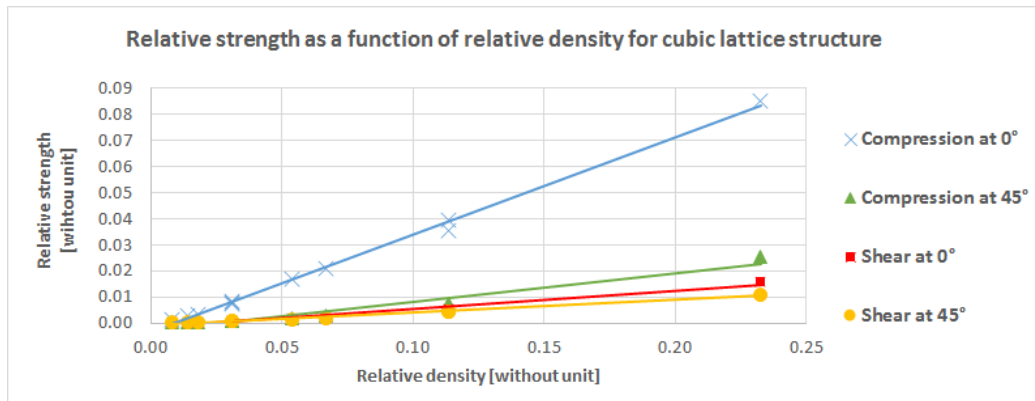


Figure 3.30: Relative strength in function of relative density for cubic lattice structure at 0° and 45° angle

Figure 3.30 shows the relative strength in function of the relative density of the cubic lattice structure for compression and shear tests at 0° and 45° position angles.

Hexa-truss lattice structure Figure 3.31 and figure 3.32 show the relative Young's modulus and the relative shear modulus in function of relative density for the hexa-truss lattice structure. The relative Young's modulus in 0° angle is higher than in the 45° angle. While the relative shear modulus is approximately the same in both 0° and 45° angle positions.

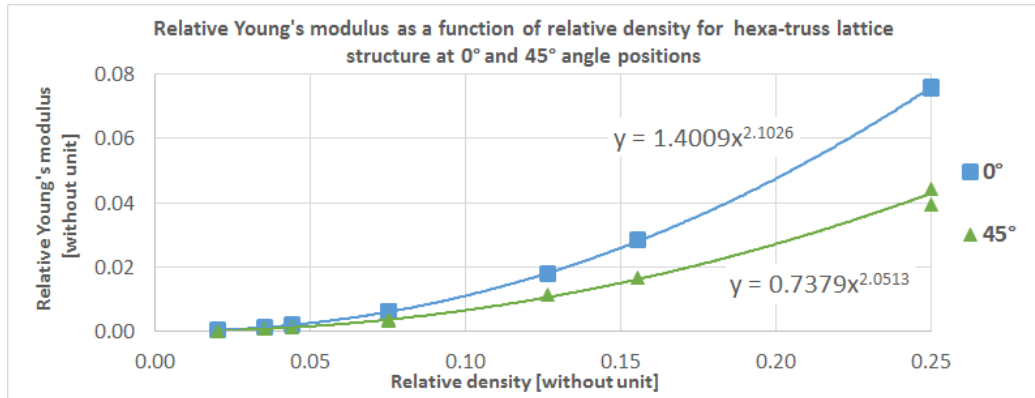


Figure 3.31: Hexa-truss lattice structure compression test at 0° and 45° angle

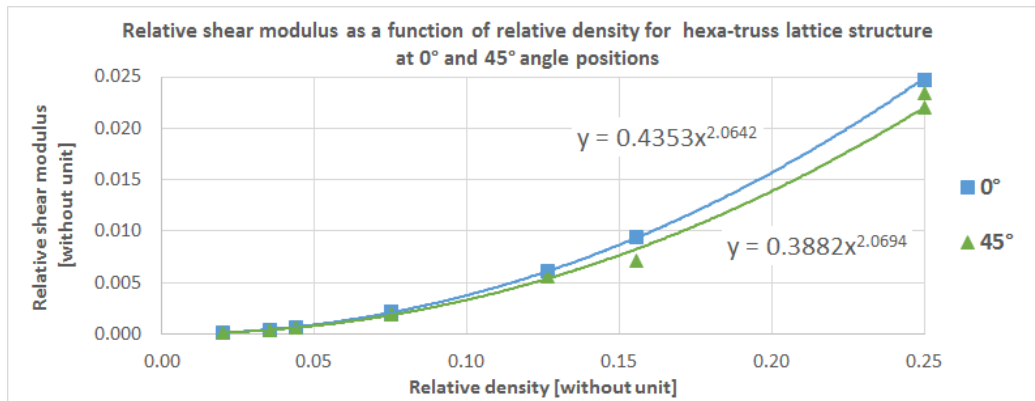


Figure 3.32: Hexa-truss lattice structure shear test at 0° and 45° angle

Figure 3.33 shows the relative strength in function of the relative density of the hexa-truss lattice structure for the compression and shear tests at 0° and 45° angle positions.

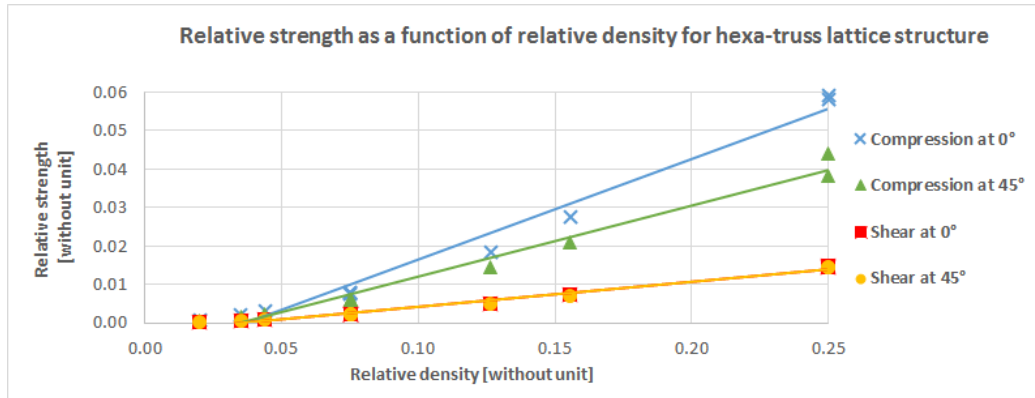


Figure 3.33: Relative strength in function of relative density for hexa-truss lattice structure at 0° and 45° angle

Open-cell foam lattice structure Figure 3.34 and figure 3.35 show that the open cell lattice structure has a higher relative Young's modulus and relative shear modulus in the 0° direction compared to 45° direction.

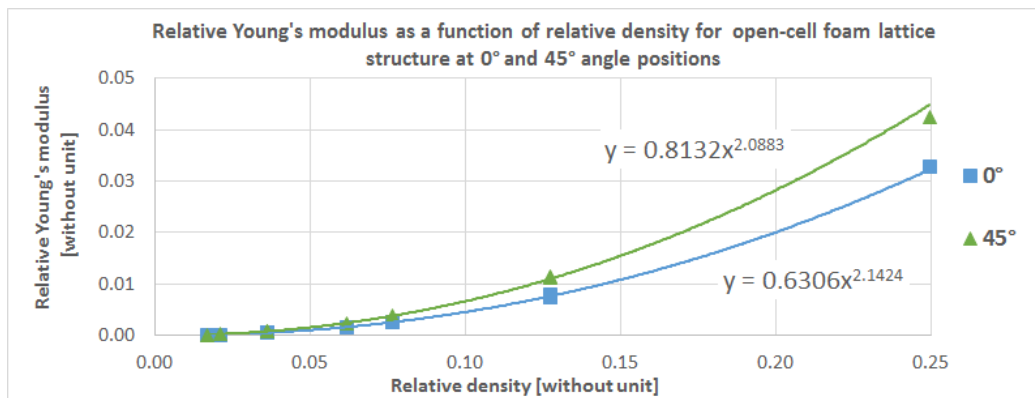


Figure 3.34: Open-cell foam lattice structure compression test at 0° and 45° angle

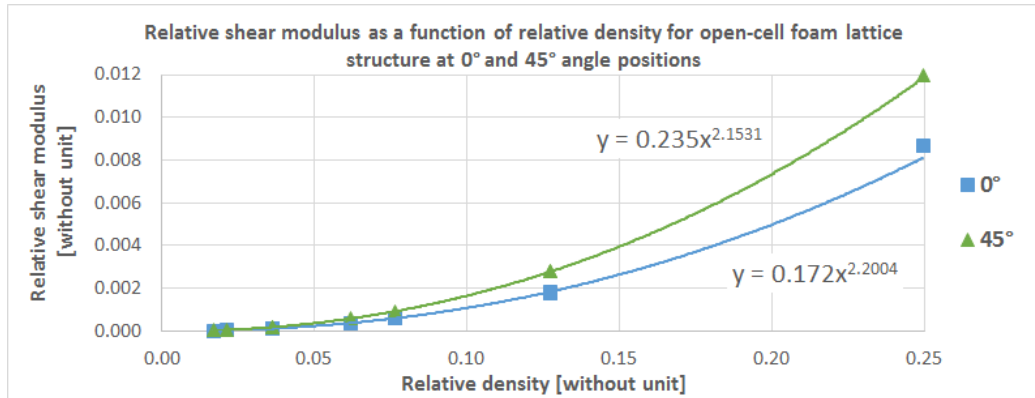


Figure 3.35: Open-cell foam lattice structure shear test at 0° and 45° angle

Figure 3.36 shows the relative strength in function of the relative density of the open-cell foam lattice structure.

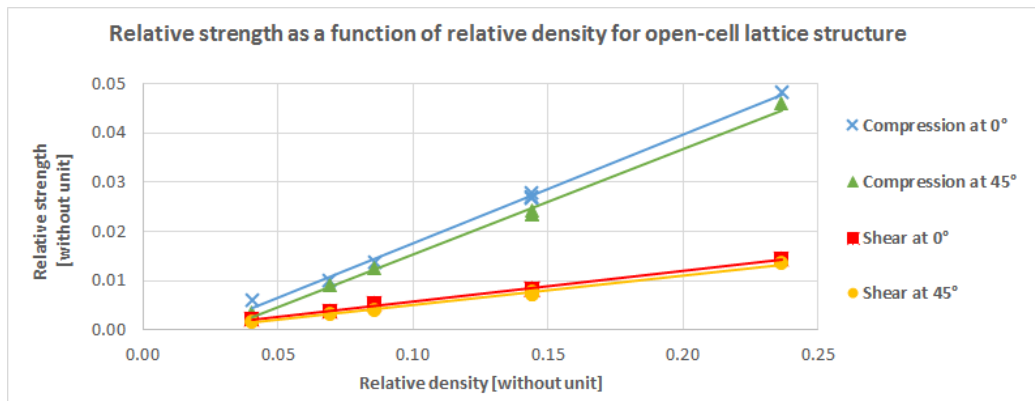


Figure 3.36: Relative strength in function of relative density for open-cell foam lattice structure at 0° and 45° angle

3.3.5 Analysis

In this section, we analyse, compare and conclude the results obtained for each lattice structure.

Influence of stretching and bending-dominated structures Figure 3.37 shows a comparison for relative Young's modulus in function of relative density at 0° angle for each lattice structure pattern. We can observe that the cubic lattice structure has the highest relative Young's modulus compared

to all other lattice structure patterns. The octet-truss and hexa-truss lattice structures have the second and third highest relative Young's modulus in function of relative density. The lowest one is the open-cell foam lattice structure. This is because of the stretching and bending-dominated characteristic of these structures. Cubic lattice structure is stretching-dominated where as the open-cell foam lattice structure is bending-dominated. The octet-truss lattice structure is stretching-dominated in both 0° and 45° angles. Octet-truss is suitable for high strength lightweight structures. Open-cell foam lattice structure is bending dominated and is suitable for energy absorption structures.

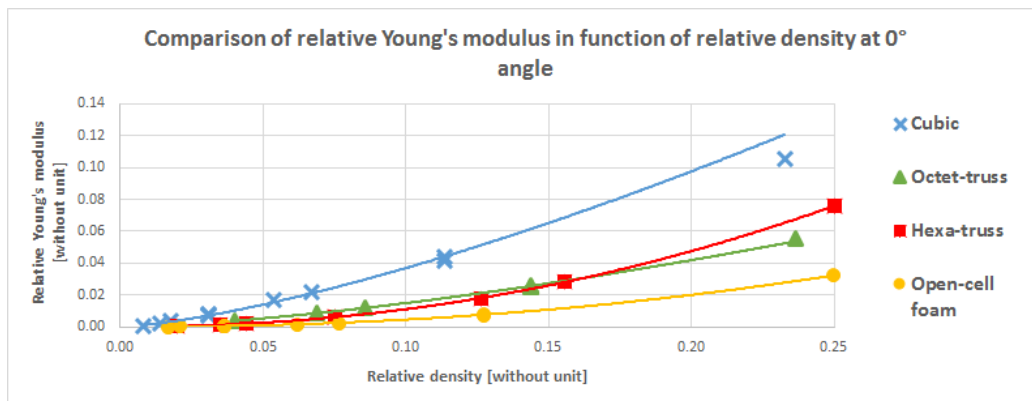


Figure 3.37: Comparison of relative Young's modulus in function of relative density at 0° angle

Influence of 0° and 45° position angles Figure 3.38 shows the relative Young's modulus in function of relative density at 45° angle. From the graph, we can analyse that the cubic lattice structure in this case has the lowest relative Young's modulus compared to the other. When positioned at a 0° angle, it has the highest relative Young's modulus compared to the rest. It is worthy here to note that the orientation of the lattice structure influences its characteristic and mechanical properties. At 0° angle, the cubic lattice structure is stretching-dominated, where as when the force is loaded at a 45° , the structure becomes bending-dominated. Where as for the octet-truss lattice structure, the relative Young's modulus is approximately the same in both 0° and 45° angle orientations. We can conclude that due to the pattern of the struts in octet-truss lattice structures, this pattern can be considered as an isotropic material. This is due to the fact that octet-truss lattice structures have struts which are oriented in both 0° and 45° angles.

Thus it is stretching-dominated in both angles. Lattice structure patterns which have struts only oriented in 0° and 90° angles can not be considered as an isotropic material. Their mechanical property changes according to the direction of the force. Figure 3.39 and figure 3.40 shows a comparison for relative shear modulus in function of relative density at 0° and 45° angles for each lattice structure pattern respectively. These findings lead us to consider lattice structures as different materials depending on their orientation.

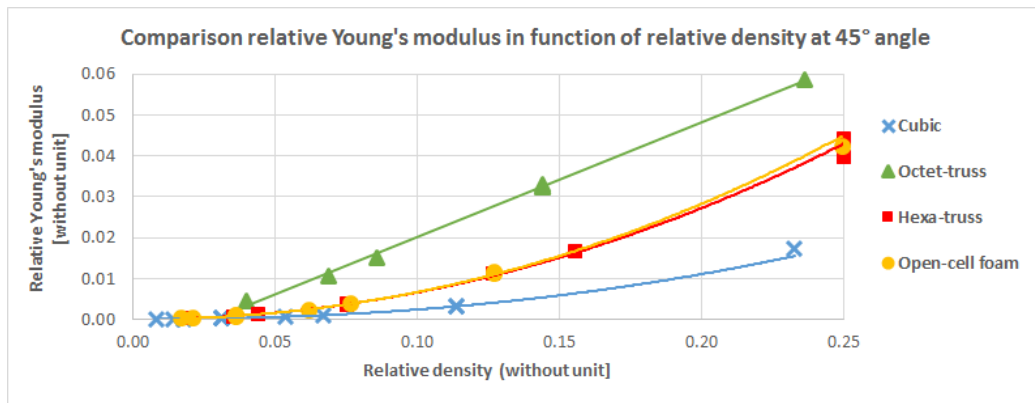


Figure 3.38: Comparison of relative Young's modulus in function of relative density at 45° angle

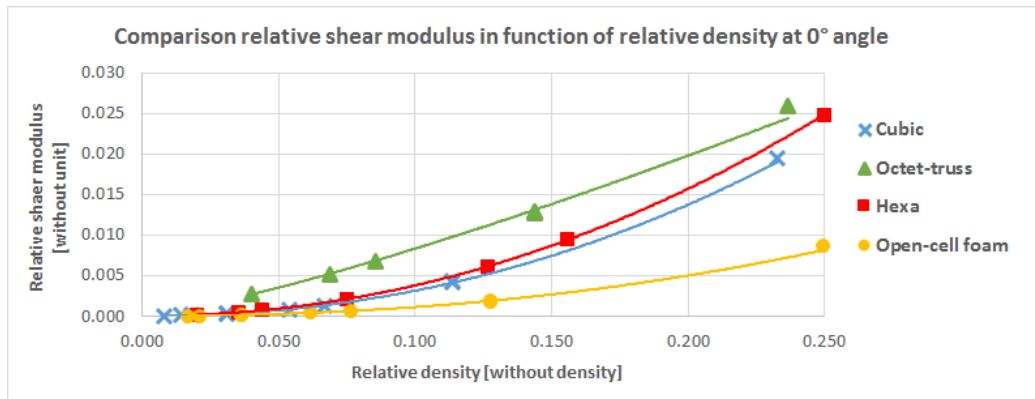


Figure 3.39: Comparison of relative shear modulus in function of relative density at 0° angle

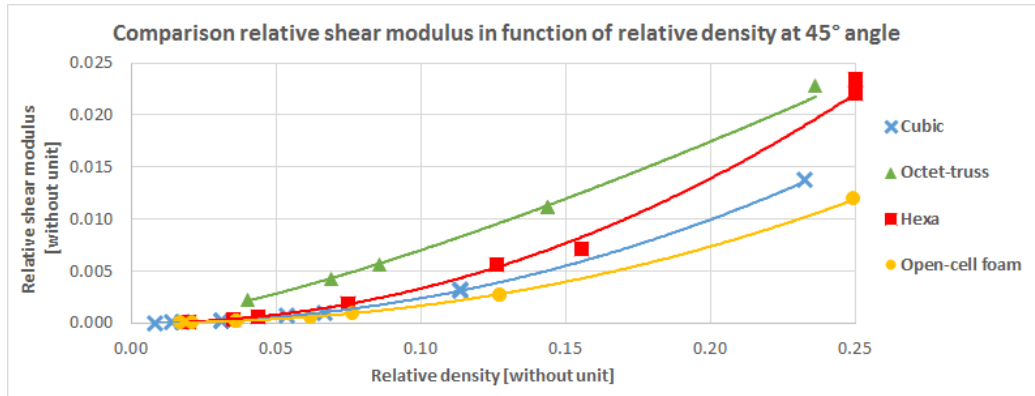


Figure 3.40: Comparison of relative shear modulus in function of relative density at 45° angle

Relative density The different combinations of struts thickness and elementary structure length that produce the same relative density will have constant relative Young's and shear modulus. For example, for the hexa-truss lattice structure, three lattice structures which have the same 7.9% relative density with different strut thickness and elementary structure length have the same relative Young's and relative shear modulus. It is also worthy to note here the effect of relative density by adjusting the struts thickness and length of the elementary structure for the reason that it directly manipulates the mechanical response of the lattice structures.

3.4 Results verification

The results obtained are compared in this section. In the section, we conducted two verifications, first by comparing with results obtained in other articles, and second by conducting case studies to compare FEA results between lattice structures and equivalent materials.

3.4.1 Comparison with results from other articles

Previous work had been published for octet-truss and diamond lattice structures to establish relations between their relative density and relative Young's modulus. We compare the FEA results that we obtained with the data published by (Suard, 2015) and (Neff, 2015) for octet-truss and diamond lattice structure respectively.

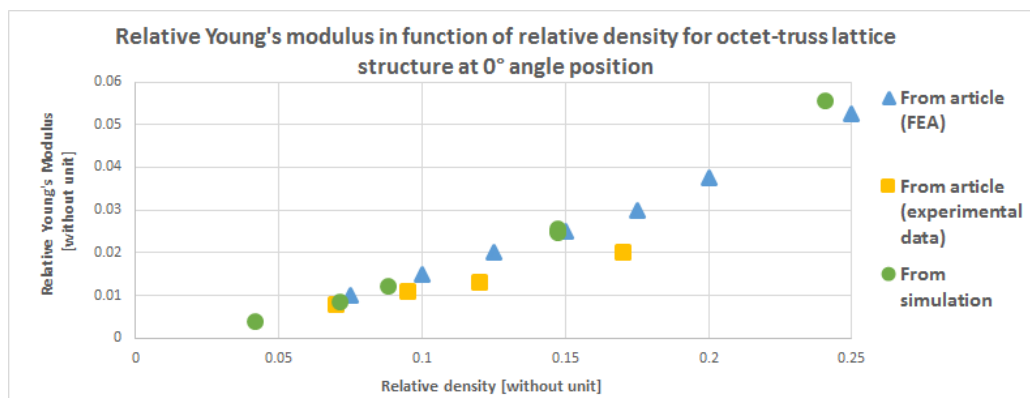


Figure 3.41: Relative Young's modulus in function of relative density for octet-truss lattice structure, in comparison with Suard's results

Figure 3.41 shows a comparison between FEA results that we obtained and the results published by (Suard, 2015). Suard et al. conducted both FEA and experimental (see figure 3.42) compression tests of octet-truss lattice structures. The results and the FEA and experimental results by Suard et al. shows good agreement. The good correlation indicates not only that the relative Young's modulus in function of relative density data that we obtained in our FEA simulations are similar to that obtained by (Suard, 2015), but also that it is in agreement with the experimental results.

We also compared with another article published for diamond lattice structure. Figure 3.43 illustrates the diamond lattice structure created by (Neff, 2015) for FEA to obtain the relative Young's modulus in function of relative density.

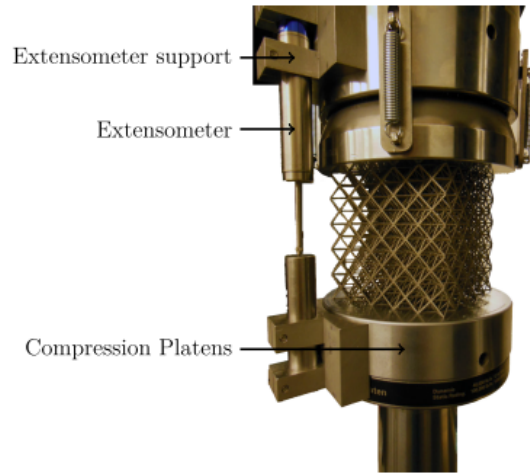


Figure 3.42: Experimental compression test of octet-truss lattice structure conducted by (Suard, 2015)

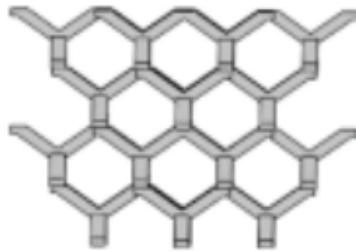


Figure 3.43: FEA on diamond lattice structure by (Neff, 2015)

We created the same lattice structure pattern and dimension and conducted a FEA compression test. The results obtained are shown in figure 3.44. From this graph, we can see that both the FEA results that we obtained and the results obtained by Neff et al. are in agreement.

Figure 3.45 shows the comparison between relative strength of ideal stretching and bending-dominated structures published by (Ashby, 2013) and the results of lattice structures from our FEA simulations.

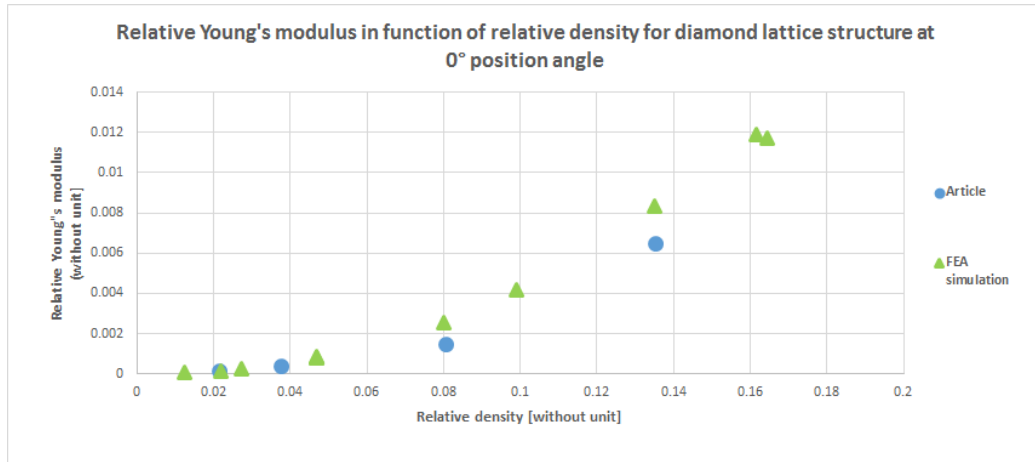


Figure 3.44: Relative Young's modulus in function of relative density for diamond lattice structure, in comparison with Neff's results

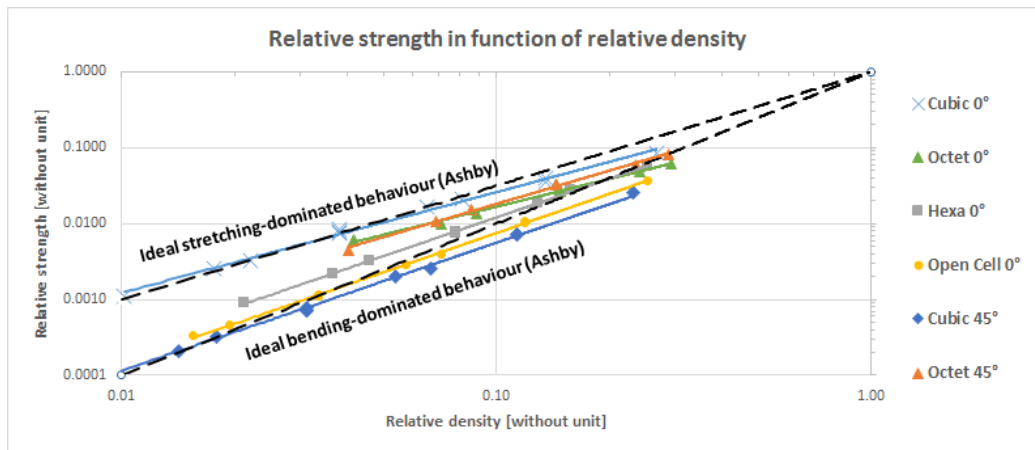


Figure 3.45: Relative strength in function of relative density for bending and stretching-dominated lattice structures, in comparison with Ashby's results

From these results, we can see that the results obtained in FEA were similar and comparable to the other results published in other papers. Thus, this verifies the reliability of the measurements and data gathered that can be used in the proposed lattice structure design method.

3.4.2 Comparison with case study results

Case study Two case studies were conducted to compare the FEA results between the lattice structure and its equivalent material, one with a L shape part, another with a C shape part. For each case study, two parts were created, first with octet-truss lattice structure, the second with the equivalent material. Both case studies have the same lattice structure pattern and relative density. The material chosen for the two case studies is titanium alloy Ti-6Al-4V. The lattice structure pattern is an octet-truss at 0° angle position with a relative density of 0.086. The results presented in section 3.3 of this chapter gives us a relative Young's modulus of 0.012 and a relative strength of 0.014.

We can thus determine the equivalent material's Young modulus from the solid material's Young's modulus using equations 3.2 and 3.5. Similarly, it is possible to calculate the equivalent material's yield strength from the solid material's yield strength using equation 3.4.

Therefore the equivalent material Young's modulus is :

$$\text{Equivalent material Young's modulus} = 0.012 \times 114 \text{ GPa} = 1.368 \text{ GPa} \quad (3.17)$$

Lattice pattern	Octet-truss at 0° angle position
Material	Ti-6Al-4V
Solid material Young's modulus (GPa)	114
Relative density	0.086
Relative Young's modulus	0.012
Relative strength	0.014
Equivalent material Young's modulus (GPa)	1.368

Table 3.1: Material properties of the octet-truss lattice structure equivalent material

The mechanical properties of the octet-truss and equivalent material are summarized in table 3.1. A 10 000 N load and clamps are applied as shown in figures 3.46 and 3.47 for the L and C shape part respectively.

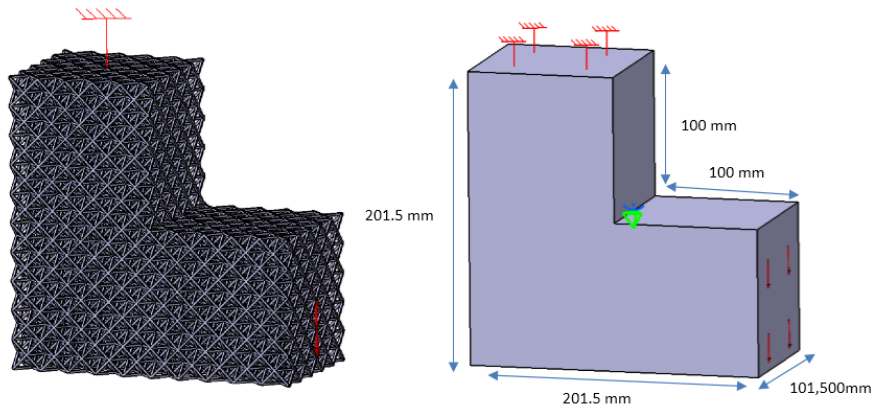


Figure 3.46: FEA on the L shaped lattice structure (left) and equivalent material (right)

A FEA simulation was executed and the displacements and the Von Mises stresses were measured. The FEA results were compared in ten elements for both parts to see the percentage difference between the two parts to verify whether equivalent material has similar mechanical properties and is able to replace the lattice structure for FEA simulation.

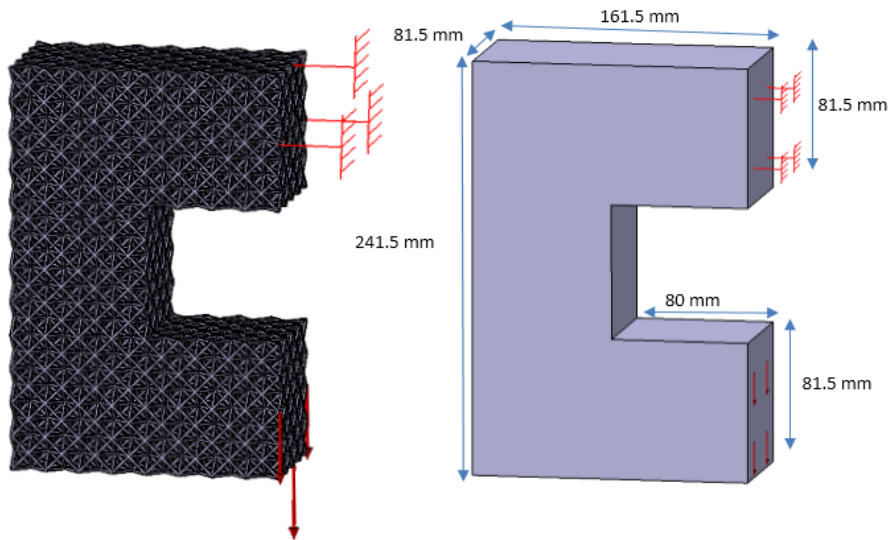


Figure 3.47: FEA on the C shaped lattice structure (left) and equivalent material (right)

Displacement: L shape part Figure 3.48 shows the displacement of the FEA result. From this image, we observe that the displacement of the lattice structure and equivalent material are in good agreement.

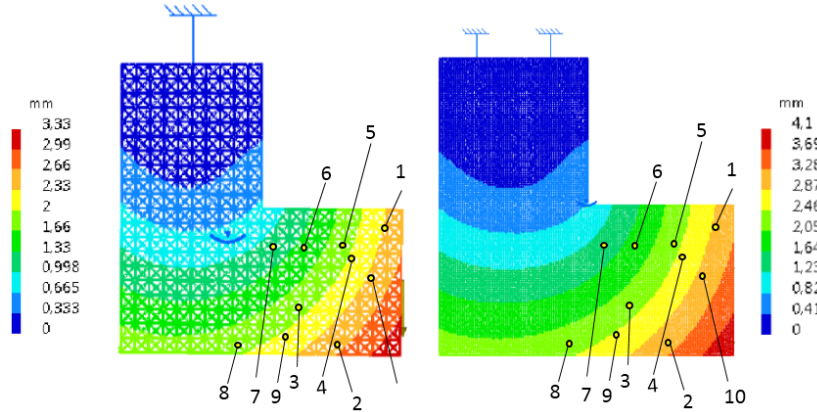


Figure 3.48: Displacements of the L shape part: Lattice structure (left) and equivalent material (right)

Element	Lattice structure				Equivalent material				Displacement difference [%]
	Coordinates of element [mm]			Displacement of element [mm]	Coordinates of element [mm]			Displacement of element [mm]	
	x	y	z		x	y	z		
1	189.5	-0.8	88.5	2.370	189.8	0.0	88.8	2.934	23.8
2	170.5	-0.8	9.7	2.731	170.8	0.0	9.8	3.345	22.5
3	140.0	-0.8	41.1	1.921	140.8	0.0	41.8	2.333	21.4
4	170.0	-0.8	70.0	2.109	169.8	0.0	70.8	2.581	22.4
5	159.5	-0.8	79.5	1.859	159.8	0.0	79.8	2.285	22.9
6	140.0	-0.8	79.4	1.529	140.8	0.0	79.8	1.875	22.6
7	119.5	-0.8	80	1.215	119.8	0.0	79.8	1.466	20.7
8	91.0	-0.8	10	1.870	90.8	0.0	9.8	2.265	21.1
9	130.2	-0.75	11	2.207	130.755	0	10.75	2.680	21.5
10	180.0	-0.75	60	2.359	180.75	0	60.75	2.915	23.6

Table 3.2: Percentage difference between the displacement of the lattice structure and the equivalent material (L shape part)

The percentage difference between both results are compared. The displacements of ten elements with the same coordinates of the lattice structure and equivalent material are compared. Table 3.2 shows the percentage difference between the two results. We can see that the difference ranges from 20

to 24%. These differences are relatively large and will undoubtedly require further developments for it to be reduced. The positive point is that the equivalent material tends to generate more displacements than the lattice structure. Consequently, it creates a security factor in the selection of the lattice structures that meet the requirements.

Von Mises stress: L shape part To compare the Von Mises stress result between the lattice structure and equivalent material, the Von Mises stress obtained from the equivalent material has to be divided by the relative strength. For the octet-truss lattice structure at 0° angle position, this value is 0.014. For example for element 1, the calculation is :

$$\frac{\text{Von Mises stress}}{\text{Relative strength}} = \frac{5.995}{0.014} = 428 \text{ MPa} \quad (3.18)$$

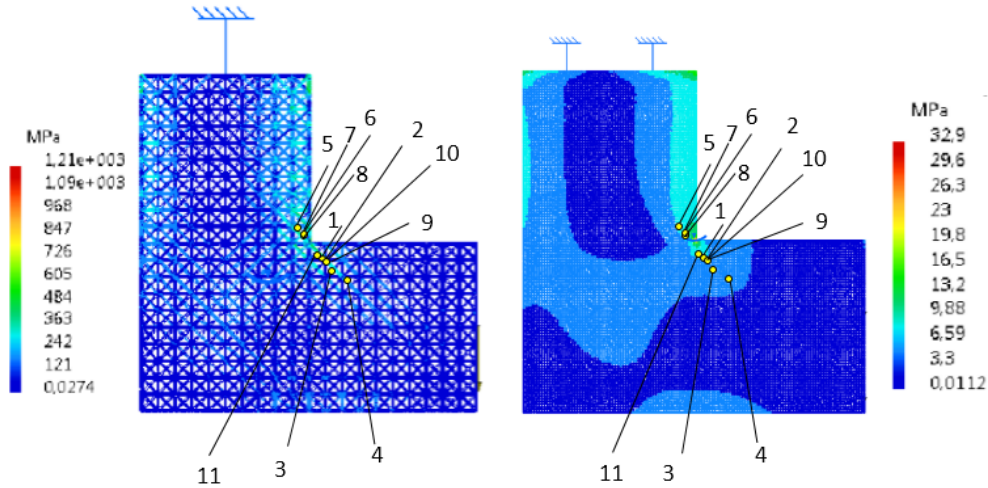


Figure 3.49: Von Mises stress of the L shape part: Lattice structure (left) and equivalent material (right)

Figure 3.49 shows the Von Mises stress repartition from the FEA result. From this image, we observe that the Von Mises stress repartition of the lattice structure and equivalent material are in good agreement. Table 3.3 shows the comparison results. We can see that the difference between the lattice structure and equivalent material is relatively important, ranging from 5% to 25%. These differences are not negligible and will undoubtedly require further development for it to be reduced. In particular not taking

into account the stress concentrations is a factor that can explain these differences, as well as the influence of the selected points, which are always in the material for the equivalent material and which can be found out of the material or at the limit for the lattice structure. The positive point is that the equivalent material tends to generate more Von Mises stress than the lattice structure. Consequently, it creates a security factor in the selection of the lattice structures that meet the requirements.

Element	Lattice structure				Equivalent material					Von Mises stress difference [%]
	Coordinates [mm]			Von Mises stress [MPa]	Coordinates [mm]			Von Mises stress [MPa]	Von Mises stress divided by relative strength [MPa]	
	x	y	z		x	y	z			
1	109.5	-0.8	90.5	358.293	109.8	0	90.8	5.995	428.214	19.5
2	110.1	-0.8	89.9	358.843	110.8	0	89.8	5.640	402.857	12.3
3	113.5	-0.8	86.6	310.190	113.8	0	86.8	4.947	353.357	13.9
4	120	-0.75	80.007	250.304	120.75	0	79.75	3.890	277.857	11.0
5	91	-0.75	109.01	409.815	91.75	0	109.75	7.169	512.071	25.0
6	92.47	-0.75	107.85	417.886	92.75	0	107.75	7.230	516.429	23.6
7	92.03	-0.75	108.03	405.673	91.75	0	107.75	6.792	485.143	19.6
8	92.85	-0.75	107.52	412.413	92.75	0	107.75	7.230	516.429	25.2
9	110.1	-0.75	89.93	358.843	110.75	0	89.75	5.640	402.857	12.3
10	110.6	-0.75	89.022	362.304	110.75	0	88.75	5.488	392.000	8.2
11	108.1	-0.75	92.149	443.277	107.75	0	91.75	6.534	466.714	5.3

Table 3.3: Percentage difference between the Von Mises stress of the lattice structure and the equivalent material (L shape part)

Displacement: C shape part Figure 3.50 shows the parts displacement. From this image, we observe that the displacement of the lattice structure and equivalent material are in good agreement.

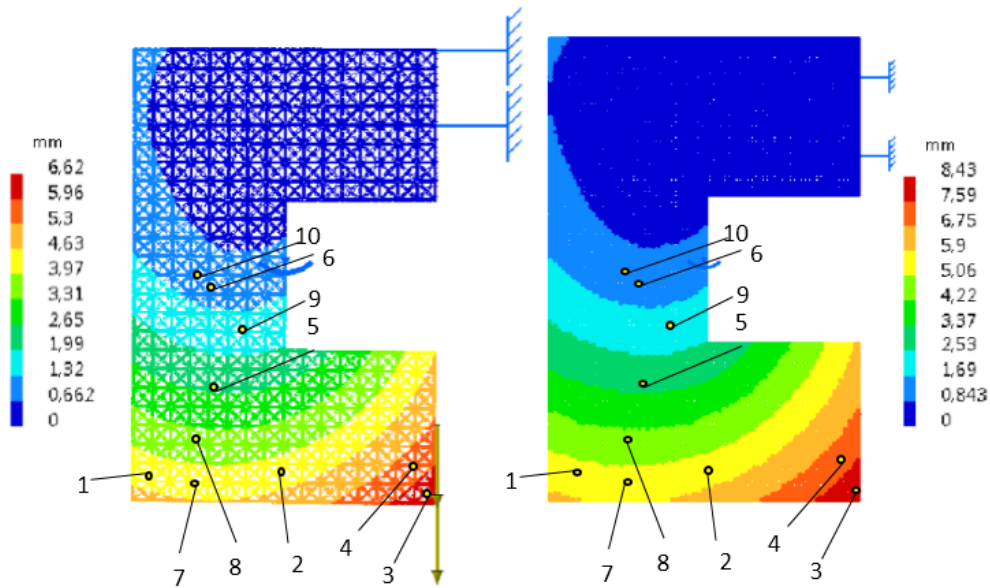


Figure 3.50: Displacements of the C shape part: Lattice structure (left) and equivalent material (right)

Table 3.4 shows the displacements results and comparison for ten elements between the lattice structure and the equivalent material.

We can see that the difference ranges from 22 to 24%. These differences are relatively large and will undoubtedly require further developments for it to be reduced. They are larger in the L shape part, due to the more complex part form and higher solicitation in the 'C' shaped part. The positive point is that the equivalent material tends to generate more displacements than the lattice structure. Consequently, it creates a security factor in the selection of the lattice structures that meet the requirements.

Element	Lattice structure				Equivalent material				Displacement difference [%]
	Coordinates of element [mm]			Displacement of element [mm]	Coordinates of element [mm]			Displacement of element [mm]	
	x	y	z		x	y	z		
1	10.5	-0.8	10.5	4.425	10.8	0.0	10.8	5.513	24.6
2	79.9	-0.8	19.9	4.152	80.9	0.0	20.5	5.201	25.2
3	159.8	0.2	1.3	6.516	159.0	0.0	1.2	8.239	26.4
4	139.4	-0.8	19.5	5.360	138.5	0.0	19.0	6.757	26.1
5	39.5	-0.8	59.5	2.577	38.7	0.0	59.1	3.253	26.2
6	40.1	-0.8	119.5	0.946	41.0	0.0	120.7	1.160	22.6
7	30.6	-0.8	10.5	4.292	30.6	0.0	11.1	5.356	24.8
8	30.4	-0.8	29.5	3.644	30.6	0.0	28.5	4.614	26.6
9	49.5	-0.8	90.5	1.588	48.9	0.0	90.7	2.000	26.0
10	39.5	-0.8	120.5	0.931	41.0	0.0	120.7	1.160	24.6

Table 3.4: Percentage difference between the displacement of the lattice structure and the equivalent material (C shape part)

Von Mises stress: C shape part Figure 3.51 shows the Von Mises stress repartition from the FEA result. From this image, we observe that the Von Mises stress repartition of the lattice structure and equivalent material are in good agreement. The table 3.5 shows the Von Mises stress results and comparison for ten elements between the lattice structure and the equivalent material. We can see that the difference between the lattice structure and equivalent material is relatively important, ranging from 0% to 25%. These differences are not negligible and will undoubtedly require further developments for it to be reduced. They are slightly higher in case of L shape part. In particular not taking into account the stress concentrations is a factor that can explain these differences, as well as the influence of the selected points, which are always in the material for the equivalent material and which can be found out of the material or at the limit for the lattice structure. The positive point is that the equivalent material tends to generate more Von Mises stress the lattice structure. Consequently, it creates a security factor in the selection of the lattice structures that meet the requirements.

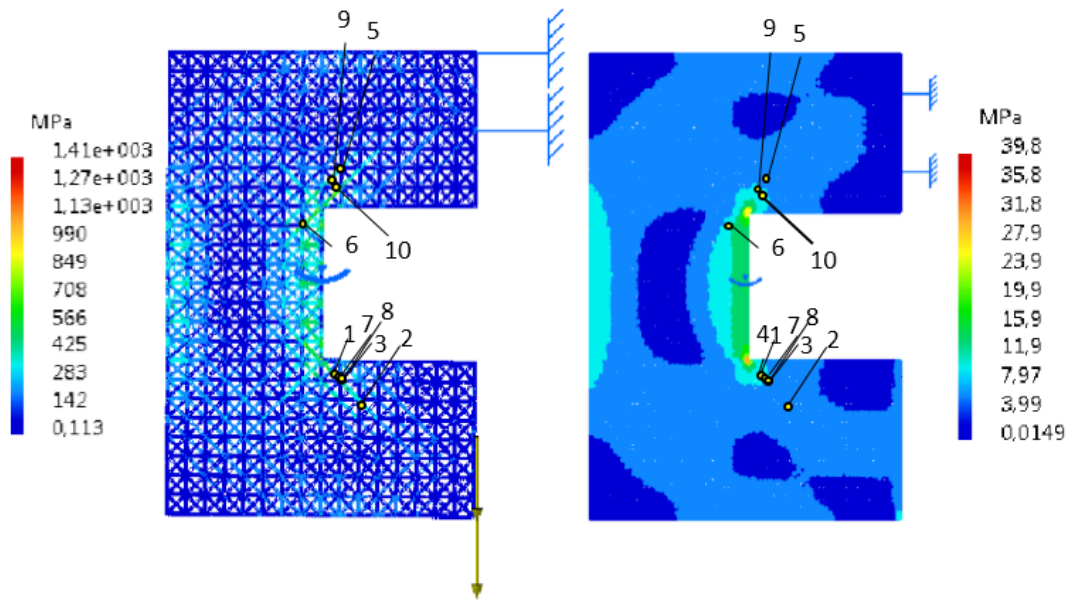


Figure 3.51: Von Mises stress of the C shape part: Lattice structure (left) and equivalent material (right)

Element	Lattice structure				Equivalent material					Von Mises stress difference [%]
	Coordinates of element [mm]			Von Mises stress of element [MPa]	Coordinates of element [mm]			Von Mises stress of element [MPa]	Von Mises stress with material equivalent coefficient [MPa]	
	x	y	z		x	y	z			
1	87.5	-0.8	72.5	610.07	86.9	0	72.9	9.60	692.64	13.5
2	96.5	9.3	53.0	292.28	95.3	0	53.1	4.88	352.29	20.5
3	89.9	-0.8	70.3	459.58	90.8	0	70.8	7.95	573.45	24.8
4	86.9	-0.8	73.4	590.34	86.9	0	72.9	9.60	692.64	17.3
5	91.9	-0.8	172.4	451.11	92.7	0	172.6	7.30	527.09	16.8
6	71.5	-0.8	151.5	600.41	71.2	0	151.5	9.95	717.96	19.6
7	88.5	-0.8	71.0	694.23	88.6	0	70.6	8.27	596.97	14.0
8	88.9	-0.8	71.4	634.11	88.9	0	72.6	8.72	629.33	0.8
9	89.0	-0.8	169.0	616.63	88.7	0	168.7	9.04	652.56	5.8
10	87.5	-0.8	167.5	610.35	88.7	0	168.7	9.04	652.56	6.9

Table 3.5: Percentage difference between the Von Mises stress of the lattice structure and the equivalent material C shape part)

3.4.3 Conclusion

The concept of equivalent material was applied in a FEA of an octet-truss lattice structure. The use of this concept for the prediction of the displacements and Von Mises stress of such a structure was validated by comparison with a FEA of the lattice structure. We observed that the differences range between 5 to 26%. This range is acceptable for the purpose of pre-sizing lattice structure CAD models. We can conclude from this study case that the equivalent materials produced can represent the lattice structure in FEA and that the methodology to obtain the equivalent material is reliable.

3.5 Summary

In this chapter, a new lattice structure design method for engineers to easily and quickly design lattice structures has been presented. This chapter proposes a new lattice structure design method, while its representation and creation will be presented in the next chapter, as shown in figure 3.52.

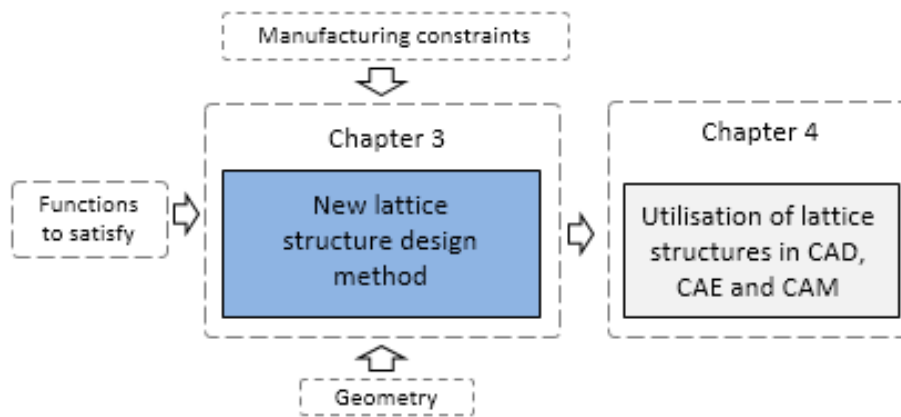


Figure 3.52: General view of the proposed lattice structures design method

New lattice structure design method A new lattice structure design method is proposed. This new method helps engineers to choose the most suitable lattice structure easily and quickly. It will help to achieve the great potential of additive manufacturing by widely integrating lattice structures in additive manufactured parts to produce lightweight high strength parts. This design method eradicates the need of creating lattice structure CAD models with struts and also improves the FEA simulations of these structures, which is a time consuming process. The lattice structures are replaced with an equivalent material which have the same mechanical properties.

Methodology for the creation of equivalent lattice structure materials In this chapter, we also presented a methodology to create equivalent lattice structure materials. This equivalent material is solid and has the same mechanical properties of lattice structures. This methodology to create equivalent materials can be used to create equivalent materials for other

lattice structure patterns. With this method, we are able to analyse the mechanical behaviour and determine whether a lattice structure is bending or stretching-dominated.

Definition and creation of the skeleton model of the lattice structures

Contents

4.1	Lattice structure configurations	103
4.1.1	Pattern	104
4.1.2	Relative density	104
4.1.3	Progressivity	106
4.1.4	Conformality	106
4.1.5	Design space	108
4.1.6	Joint shape	109
4.2	Creation of skeleton model	109
4.2.1	Skeleton model concept	109
4.2.2	Skeleton model algorithm	111
4.3	Visualisation	119
4.4	Manufacturing	121
4.5	Summary	123

Chapter 4. Definition and creation of the skeleton model of the lattice structures

In this chapter we will deal with the problem of visualization and manufacturing of lattice structures. The type of lattice structure (pattern, density, etc.) being determined, it is necessary to give to the designer a representation in a CAD environment. This is achieved by uploading to the graphic card the facets, results of the discretization of the boundary surfaces of all the elements of the structure. The structure being validated by the designer, its manufacturing requires the determination of the contours and the fusion trajectory for each layer. This is usually done once again from the boundary surface (skin) discretized or not. We have shown in Chapter 2 that the modelling in a usual CAD environment and the use of the boundary surface is not appropriate in terms of ergonomics and resource consumption. It is therefore necessary to propose a new way of modeling these lattices from the data collected in Chapter 3 and then to visualize them and to prepare their manufacturing.

For this, the proposal is to go through a skeleton model, the information about the skin being used at the time of the calculation of the visualization data by the graphics card or the manufacturing data by the CAM software. The skeleton model is created from the geometric data of the lattice structure as shown in figure 4.1. In this chapter, first the data necessary to describe a lattice structure will be listed and described in section 4.1. Then the algorithm to create the skeleton model from these data will be presented in section 4.2. Finally how visualisation and calculation of the manufacturing from the skeleton model is imagined will be exposed in section 4.3.

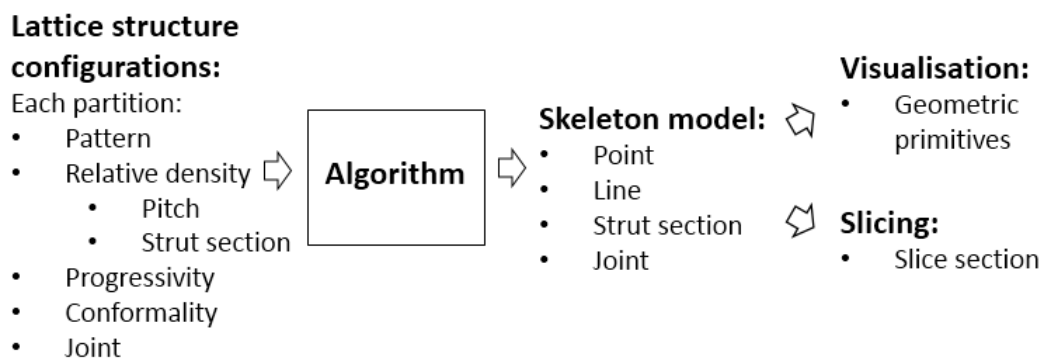


Figure 4.1: Chapter 4

4.1 Lattice structure configurations

In this section, the different types of lattice structure configurations that have to be described and created is examined. Figure 4.2 summarises the different lattice structure configurations and variables. There are six variables: pattern, design space, density, progressivity, conformality and joint. In the following subsections, the variables are explained in detail.

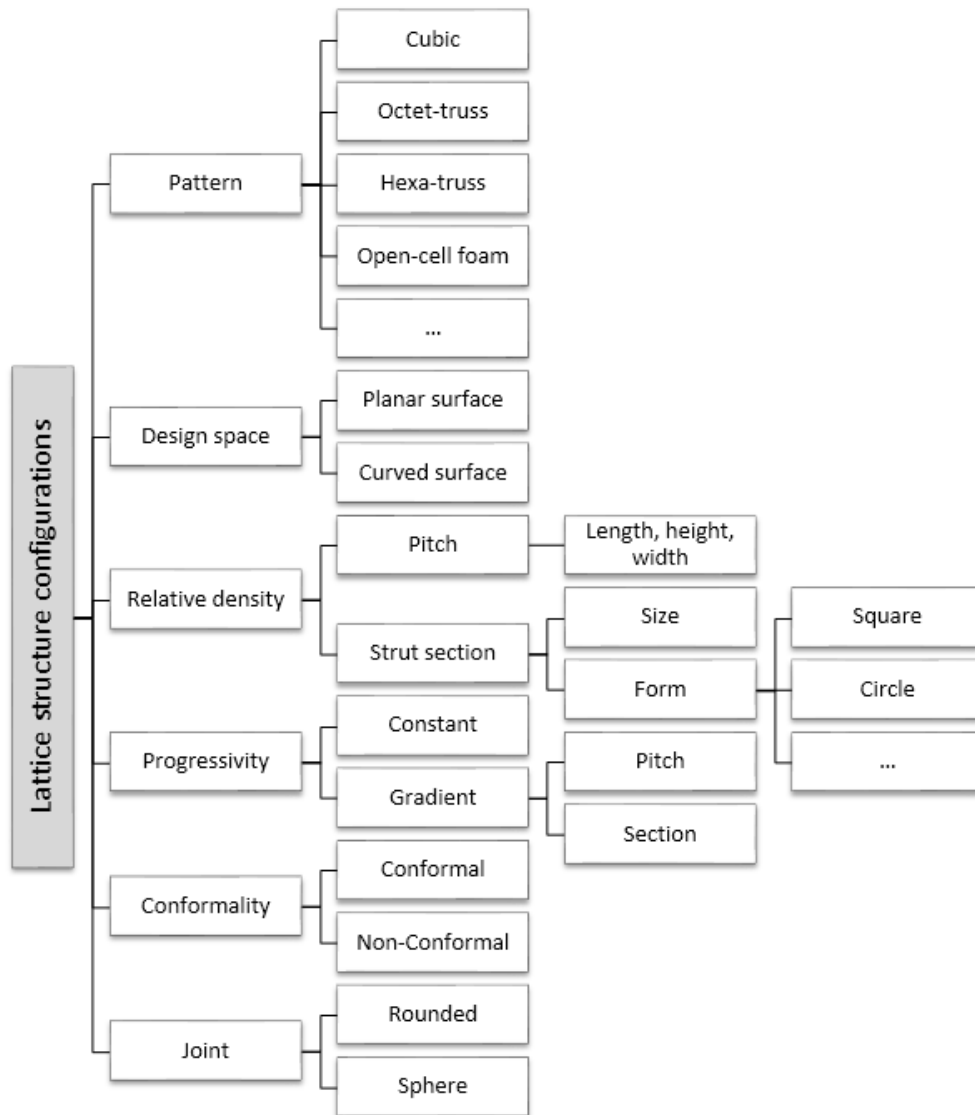


Figure 4.2: Lattice structure configurations

4.1.1 Pattern

The lattice pattern is the basic element of its geometric structure. It is based on nodes positions and struts connection between these nodes. There are many types of lattice structure patterns. The most used are the four following ones.

- Cubic
- Octet-truss
- Hexa-truss
- Open-cell foam
- Diamond

Figure 3.16 shows a representation and table 4.1 the number of points and lines for these four lattice structure pattern. An open format to describe existing and new pattern is presented in section 4.2. The pattern is then repeated in the volume, deformed and adjusted to create the final lattice structure.

	Cubic	Octet-truss	Hexa-truss	Open-cell foam
Number of points	8	14	24	32
Number of lines	12	28	36	24

Table 4.1: Number of points and lines for cubic, octet-truss, hexa-truss and open-cell foam elementary structure

4.1.2 Relative density

The relative density is the ratio between the volume of material of the lattice structure and the volume of the bounding box. It is a function of the geometrical parameters and of the strut section. Equation 3.1 and figure 3.2 illustrate the relative density. The volume of material of the lattice structure depends on the pitch and strut section dimension. The pitch dimension can vary along the X, Y and Z-axis. The section can be circular, square or any other geometries.

At a first order the relative density can be approximated for each pattern as a function of pitch and section for a constant pitch and section. For an octet-truss lattice structure the first order approximation is given in equation 4.1 and for a cubic lattice structure by the equation 4.2 where l is the pitch and s is the section. This approximation is realistic for low density but

the error becomes larger for higher densities as overlapping volume at the connections become more important. Figures 4.3 and 4.4 shows the first order relative density as a function of the true relative density, which has been measured from the CAD model of a unit cell.

$$\rho^{1st} = 12\sqrt{2}\left(\frac{s}{l^2}\right) \quad (4.1)$$

$$\rho^{1st} = \left(\frac{3 * s}{l^2}\right) \quad (4.2)$$

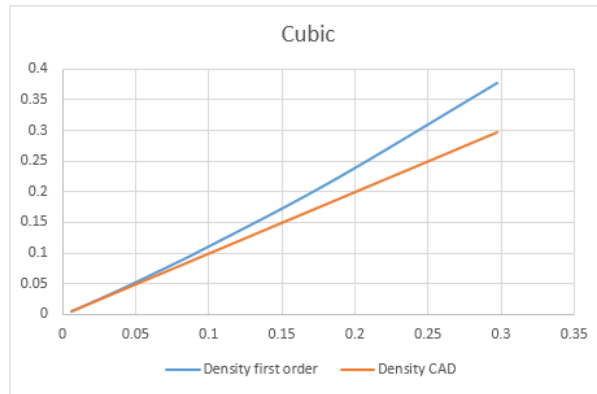


Figure 4.3: First order relative density as a function of the true relative density for the cubic lattice structure. The red line represents the isovalue

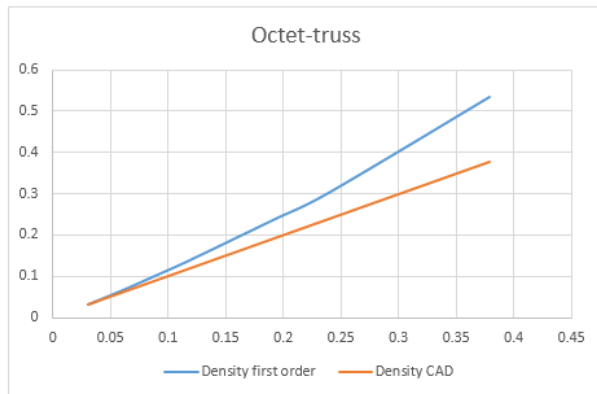


Figure 4.4: First order relative density as a function of the true relative density for the octet-truss lattice structure.

4.1.3 Progressivity

Lattice structures relative density can be uniform or gradient. For uniform lattice structures, the size and dimensions of each elementary structure are constant throughout the whole design space. As for gradient lattice structures, the dimensions of each elementary lattice structure vary throughout the part. The sections of the struts can also vary to produce gradient lattice structures and with a variable relative density. Table 4.2 shows examples of constant and gradient lattice structures for each pattern. This ability to optimise lattice structures using gradient lattice structures creates different relative densities in each area of the part. With the same material, a lattice structure with higher relative density will have higher strength and stiffness. By locally optimising the relative density and properties of a lattice structure, it is possible to meet the requirements of a specific loading in an area of a part. This gradient form can be designed to follow the direction and magnitudes of the loads applied to the part. In areas where high stress is applied, a higher relative density lattice structure will be needed, while in areas where lower stress is applied, lower relative density is needed.

4.1.4 Conformality

Lattice structures can follow different design space forms, such as curved or planar surfaces. This characteristic is categorised as conformal lattice structure. Struts in conformal lattice structures are oriented in accordance with the form of the design space, whereas in non-conformal lattice structures, the struts are oriented independently from the design space along three perpendicular directions. Figure 4.5 shows examples in 2D of different design space forms and the corresponding conformal lattice structures. There are two types: first the opposite surfaces are parallel, second they are not parallel. The definition of the conformality is versatile and complex has not been deeply studied. It will mainly be driven by meshing parameters. Only conformality in one direction has been considered with two cases, the two opposite surfaces are parallel or not.

Chapter 4. Definition and creation of the skeleton model of the lattice structures



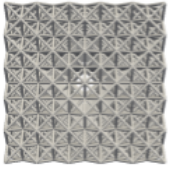
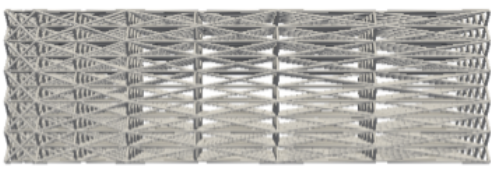
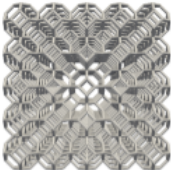
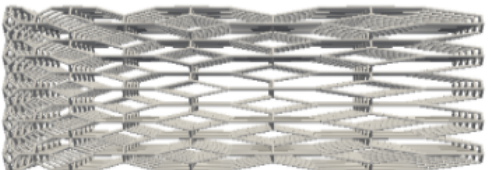
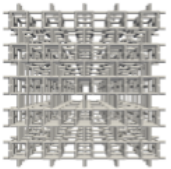

Pattern	Constant	Gradient
Cubic		
Octet-truss		
Hexa-truss		
Open-cell foam		

Table 4.2: Constant and gradient lattice structures

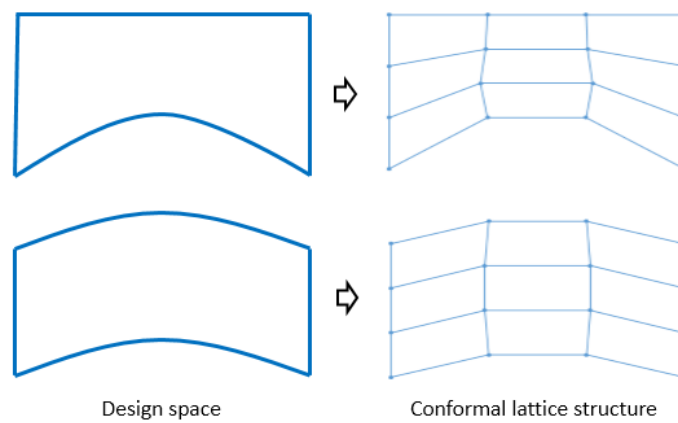


Figure 4.5: Different types of conformal lattice structures

4.1.5 Design space

Design space or zone from chapter 3, is the area of 3D space where the defined lattice is built. It is defined by its boundary surfaces and the mesh is adjusted to keep only the portion inside these surfaces, as shown in figure 4.6. The lattice is adjusted in relation to this design space and different solutions for the connections between the lattice and the edge of the design space can be designed.

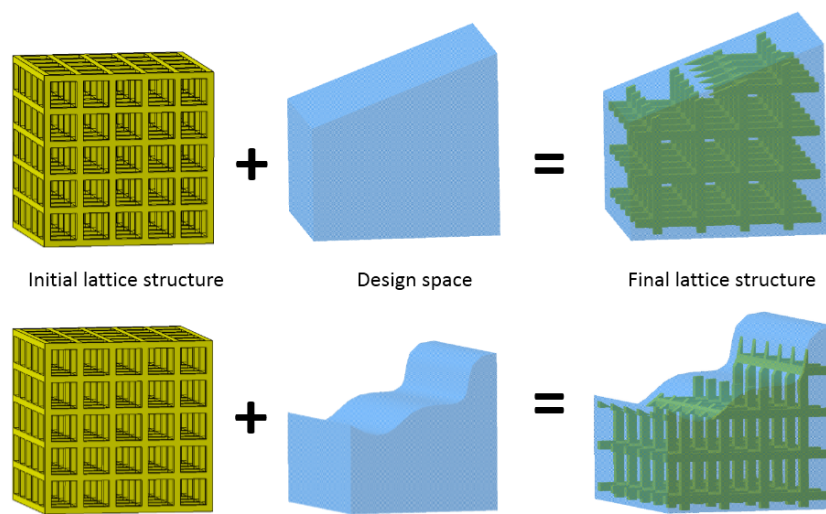


Figure 4.6: Example of a cubic lattice structure with an upper planar and curved surface of the design space

There are two types of connections between the lattice structure extremity struts and the design space boundary surface. Figure 4.7 shows an example of the two types. The first type of connection is the non-conformal extremity strut connection, whereas the second connection is the conformal extremity struts connection. In the non-conformal extremity struts, struts that cut the boundary are only adjusted while in the conformal extremity struts, the orientation of the extremity struts are modified to follow the orientation of the surface of the design space. As for conformal lattice, conformal extremity has a lot of possibilities and has not been deeply studied in this manuscript.

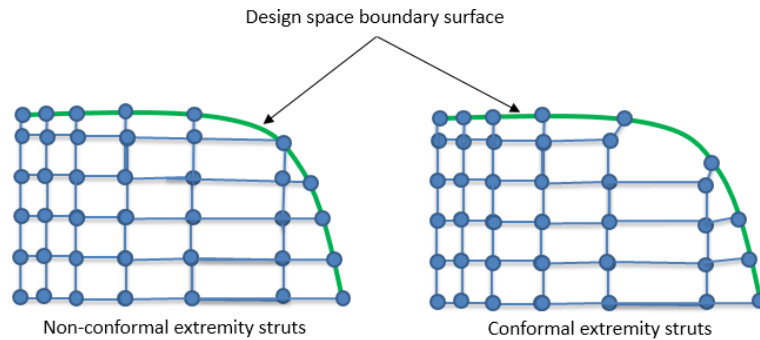


Figure 4.7: Connection between extremity struts and design space

4.1.6 Joint shape

The connection between the struts forms a joint. At each joint, forms are added to form the joint. These forms can be either rounded edges or spheres. Figure 4.8 is an example of a cubic lattice structure with rounded joint edges.

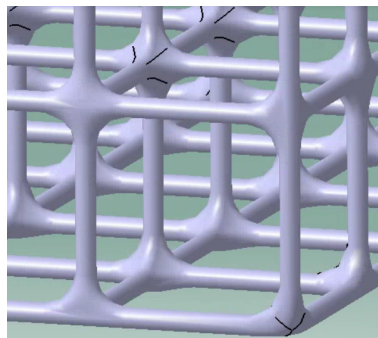


Figure 4.8: Cubic lattice structure with rounded joint edges

4.2 Creation of skeleton model

4.2.1 Skeleton model concept

In this chapter, the objective is to propose an alternative to skin or B-Rep models. Current CAD tools currently create and represent lattice structures using surfaces and volumes. This thus contributes to large file sizes, high RAM consumption, as well as time-consuming creations and operations. Hence, a better way to create lattice structure parts than the current method

is by defining it with four elements, which are points, lines, strut sections and joints. These four elements define a skeleton model. Table 4.3 shows the point, line, section and connection list for an elementary octet-truss structure. The point list contains the coordinates of each point (X, Y, Z) and the line list contains the lines (struts) connecting these points, it is described by a beginning point and ending point. The section list describes the size of the section for each line to define a strut. It is described by a section size at the beginning and end of the line. The connection line describes the type of joint at each corresponding point. The following subsections will explain how the skeleton model is created.

Point list				Line list			Section list			Connection list	
Index	X	Y	Z	Index	Begin (point)	End (point)	Line	Begin (size)	Begin (Size)	Index	Type
1	0	0	0	1	2	5	1	1	1	1	Rounded
2	2	0	0	2	3	4	2	1	1	2	Rounded
3	0	0	2	3	6	9	3	1	1	3	Rounded
4	2	0	2	4	7	8	4	1	1	4	Rounded
5	0	2	0	5	4	6	5	1	1	5	Rounded
6	2	2	0	6	2	8	6	1	1	6	Rounded
7	0	2	2	7	5	7	7	1	1	7	Rounded
8	2	2	2	8	3	9	8	1	1	8	Rounded
9	1	0	1	9	8	5	9	1	1	9	Rounded
10	0	1	1	10	4	9	10	1	1	10	Rounded
11	1	1	0	11	2	7	11	1	1	11	Rounded
12	2	1	1	12	6	3	12	1	1	12	Rounded
13	1	1	2	13	6	4	13	1	1	13	Rounded
14	1	2	1	14	2	8	14	1	1	14	Rounded
				15	5	7	15	1	1		
				16	3	9	16	1	1		
				17	10	11	17	1	1		
				18	10	12	18	1	1		
				19	10	13	19	1	1		
				20	10	14	20	1	1		
				21	15	11	21	1	1		
				22	15	12	22	1	1		
				23	15	13	23	1	1		
				24	15	14	24	1	1		
				25	11	12	25	1	1		
				26	12	13	26	1	1		
				27	13	14	27	1	1		
				28	11	14	28	1	1		

Table 4.3: Elementary octet-truss structure: Point, line, section and connection list

Figure 4.9 illustrates a cubic lattice structure defined with a skeleton model. The lattice structure on the left is created with only points and lines, whereas for the lattice structure on the right, the strut sections are added.

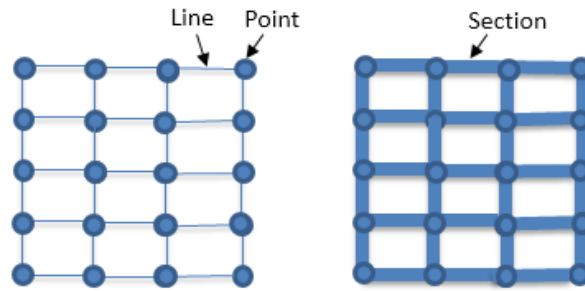


Figure 4.9: Skeleton model: Lattice structure defined by points, lines and sections

4.2.2 Skeleton model algorithm

The algorithm to create the skeleton model is presented in this section.

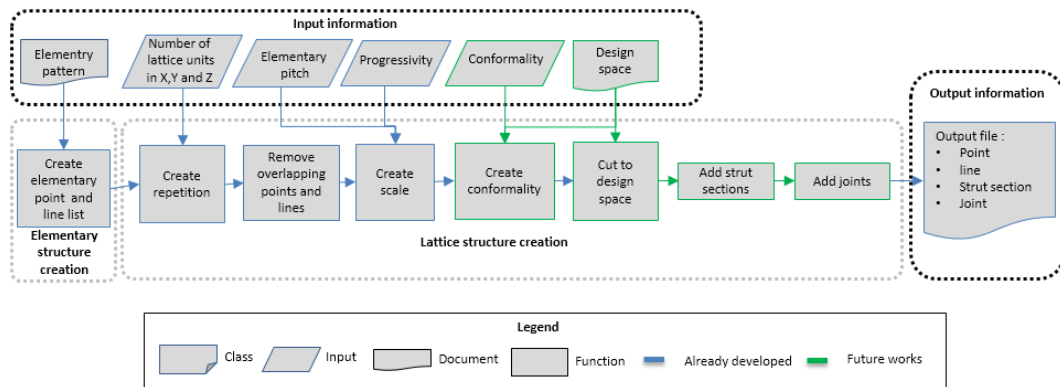


Figure 4.10: Class, functions, input and output information of the algorithm

Figure 4.10 shows the workflow to create the skeleton model from the characteristics of the lattice structure defined in section 4.1. In blue are the steps that has already been implemented, while in green are those to be developed in future works. The following paragraphs explain the successive steps of the algorithm.

Elementary structure creation The elementary pattern is described in a unit cube by the coordinates of the points and the lines linking these points. For example, to create a cubic lattice structure, eight points are needed to define the cubic elementary structure, as shown in table 4.4. The number of each point corresponds to its index number in the algorithm. The coordinates of each point are shown in the corresponding columns in the table. The eight points are connected with twelve lines. The column on the left and right indicates the index of the points connected to construct each line. The point and line lists of the octet-truss, hexa-truss and open-cell foam elementary structure are presented in tables B.1, B.2 and B.3 in appendix B.

Point list				Line list		
Index	X	Y	Z	Index	Begin (point)	End (point)
1	0	0	0	1	1	2
2	1	0	0	2	2	4
3	0	1	0	3	4	3
4	1	1	0	4	3	1
5	0	0	1	5	5	6
6	1	0	1	6	6	8
7	0	1	1	7	8	7
8	1	1	1	8	7	5
				9	1	5
				10	2	6
				11	3	7
				12	4	8

Table 4.4: Elementary cubic structure: Point and line list

A point is defined by its coordinates. Here we use the Cartesian coordinate system to describe the coordinates of the points. Therefore, a point class consists of the coordinates X, Y and Z. In this class, we also attribute an index to each point. The index of the point refers to the position of the point in the points list.

A line connects two points. Therefore it is defined by the point at the beginning of the line and the point at the end of the line. The lines defined are straight (having no curvature). Each line is attributed an index, which refers to the position of the line in the line list.

A section is defined by its geometry and its dimensions. Here only circular and square sections have been considered. A section is assigned to each extremity (beginning and end) of each line.

A joint is described by its form, for example rounded edges or spheres and its dimensions. Each point is attributed a joint form in the joint list.

Create repetition To create the lattice structure, a repetition of the elementary structure is carried out. The elementary structure is repeated with a pitch of one in each direction till the desired number of cells is obtained. Figure 4.11 shows the repetition of an elementary structure repetition in the X, Y and Z-axis to obtain a 3 x 3 x 3 unit cubic lattice structure. Here we note that during the repetition of two elementary structures, overlapping points and lines were created. Thus a function is required to delete these overlapping points and lines. Table B.4 in appendix B contains the point and line lists for this 3 x 3 x 3 unit cubic lattice structure.

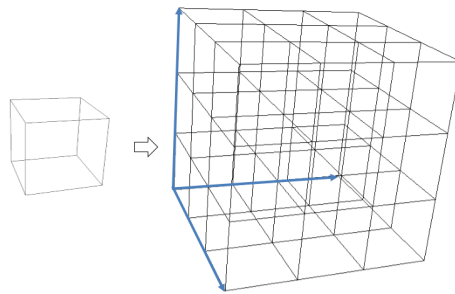


Figure 4.11: Elementary structure repetition to obtain 3 x 3 x 3 unit lattice structure

Remove duplicated points and lines Next, we remove the overlapping points and lines which exist after the elementary structure repetition, as shown in figure 4.12.

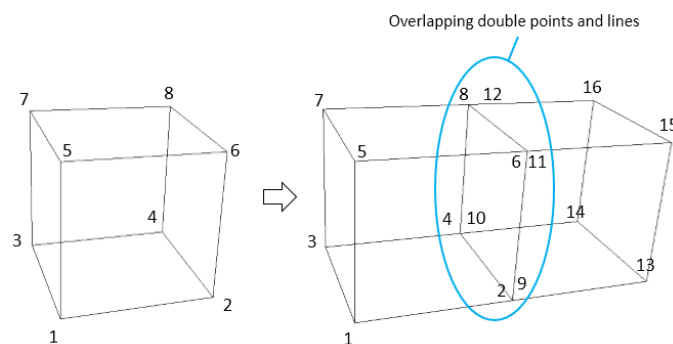


Figure 4.12: Overlapping points and lines after elementary structure repetition

In step one, first an empty point list is created. This list is referred to as

the filtered point list. Then, each point in the initial point list is compared to the points in the filtered point list. If it does not yet exist in the filtered point list, then the point is added to the list. For example in figure 4.13 case one, point three has a coordinate of (0,1,0), which does not yet exist in the filtered point list. Thus it is added to the list. The indexes of the point in the initial point list and the filtered point list are added in the corresponding initial and filtered point list. If the point in the initial point list already exists in the filtered point list, as in figure 4.13 case 2, thus the point is not added to the list. The index of the two overlapping points are added in the corresponding initial and filtered points list.

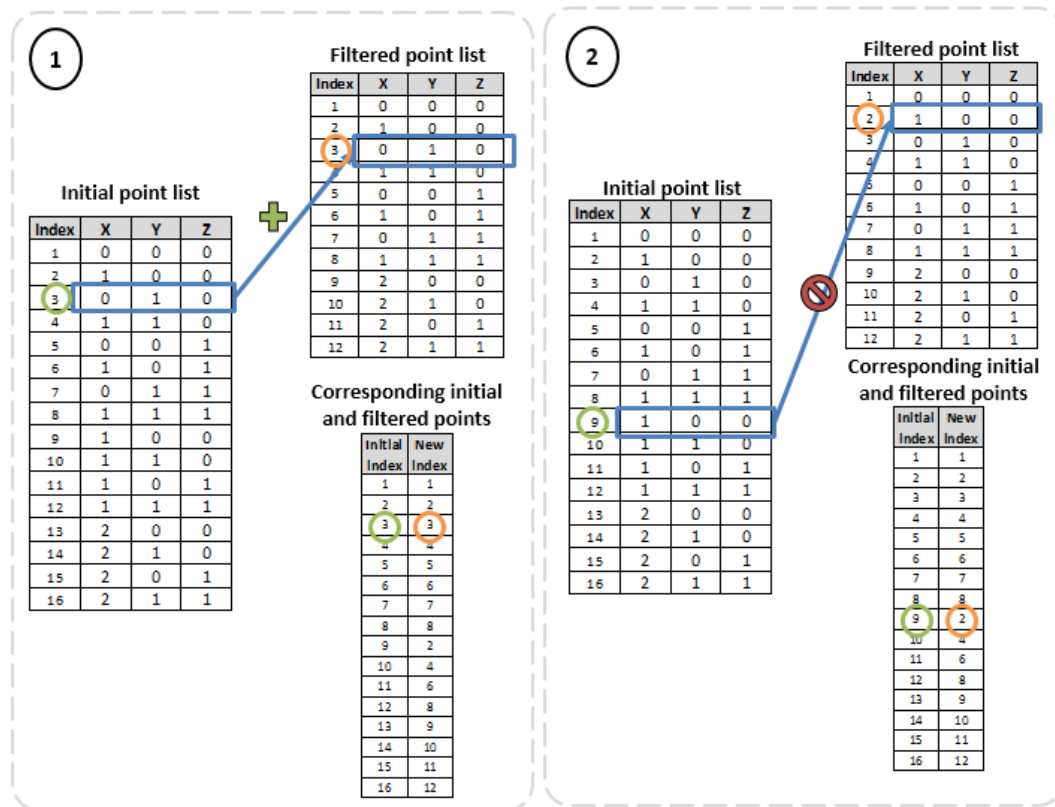


Figure 4.13: Step one case one and two

In the second step, the begin and end point for each line in the initial line list is replaced by the new point from the corresponding initial and filtered points list. The corresponding line list is obtained, as shown in figure 4.14.

Chapter 4. Definition and creation of the skeleton model of the lattice structures

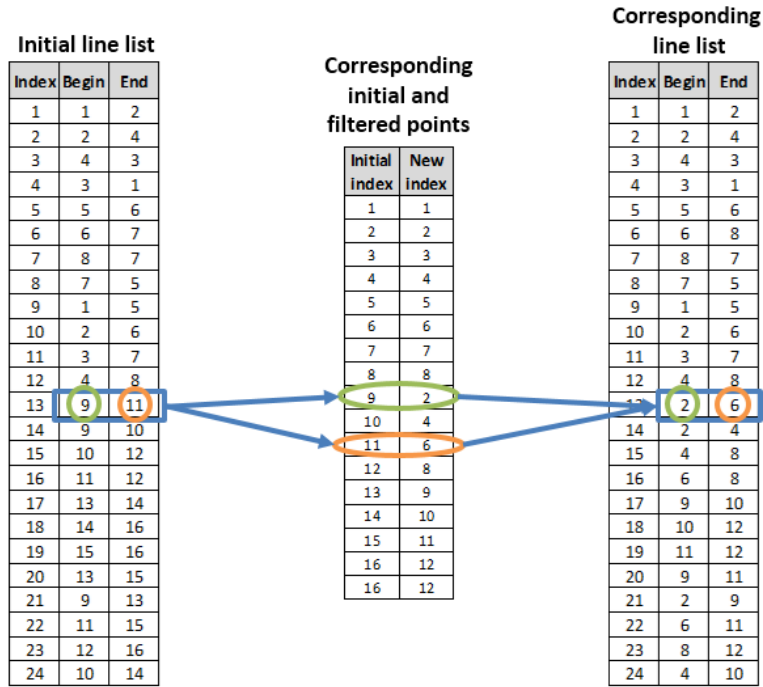


Figure 4.14: Step two

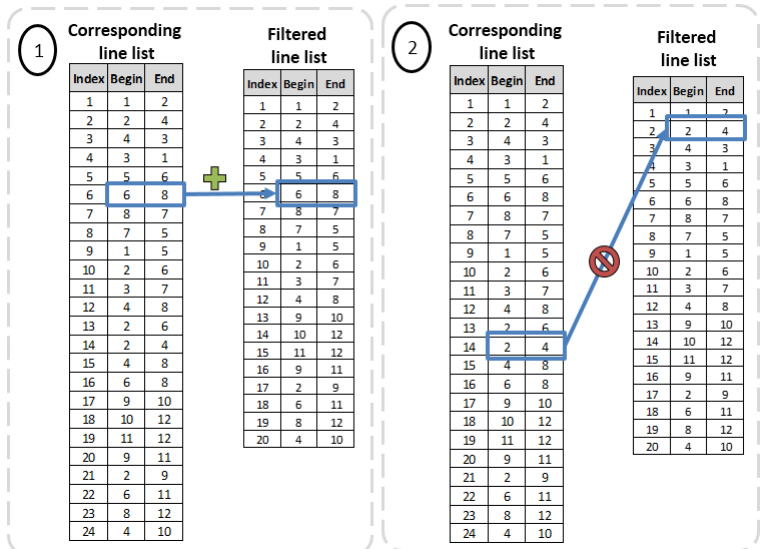


Figure 4.15: Step three case one and two

In the third step, an empty line list is created. This list is referred to as

filtered line list. Then, each line in the initial line list is compared to the line in the filtered point list. If it does not yet exist in the filtered line list, the point is then added to the list, as shown in figure 4.15 case one. If the line in the initial line list already exists in the filtered line list, thus the line is not added to the list, as shown in figure 4.15 case two.

Create scale The lattice structure being defined with a unit pitch, it has to be scaled so that its pitch becomes the one defined by the designer. The scale can be either constant or gradient depending on the progressivity defined by the designer.

Figure 4.16 shows an example a constant $3 \times 3 \times 3$ unit scale lattice structure with a pitch dimension of 2 mm. As we can see in the point and line lists is shown in table B.5 in appendix B, the line list is the same as an unscaled structure in table B.4, the only changes occur in the coordinates of the points list, where each point in the elementary structure is multiplied by two.

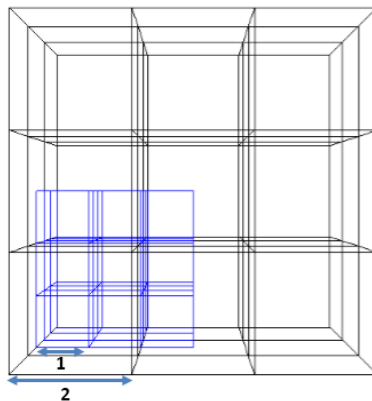


Figure 4.16: Constant scaled $3 \times 3 \times 3$ unit cubit lattice structure with a pitch dimension of 2

Figure 4.17 is an example of a scale gradient lattice structure. Here the algorithm is the same used as for the scaled constant lattice structure, the only difference being the multiplication of the coordinates of the points. Here, instead of multiplying with a constant, the coordinates of the points are multiplied with maths formulas such as exponential, square or power. As we can see in the point and line lists shown in table B.6 in appendix B, the line list is the same as an unscaled structure in table B.4, the only changes occur in the coordinates of the points list, where each point in the elementary structure is multiplied by the maths formula applied.

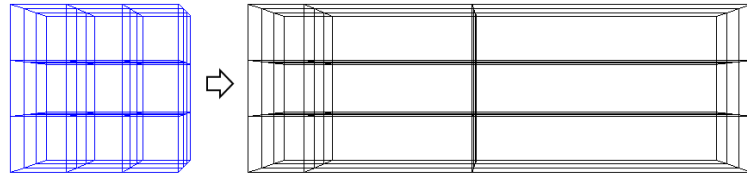


Figure 4.17: Progressive scaled 3 x 3 x 3 unit cubit lattice structure

To obtain the constant or gradient lattice structure, the following algorithm is used :

For Point in Pointlist :

$X = x * (\text{maths formula or constant dimension})$

$Y = y * (\text{maths formula or constant dimension})$

$Z = z * (\text{maths formula or constant dimension})$

Create conformality Conformal lattice structures are created from the previous point list by moving the points according to the driving surfaces. Here we propose three different methods to move the points. The first method consists of measuring the distance between the horizontal and vertical design space boundaries. Next, each distance is divided by the number of units in the lattice structure to obtain an equal spacing between each line in the vertical and horizontal direction. This method is illustrated in figure 4.18. In this example, a 4 x 4 x 1 unit cubic lattice structure conforms to the design space. Table B.7 in appendix B shows the point and line list of this conformal cubic lattice structure.

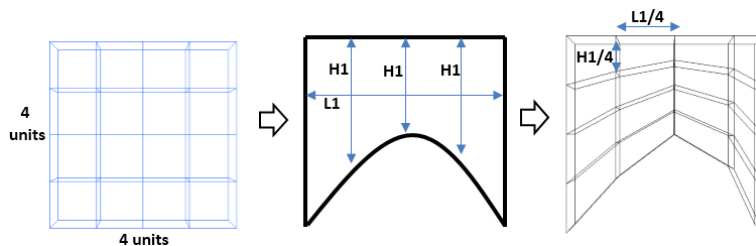


Figure 4.18: Method one

The second proposed method is for conformal lattice structures with parallel design space boundaries. In this case, the idea proposed is to measure the distance of the lower design space boundary to the origin of the axis. Then,

each coordinate in this direction is translated with the distance measured, as shown in figure 4.19 to translate all the points. Table B.8 in appendix B shows the point and line list of this conformal cubic lattice structure.

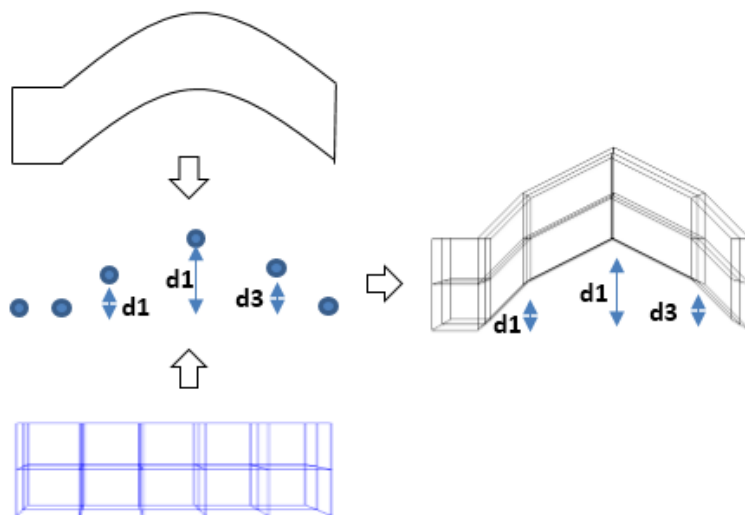


Figure 4.19: Method two

The third method is similar to the first method, the only difference being the method to calculate the distance between the points. Instead of dividing the distance between the design space boundaries by the number of units as in method one, here we use the minmax formula to create equal distances between the points in each direction. An illustration of this third method is given in figure 4.5.

Cut to design space There are two types of connections between the lattice structure extremity and boundary of the design space, as shown in figure 4.7. The connections are created by modifying the position of the points of the extremity struts on the boundary surface of the design space to obtain lines which connects the extremities of the lattice structure to the design space surface. The method to obtain the non-conformal extremity struts is shown in figure 4.20 and the conformal one has not been addressed in this manuscript. First the line for which the two points are outside the design space are deleted. Then for the lines having one point inside the design and one point outside the design space, a point is created at the intersection of the line and the design space boundary and then the outside point is replaced by the new point. Finally the points which are not any more connected to a line are deleted. The same approach can be carried out to obtain conformal

extremity struts, except in this case, creation of the new points is carried out differently. Here, the points are repositioned according the orientation of the design space boundary surface.

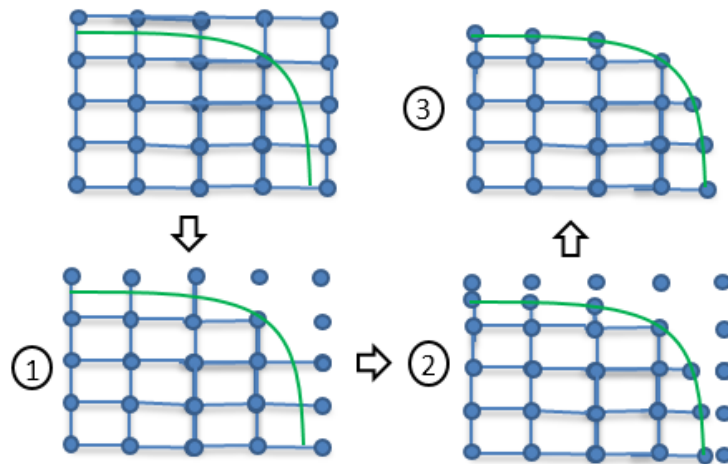


Figure 4.20: Method to obtain non-conformal extremity struts

Output information The output information contains the lists of the points, lines, strut sections and joints. In the points list, each line contains the coordinates of the point. The lines list contains the index of the points to which they are connected. The section list contains section characteristics for each strut extremity and the joint list contains the joint type. Figure 4.21 is an example of a cubic, octet-truss and hexa-truss lattice structure created with points and lines, and visualised in a viewer (Paraview).

Tables B.9 and B.10 in appendix B is an example of a 3 x 3 x 3 cubic lattice structure. It contains point, line, section and joint shapes lists.

4.3 Visualisation

Proposed visualisation method The idea for the proposed method is to avoid the need to create lattice structures with surfaces and volumes by replacing them with lines, points and sections. From the skeleton model, the solution is to use geometric primitives to visualise the lattice structures in CAD. Geometric primitives are the simplest geometric objects that a CAD system can draw and store. Commonly used geometric primitives include:

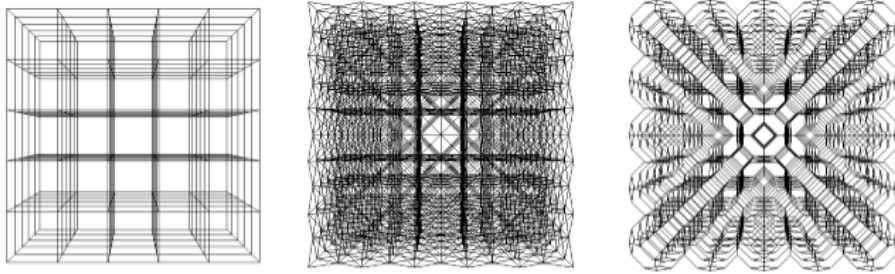


Figure 4.21: Example of a cubic, octet-truss and hexa-truss lattice structure created with points and lines visualised in a viewer (Paraview)

- Points
- Lines and line segments
- Planes
- Circles and ellipses
- Triangles and other polygons
- Spline curves

Whereas in 3D applications, basic geometric forms and shapes are considered to be primitives, for example:

- Spheres
- Cubes or boxes
- Toroids
- Cylinders
- Pyramids

Figure 4.22 shows an example of a cubic lattice structure visualised in the CAD software by adding the section of the struts. Lattice structures can be built with geometric primitives such as cylinders and spheres. The idea is to send to the graphic card the primitives (for example a cylinder) based on the information of the skeleton model. The graphic card will then calculate the facet to create the visualisation model of the lattice.

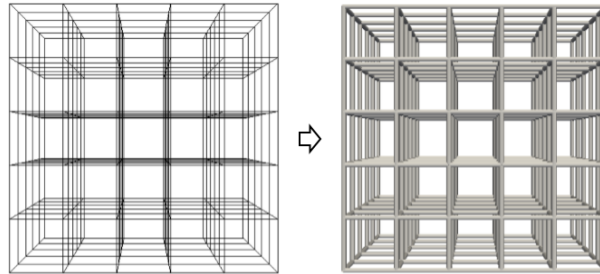


Figure 4.22: Visualisation of lattice structure built by geometric primitive lines and cylinders

4.4 Manufacturing

Proposed slicing method The data sent to the usual machine in additive manufacturing are the contour of the melted zones for each layer. The 3D model of the part has to be sliced to determine these contours. In our case, the skin of the part is not known and the slicing has to be done from the skeleton. The lines are sliced to obtain the centre of the contours. Then, from the section list and the orientation of the struts, we create the contours and finally the outer contour of the form. The joint forms, for example rounded or sphere joints, are not addressed in this manuscript. It will be for future works.

Figure 4.23 shows the two steps.

Strut section The form of the contour around the mean line depends on the section and the orientation of the strut. For example, for a circular section, a strut oriented at a 90° angle has a circular section, while struts which are not at 90° angles have ellipse-shaped sections. The exact shape of the ellipse depends on the angle of the orientation.

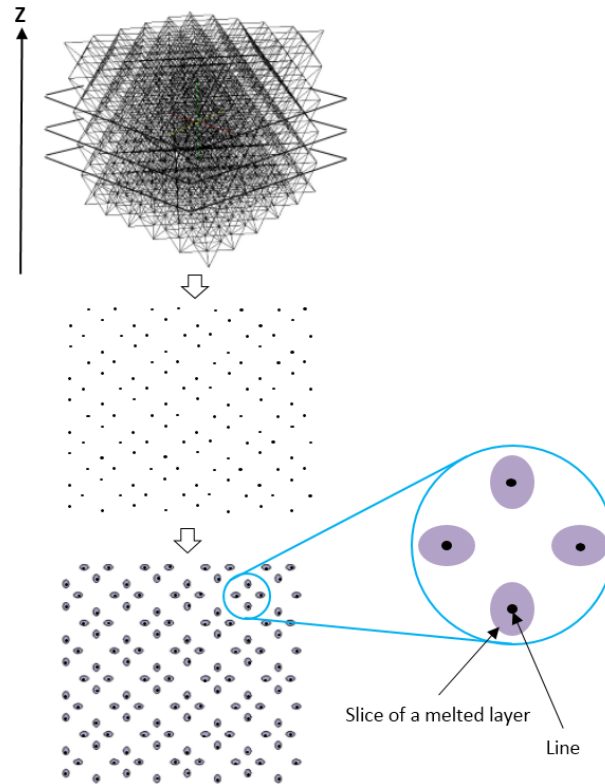


Figure 4.23: Slicing lattice structure lines into layers and adding section to sliced lines

Strut joint The section form in a strut joint is a combination of joint ellipses, as shown in figure 4.24. Here we see the joint in an octet-truss lattice structure, where four struts are connected at the joint at an inclined angle. First the lines at the joint is sliced to obtain four points, then an ellipse contour is added surrounding each point. Next, the contours of the ellipse are joined together, by keeping only the outer contour, to obtain the final section form.

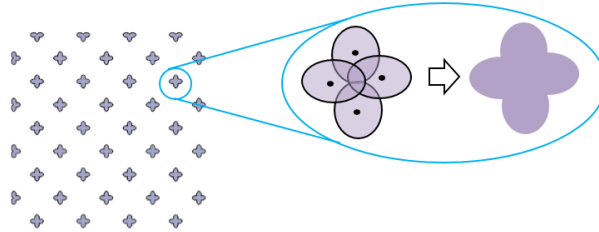


Figure 4.24: Adding section to sliced lines

4.5 Summary

Two advances are presented in this chapter. First, the determination of lattice structure part configurations for metallic additive manufacturing. Second, a new proposed method to visualise lattice structure in CAD and slice it in CAM. First the requirements and problems encountered were determined. The core of this proposed methodology is the representation and creation of lattice structures with points, lines and section sizes, referred to as the skeleton model. The creation of the skeleton model is described. A algorithm was created based on this concept. A method was proposed to visualise the lattice structures in CAD software by using geometric primitives. In CAM environment, a new method was proposed to slice lattice structures using the skeleton model. This PhD serves as a starting point for future developments in the creation of conformal lattice structures, cutting to the design space, section, joints and connections contributing to new and improved CAD and CAM tools for additive manufacturing and also a new additive manufacturing file format.

General conclusion

Aim and strategy

The aim of this PhD is to facilitate and improve the integration of lattice structures in additive manufacturing parts. The problematic has been split into difference parts. First, the design aspect of the lattice structures, where the goal is to help designers have the necessary information to be able to choose and integrate the correct type of lattice structures based on a part's requirements. Then, the definition of a skeleton model for visualisation and creation of manufacturing data. The outcome will contribute to the wide use of lattice structures in additive manufactured parts.

Main results

New lattice structure design method

A new lattice structure design method is proposed for better lattice structure integration in part designs. This design method enables designers to choose the correct lattice pattern and density. An essential part of this proposition is the use of equivalent lattice structure materials. This eradicates the need to design lattice structure CAD models and reduces FEA simulation time.

Methodology to create an equivalent lattice structure material

A methodology to create an equivalent material is presented in this Phd thesis. It enables engineers to replace lattice structure CAD models with CAD solid models which have the same mechanical properties. This methodology can be used to define equivalent materials for other lattice structure patterns. The equivalent materials reduces FEA simulation time.

Evaluation of current CAD tools performances in additive manufacturing

The performances of current CAD tools were assessed to determine whether they are adequate enough for the requirements of additive manufacturing. Results show that current CAD software are not practical for designers to

design lattice structures easily and quickly for additive manufacturing and that current CAE software are not up to scratch in terms of performances to execute finite-element-analysis of lattice structures. Improvements in CAD and CAE software are needed.

Definition and creation of the skeleton model for lattice structures

A representation and creation of lattice structures with points, lines and section sizes, referred to as the skeleton model was created. Lattice structure geometrical characteristics were determined and an algorithm for the creation of a skeleton model for these characteristics were presented.

Future work

New CAD tools to design lattice structures

To overcome the problem of having to design lattice structures manually in CAD software, CAD tools must be able to automatically create the lattice structures CAD models. One which enables designers to choose from a library the lattice pattern, struts thickness and length, and functions to automatically create the lattice structures. This work is a basis for future work to create new CAD tools to design lattice structures

CAD file formats for additive manufacturing

A new CAD file format suitable for lattice structure is needed. One that stores lattice structure information based on points and lines instead of surfaces and volumes. Lattice part designs, CAD, CAE and CAM requirements have to be taken into consideration for the creation of this new CAD file format for additive manufacturing, as shown in figure 4.25. This work is a starting point for the creation of a new CAD file format for additive manufacturing.

Lattice structure optimisation and stress concentration

The proposed lattice structure design method allows engineers to choose the correct lattice structure pattern and density. A preliminary study regarding stress concentration in lattice structures is assessed in this Phd. However,

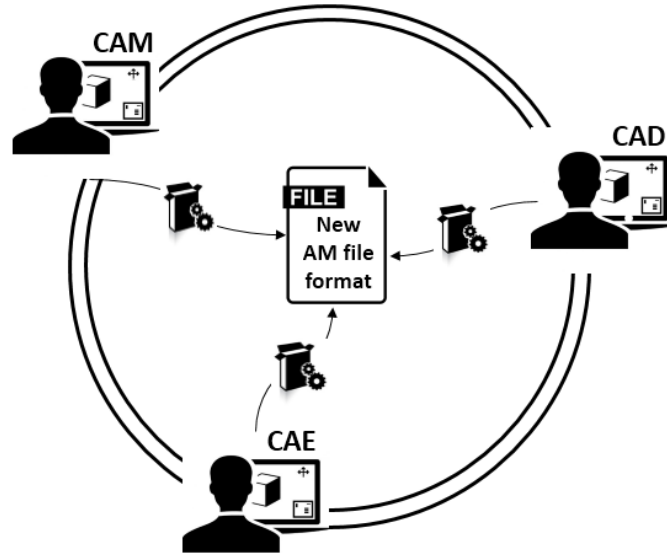


Figure 4.25: Proposal of a new CAD file format for additive manufacturing taking into aspect CAD, CAE and CAM requirements

future work is needed to optimise the lattice structure struts and overcome the stress concentration areas.

Lattice structure partitioning

In the proposed lattice structure design method, the partitions were defined by the engineer based on the FEA results. However, it would be interesting to have a detail method to define this partitions. This will help engineers to choose the most optimised partitions. The approach proposed in this work opens the path for future research in this area.

Bibliography

- Al-Ahmari, A. and K. Moiduddin
2014. Cad issues in additive manufacturing. *Comprehensive Materials Processing. Advances in Additive Manufacturing and Tooling*, 10:375–399.
- Ashby, M.
2006. The properties of foams and lattices. *Philosophical Transactions of the Royal Society of London A: Mathematical, Physical and Engineering Sciences*, 364(1838):15–30.
- Ashby, M.
2013. Designing architected materials. *Scripta Materialia*, 68(1):4–7.
- Ashby, M. F., T. Evans, N. A. Fleck, J. Hutchinson, H. Wadley, and L. Gibson
2000. *Metal Foams: A Design Guide*. Elsevier.
- Beyer, C.
2014. Strategic implications of current trends in additive manufacturing. *Journal of Manufacturing Science and Engineering*, 136(6):064701.
- Bhandarkar, M. P., B. Downie, M. Hardwick, and R. Nagi
2000. Migrating from iges to step: one to one translation of iges drawing to step drafting data. *Computers in industry*, 41(3):261–277.
- Brackett, D., I. Ashcroft, and R. Hague
2011. Topology optimization for additive manufacturing. In *Proceedings of the Solid Freeform Fabrication Symposium, Austin, TX*, Pp. 348–362.
- Campbell, I., D. Bourell, and I. Gibson
2012. Additive manufacturing: rapid prototyping comes of age. *Rapid Prototyping Journal*, 18(4):255–258.
- Chu, C., G. Graf, and D. W. Rosen
2008. Design for additive manufacturing of cellular structures. *Computer-Aided Design and Applications*, 5(5):686–696.
- Cooper, D. E., M. Stanford, K. A. Kibble, and G. J. Gibbons
2012. Additive manufacturing for product improvement at red bull technology. *Materials & Design*, 41:226–230.

Bibliography

- Darwish, S. M. and M. U. Aslam
2016. Auxetic cellular structures for custom made orthopedic implants using additive manufacturing. *International Journal of Engineering and Advanced Technology (IJEAT)*, 4(2).
- Deshpande, V., M. Ashby, and N. Fleck
2001. Foam topology: bending versus stretching dominated architectures. *Acta Materialia*, 49(6):1035–1040.
- Dong, L., V. Deshpande, and H. Wadley
2015. Mechanical response of ti-6al-4v octet-truss lattice structures. *International Journal of Solids and Structures*, 60:107–124.
- Dutta, B. and F. Froes
2015. 24-the additive manufacturing (am) of titanium alloys. *Titanium Powder Metallurgy, Butterworth-Heinemann, Boston*, Pp. 447–468.
- Evans, A. G., J. W. Hutchinson, N. A. Fleck, M. Ashby, and H. Wadley
2001. The topological design of multifunctional cellular metals. *Progress in Materials Science*, 46(3):309–327.
- Fall, G. C.
2013. Industry research monitor: Additive manufacturing. *General Electric Corporation, (accessed in April 2014) http://www.americas.gecapital.com/GECA_Document/Additive_Manufacturing_Fall_201*, 3.
- Finnegan, K., G. Kooistra, H. N. Wadley, and V. Deshpande
2007. The compressive response of carbon fiber composite pyramidal truss sandwich cores. *International Journal of Materials Research*, 98(12):1264–1272.
- Froes, F. and B. Dutta
2014. The additive manufacturing (am) of titanium alloys. In *Advanced Materials Research*, volume 1019, Pp. 19–25. Trans Tech Publ.
- Gibson, L. J.
2005. Biomechanics of cellular solids. *Journal of biomechanics*, 38(3):377–399.
- Gibson, L. J. and M. F. Ashby
1999. *Cellular solids: structure and properties*. Cambridge university press.

- Hiller, J. D. and H. Lipson
2009. Stl 2.0: a proposal for a universal multi-material additive manufacturing file format. In *Proceedings of the Solid Freeform Fabrication Symposium*, number 1, Pp. 266–278. Citeseer.
- Iyer, A., S. G. Kapoor, and R. E. DeVor
2001. Cad data visualization for machining simulation using the step standard. *Journal of manufacturing systems*, 20(3):198.
- Kooistra, G. W. and H. N. Wadley
2007. Lattice truss structures from expanded metal sheet. *Materials & Design*, 28(2):507–514.
- Kranz, J., D. Herzog, and C. Emmelmann
2015. Design guidelines for laser additive manufacturing of lightweight structures in tial6v4. *Journal of Laser Applications*, 27(S1):S14001.
- Li, Q., E. Y. Chen, D. R. Bice, and D. C. Dunand
2008. Mechanical properties of cast ti-6al-4v lattice block structures. *Metallurgical and Materials Transactions A*, 39(2):441–449.
- Lu, W., F. Lin, J. Han, H. Qi, and N. Yan
2009. Scan strategy in electron beam selective melting. *Tsinghua Science & Technology*, 14:120–126.
- Manfredi, D., E. Ambrosio, F. Calignano, M. Krishnan, R. Canali, S. Biamino, M. Pavese, E. Atzeni, L. Iuliano, P. Fino, et al.
2014. Direct metal laser sintering: an additive manufacturing technology ready to produce lightweight structural parts for robotic applications. *La metallurgia italiana*, (10).
- McHenry, K. and P. Bajcsy
2008. An overview of 3d data content, file formats and viewers. *National Center for Supercomputing Applications*, 1205.
- McMains, S., J. Smith, and C. Séquin
2002. The evolution of a layered manufacturing interchange format. In *ASME 2002 International Design Engineering Technical Conferences and Computers and Information in Engineering Conference*, Pp. 945–953. American Society of Mechanical Engineers.
- Moongkhamklang, P., D. M. Elzey, and H. N. Wadley
2008. Titanium matrix composite lattice structures. *Composites Part A: applied science and manufacturing*, 39(2):176–187.

Bibliography

- Mun, J., B.-G. Yun, J. Ju, and B.-M. Chang
2015. Indirect additive manufacturing based casting of a periodic 3d cellular metal–flow simulation of molten aluminum alloy. *Journal of Manufacturing Processes*, 17:28–40.
- Nadeau, D. R., J. L. Moreland, and M. M. Heck
1998. Introduction to vrml 97. *ACM SIGGRAPH '98 Course Notes*.
- Neff, C.
2015. *Mechanical Properties of Laser-Sintered-Nylon Diamond Lattices*. PhD thesis, University of South Florida.
- Ponader, S., E. Vairaktaris, P. Heintz, C. v. Wilmowsky, A. Rottmair, C. Körner, R. F. Singer, S. Holst, K. A. Schlegel, F. W. Neukam, et al.
2008. Effects of topographical surface modifications of electron beam melted ti-6al-4v titanium on human fetal osteoblasts. *Journal of biomedical materials research Part A*, 84(4):1111–1119.
- Queheillalt, D. T. and H. N. Wadley
2005. Cellular metal lattices with hollow trusses. *Acta Materialia*, 53(2):303–313.
- Rashed, M., M. Ashraf, R. Mines, and P. J. Hazell
2016. Metallic microlattice materials: A current state of the art on manufacturing, mechanical properties and applications. *Materials & Design*, 95:518–533.
- Reinhart, G. and S. Teufelhart
2011. Load-adapted design of generative manufactured lattice structures. *Physics Procedia*, 12:385–392.
- Rochus, P., J.-Y. Plessier, M. Van Elsen, J.-P. Kruth, R. Carrus, and T. Dormal
2007. New applications of rapid prototyping and rapid manufacturing (rp/rm) technologies for space instrumentation. *Acta Astronautica*, 61(1):352–359.
- Rosen, D. W.
2007. Computer-aided design for additive manufacturing of cellular structures. *Computer-Aided Design and Applications*, 4(5):585–594.
- Standard, A.
2012. F2792. 2012. standard terminology for additive manufacturing technologies. *ASTM F2792-10e1*.

Bibliography

Suard, M.

2015. *Characterization and optimization of lattice structures made by Electron Beam Melting*. PhD thesis, Univ. Grenoble Alpes.

Tang, Y., J.-Y. Hascoet, and Y. F. Zhao

2014. Integration of topological and functional optimization in design for additive manufacturing. In *ASME 2014 12th Biennial Conference on Engineering Systems Design and Analysis*, Pp. V001T06A006–V001T06A006. American Society of Mechanical Engineers.

Thompson, M. K., G. Moroni, T. Vaneker, G. Fadel, R. I. Campbell, I. Gibson, A. Bernard, J. Schulz, P. Graf, B. Ahuja, et al.

2016. Design for additive manufacturing: Trends, opportunities, considerations, and constraints. *CIRP Annals-Manufacturing Technology*, 65(2):737–760.

Vayre, B., F. Vignat, and F. Villeneuve

2012a. Designing for additive manufacturing. *Procedia CIRP*, 3:632–637.

Vayre, B., F. Vignat, and F. Villeneuve

2012b. Metallic additive manufacturing: state-of-the-art review and prospects. *Mechanics & Industry*, 13(02):89–96.

Wadley, H. N.

2002. Cellular metals manufacturing. *Advanced Engineering Materials*, 4(10):726–733.

Wadley, H. N.

2006. Multifunctional periodic cellular metals. *Philosophical Transactions of the Royal Society of London A: Mathematical, Physical and Engineering Sciences*, 364(1838):31–68.

Wadley, H. N., N. A. Fleck, and A. G. Evans

2003. Fabrication and structural performance of periodic cellular metal sandwich structures. *Composites Science and Technology*, 63(16):2331–2343.

Wang, J., A. Evans, K. Dharmasena, and H. Wadley

2003. On the performance of truss panels with kagome cores. *International Journal of Solids and Structures*, 40(25):6981–6988.

Wolcott, M. P.

1990. Cellular solids: Structure and properties: by lorna j. gibson and michael f. ashby; published by pergamon, oxford, 1988; 358 pp.

Bibliography

- Wong, K. V. and A. Hernandez
2012. A review of additive manufacturing. *ISRN Mechanical Engineering*.
- Zhang, P., J. Toman, Y. Yu, E. Biyikli, M. Kirca, M. Chmielus, and A. C. To
2015. Efficient design-optimization of variable-density hexagonal cellular structure by additive manufacturing: theory and validation. *Journal of Manufacturing Science and Engineering*, 137(2):021004.
- Zheng, X., H. Lee, T. H. Weisgraber, M. Shusteff, J. DeOtte, E. B. Duoss, J. D. Kuntz, M. M. Biener, Q. Ge, J. A. Jackson, et al.
2014. Ultralight, ultrastiff mechanical metamaterials. *Science*, 344(6190):1373–1377.
- Zhu, H., J. Knott, and N. Mills
1997. Analysis of the elastic properties of open-cell foams with tetrakaidecahedral cells. *Journal of the Mechanics and Physics of Solids*, 45(3):319–343.

APPENDIX A

Detailed FEA simulation results for the lattice structures

Table A.1 shows the result for the cubic lattice structure which contains the relative Young's modulus, relative shear modulus and relative strength in function of the relative density for 0° and 45° angle positions.

		Cubic lattice structure									
		Positioned at 0° angle					Positioned at 45° angle				
		Compression			Shear		Compression			Shear	
Elementary Structure Length [mm]	Thickness [mm]	Relative density [without unit]	Relative Young's modulus [without unit]	Relative strength [without unit]	Relative shear modulus [without unit]	Relative strength [without unit]	Relative Young's modulus [without unit]	Relative strength [without unit]	Relative shear modulus [without unit]	Relative strength [without unit]	
5	1	0.11	0.044	0.039	4.25E-03	5.22E-03	3.11E-03	7.13E-03	3.13E-03	4.14E-03	
5	1.5	0.23	0.106	0.085	1.94E-02	1.57E-02	1.73E-02	2.53E-02	1.37E-02	1.10E-02	
5	2	0.37	0.197	0.150	5.52E-02	3.65E-02	5.94E-02	6.37E-02	3.85E-02	2.50E-02	
10	1	0.03	0.008	0.008	2.53E-04	5.90E-04	1.63E-04	7.23E-04	2.08E-04	5.50E-04	
10	1.5	0.07	0.022	0.021	1.25E-03	1.90E-03	9.06E-04	2.58E-03	1.02E-03	1.68E-03	
10	2	0.11	0.042	0.035	4.17E-03	5.07E-03	3.21E-03	7.10E-03	3.17E-03	4.12E-03	
15	1	0.01	0.002	0.003	4.88E-05	1.71E-04	3.09E-05	2.12E-04	4.22E-05	1.61E-04	
15	1.5	0.03	0.008	0.008	2.42E-04	5.52E-04	1.67E-04	7.19E-04	2.09E-04	5.12E-04	
15	2	0.05	0.017	0.017	8.38E-04	1.54E-03	5.91E-04	2.00E-03	6.68E-04	1.28E-03	
20	1	0.01	0.001	0.001	1.53E-05	7.03E-05	1.01E-05	8.97E-05	1.40E-05	6.88E-05	
20	1.5	0.02	0.003	0.003	7.46E-05	2.28E-04	5.30E-05	3.22E-04	6.76E-05	2.37E-04	
20	2	0.03	0.007	0.008	2.53E-04	5.85E-04	1.73E-04	7.83E-04	2.10E-04	5.64E-04	

Table A.1: Relative Young's modulus and relative strength for cubic lattice structure compression and shear test at 0° and 45° angle

Table A.2 shows the result for the octet-truss lattice structure which contains the relative Young's modulus, relative shear modulus and relative strength in function of the relative density.

Appendix A. Detailed FEA simulation results for the lattice structures

		Octet-truss lattice structure								
		Positioned at 0° angle					Positioned at 45° angle			
		Compression			Shear		Compression		Shear	
Elementary Structure Length [mm]	Thickness [mm]	Relative density [without unit]	Relative Young's modulus [without unit]	Relative strength [without unit]	Relative shear modulus [without unit]	Relative strength [without unit]	Relative Young's modulus [without unit]	Relative strength [without unit]	Relative shear modulus [without unit]	Relative strength [without unit]
5	1	0.45	0.188	0.124	0.077	0.035	0.133	0.088	0.069	0.034
5	1.5	N/A	N/A	N/A	N/A	N/A	N/A	N/A	N/A	N/A
5	2	N/A	N/A	N/A	N/A	N/A	N/A	N/A	N/A	N/A
10	1	0.14	0.025	0.027	0.013	0.008	0.032	0.023	0.011	0.007
10	1.5	0.29	0.078	0.062	0.035	0.019	0.081	0.060	0.031	0.017
10	2	0.45	0.188	0.125	0.078	0.036	0.134	0.087	0.069	0.033
15	1	0.07	0.009	0.010	0.005	0.004	0.011	0.009	0.004	0.003
15	1.5	0.14	0.026	0.028	0.013	0.008	0.033	0.024	0.011	0.008
15	2	0.24	0.056	0.048	0.026	0.014	0.059	0.046	0.023	0.014
20	1	0.04	0.004	0.006	0.003	0.002	0.004	0.003	0.002	0.002
20	1.5	0.09	0.012	0.014	0.007	0.005	0.015	0.012	0.006	0.004
20	2	0.14	0.025	0.027	0.013	0.008	0.032	0.024	0.011	0.007

Table A.2: Relative Young's modulus and relative strength for octet-truss lattice structure compression and shear test at 0° and 45° angle

Table A.3 shows the result for the hexa-truss lattice structure which contains the relative Young's modulus, relative shear modulus and relative strength in function of the relative density.

		Hexa lattice structure								
		Positioned at 0° angle					Positioned at 45° angle			
		Compression			Shear		Compression		Shear	
Elementary Structure Length [mm]	Thickness [mm]	Relative density [without unit]	Relative Young's modulus [without unit]	Relative strength [without unit]	Relative shear modulus [without unit]	Relative strength [without unit]	Relative Young's modulus [without unit]	Relative strength [without unit]	Relative shear modulus [without unit]	Relative strength [without unit]
5	1	0.25	7.60E-02	5.80E-02	2.47E-02	1.46E-02	4.42E-02	4.41E-02	2.34E-02	1.43E-02
5	1.5	N/A	N/A	N/A	N/A	N/A	N/A	N/A	N/A	N/A
5	2	N/A	N/A	N/A	N/A	N/A	N/A	N/A	N/A	N/A
10	1	0.08	5.98E-03	7.72E-03	2.12E-03	2.24E-03	3.69E-03	6.09E-03	1.89E-03	2.22E-03
10	1.5	0.16	2.83E-02	2.75E-02	9.39E-03	7.22E-03	1.67E-02	2.08E-02	7.07E-03	6.88E-03
10	2	0.25	7.56E-02	5.90E-02	2.47E-02	1.48E-02	3.96E-02	3.82E-02	2.21E-02	1.46E-02
15	1	0.04	1.24E-03	2.16E-03	4.33E-04	6.49E-04	7.78E-04	1.77E-03	3.80E-04	6.83E-04
15	1.5	0.08	6.07E-03	7.73E-03	2.08E-03	2.18E-03	3.64E-03	6.01E-03	1.87E-03	2.23E-03
15	2	0.13	1.81E-02	1.85E-02	6.13E-03	5.12E-03	1.13E-02	1.46E-02	5.57E-03	5.01E-03
20	1	0.02	3.82E-04	9.08E-04	1.38E-04	2.73E-04	2.46E-04	7.34E-04	1.19E-04	2.81E-04
20	1.5	0.04	1.98E-03	3.29E-03	6.89E-04	9.54E-04	1.20E-03	2.41E-03	6.11E-04	9.63E-04
20	2	0.08	6.11E-03	7.56E-03	2.10E-03	2.23E-03	3.51E-03	5.91E-03	1.88E-03	2.25E-03

Table A.3: Relative Young's modulus and relative strength for hexa-truss lattice structure compression and shear test at 0° and 45° angle

Table A.4 shows the result for the open-cell foam lattice structure which

Appendix A. Detailed FEA simulation results for the lattice structures

contains the relative Young's modulus, relative shear modulus and relative strength in function of the relative density for tests in 0° and 45° position angles.

Open-cell foam lattice structure										
		Positioned at 0° angle					Positioned at 45° angle			
		Compression			Shear		Compression		Shear	
Elementary Structure Length [mm]	Thickness [mm]	Relative density [without unit]	Relative Young's modulus [without unit]	Relative strength [without unit]	Relative shear modulus [without unit]	Relative strength [without unit]	Relative Young's modulus [without unit]	Relative strength [without unit]	Relative shear modulus [without unit]	Relative strength [without unit]
5	1	0.13	7.47E-03	1.03E-02	1.78E-03	2.64E-03	1.16E-02	1.09E-02	2.78E-03	3.23E-03
5	1.5	0.25	3.28E-02	3.68E-02	8.70E-03	8.75E-03	4.23E-02	3.34E-02	1.20E-02	9.78E-03
5	2	0.39	8.64E-02	6.84E-02	2.45E-02	1.67E-02	9.75E-03	6.56E-02	1.82E-02	2.02E-02
10	1	0.04	5.32E-04	1.11E-03	1.16E-04	3.16E-04	8.53E-04	1.62E-03	1.92E-04	4.31E-04
10	1.5	0.08	2.51E-03	4.00E-03	5.85E-04	1.10E-03	3.86E-03	4.85E-03	9.16E-04	1.45E-03
10	2	0.13	7.81E-03	1.06E-02	1.82E-03	2.72E-03	1.12E-02	1.12E-02	2.78E-03	3.46E-03
15	1	0.02	1.04E-04	3.31E-04	2.24E-05	9.43E-05	1.56E-04	4.35E-04	3.62E-05	1.17E-04
15	1.5	0.04	5.00E-04	1.12E-03	1.15E-04	3.15E-04	8.05E-04	1.49E-03	1.85E-04	4.25E-04
15	2	0.06	1.59E-03	2.89E-03	3.67E-04	7.90E-04	2.36E-03	3.44E-03	5.80E-04	9.78E-04
20	1	N/A	N/A	N/A	N/A	N/A	N/A	N/A	N/A	N/A
20	1.5	0.02	1.59E-04	4.54E-04	3.62E-05	1.30E-04	2.57E-04	6.43E-04	5.87E-05	1.78E-04
20	2	0.04	5.33E-04	1.17E-03	1.18E-04	3.24E-04	7.83E-04	1.47E-03	1.83E-04	4.08E-04

Table A.4: Relative Young's modulus and relative strength for open-cell lattice structure compression and shear test at 0° and 45° angle

APPENDIX B

Skeleton model points, lines, sections and joints lists

Point list				Line list		
Index	X	Y	Z	Index	Begin (point)	End (point)
1	0	0	0	1	1	4
2	1	0	0	2	2	3
3	0	0	1	3	5	8
4	1	0	1	4	6	7
5	0	1	0	5	3	5
6	1	1	0	6	1	7
7	0	1	1	7	4	6
8	1	1	1	8	2	8
9	0.5	0	0.5	9	7	4
10	0	0.5	0.5	10	3	8
11	0.5	0.5	0	11	1	6
12	1	0.5	0.5	12	5	2
13	0.5	0.5	1	13	5	3
14	0.5	1	0.5	14	1	7
				15	4	6
				16	2	8
				17	9	10
				18	9	11
				19	9	12
				20	9	13
				21	14	10
				22	14	11
				23	14	12
				24	14	13
				25	10	11
				26	11	12
				27	12	13
				28	10	13

Table B.1: Elementary octet-truss structure: Point and line list

Appendix B. Skeleton model points, lines, sections and joints lists

Point list				Line list		
Index	X	Y	Z	Index	Begin (point)	End (point)
1	0.25	0.5	0	1	1	7
2	0.5	0.25	0	2	3	9
3	0.75	0.5	0	3	11	15
4	0.5	0.75	0	4	13	5
5	0	0.5	0.75	5	2	18
6	0	0.25	0.5	6	6	17
7	0	0.5	0.25	7	10	19
8	0	0.75	0.5	8	14	20
9	1	0.5	0.25	9	8	21
10	1	0.25	0.5	10	4	22
11	1	0.5	0.75	11	12	23
12	1	0.75	0.5	12	16	24
13	0.25	0.5	1	13	1	2
14	0.5	0.25	1	14	2	3
15	0.75	0.5	1	15	3	4
16	0.5	0.75	1	16	4	1
17	0.25	0	0.5	17	5	6
18	0.5	0	0.25	18	6	7
19	0.75	0	0.5	19	7	8
20	0.5	0	0.75	20	8	5
21	0.25	1	0.5	21	9	10
22	0.5	1	0.25	22	10	11
23	0.75	1	0.5	23	11	12
24	0.5	1	0.75	24	12	9
				25	13	14
				26	14	15
				27	15	16
				28	16	13
				29	17	18
				30	18	19
				31	19	20
				32	20	17
				33	21	22
				34	22	23
				35	23	24
				36	24	21

Table B.2: Elementary hexa-truss structure: Point and line list

Appendix B. Skeleton model points, lines, sections and joints lists

Point list				Line list		
Index	X	Y	Z	Index	Begin (point)	End (point)
1	2.5	2.5	2.5	1	1	2
2	7.5	2.5	2.5	2	2	4
3	2.5	7.5	2.5	3	4	3
4	7.5	7.5	2.5	4	3	1
5	2.5	2.5	7.5	5	5	6
6	7.5	2.5	7.5	6	6	8
7	2.5	7.5	7.5	7	8	7
8	7.5	7.5	7.5	8	7	5
9	5	0	2.5	9	1	5
10	5	2.5	2.5	10	2	6
11	5	0	7.5	11	3	7
12	5	2.5	7.5	12	4	8
13	5	7.5	2.5	13	9	10
14	5	10	2.5	14	11	12
15	5	7.5	7.5	15	13	14
16	5	10	7.5	16	15	16
17	2.5	5	0	17	17	18
18	2.5	5	2.5	18	19	20
19	7.5	5	0	19	21	22
20	7.5	5	2.5	20	23	24
21	2.5	5	7.5	21	25	26
22	2.5	5	10	22	27	28
23	7.5	5	7.5	23	29	30
24	7.5	5	10	24	31	32
25	0	2.5	5			
26	2.5	2.5	5			
27	0	7.5	5			
28	2.5	7.5	5			
29	7.5	2.5	5			
30	10	2.5	5			
31	7.5	7.5	5			
32	10	7.5	5			

Table B.3: Elementary open-cell foam structure: Point and line list

Appendix B. Skeleton model points, lines, sections and joints lists

Points : 64				Lines: 144															
Index	X	Y	Z	Index	X	Y	Z	Index	Begin	End	Index	Begin	End	Index	Begin	End	Index	Begin	End
1	0.0	0.0	0.0	44	2.0	2.0	3.0	1	1	2	44	23	15	87	41	42	130	58	59
2	1.0	0.0	0.0	45	2.0	3.0	0.0	2	2	4	45	21	23	88	38	43	131	56	60
3	0.0	1.0	0.0	46	2.0	3.0	1.0	3	4	3	46	22	24	89	43	22	132	60	44
4	1.0	1.0	0.0	47	2.0	3.0	2.0	4	3	1	47	18	26	90	42	43	133	59	60
5	0.0	0.0	1.0	48	2.0	3.0	3.0	5	5	6	48	26	25	91	40	44	134	57	61
6	1.0	0.0	1.0	49	3.0	0.0	0.0	6	6	8	49	25	17	92	44	24	135	61	45
7	0.0	1.0	1.0	50	3.0	1.0	0.0	7	8	7	50	20	28	93	43	44	136	58	62
8	1.0	1.0	1.0	51	3.0	0.0	1.0	8	7	5	51	28	27	94	41	45	137	62	46
9	0.0	0.0	2.0	52	3.0	1.0	1.0	9	1	5	52	27	19	95	45	26	138	61	62
10	1.0	0.0	2.0	53	3.0	0.0	2.0	10	2	6	53	25	27	96	42	46	139	59	63
11	0.0	1.0	2.0	54	3.0	1.0	2.0	11	3	7	54	26	28	97	46	28	140	63	47
12	1.0	1.0	2.0	55	3.0	0.0	3.0	12	4	8	55	22	30	98	45	46	141	62	63
13	0.0	0.0	3.0	56	3.0	1.0	3.0	13	9	10	56	30	29	99	43	47	142	60	64
14	1.0	0.0	3.0	57	3.0	2.0	0.0	14	10	12	57	29	21	100	47	30	143	64	48
15	0.0	1.0	3.0	58	3.0	2.0	1.0	15	12	11	58	27	29	101	46	47	144	63	64
16	1.0	1.0	3.0	59	3.0	2.0	2.0	16	11	9	59	28	30	102	44	48			
17	0.0	2.0	0.0	60	3.0	2.0	3.0	17	5	9	60	24	32	103	48	32			
18	1.0	2.0	0.0	61	3.0	3.0	0.0	18	6	10	61	32	31	104	47	48			
19	0.0	2.0	1.0	62	3.0	3.0	1.0	19	7	11	62	31	23	105	33	49			
20	1.0	2.0	1.0	63	3.0	3.0	2.0	20	8	12	63	29	31	106	49	50			
21	0.0	2.0	2.0	64	3.0	3.0	3.0	21	13	14	64	30	32	107	50	34			
22	1.0	2.0	2.0					22	14	16	65	2	33	108	35	51			
23	0.0	2.0	3.0					23	16	15	66	33	34	109	51	52			
24	1.0	2.0	3.0					24	15	13	67	34	4	110	52	36			
25	0.0	3.0	0.0					25	9	13	68	6	35	111	49	51			
26	1.0	3.0	0.0					26	10	14	69	35	36	112	50	52			
27	0.0	3.0	1.0					27	11	15	70	36	8	113	37	53			
28	1.0	3.0	1.0					28	12	16	71	33	35	114	53	54			
29	0.0	3.0	2.0					29	4	18	72	34	36	115	54	38			
30	1.0	3.0	2.0					30	18	17	73	10	37	116	51	53			
31	0.0	3.0	3.0					31	17	3	74	37	38	117	52	54			
32	1.0	3.0	3.0					32	8	20	75	38	12	118	39	55			
33	2.0	0.0	0.0					33	20	19	76	35	37	119	55	56			
34	2.0	1.0	0.0					34	19	7	77	36	38	120	56	40			
35	2.0	0.0	1.0					35	17	19	78	14	39	121	53	55			
36	2.0	1.0	1.0					36	18	20	79	39	40	122	54	56			
37	2.0	0.0	2.0					37	12	22	80	40	16	123	50	57			
38	2.0	1.0	2.0					38	22	21	81	37	39	124	57	41			
39	2.0	0.0	3.0					39	21	11	82	38	40	125	52	58			
40	2.0	1.0	3.0					40	19	21	83	34	41	126	58	42			
41	2.0	2.0	0.0					41	20	22	84	41	18	127	57	58			
42	2.0	2.0	1.0					42	16	24	85	36	42	128	54	59			
43	2.0	2.0	2.0					43	24	23	86	42	20	129	59	43			

Table B.4: 3 x 3 x 3 unit cubic lattice structure with with a pitch size of one

Appendix B. Skeleton model points, lines, sections and joints lists

Points : 64				Lines: 144												
Index	X	Y	Z	Index	X	Y	Z	Index	Begin	End	Index	Begin	End	Index	Begin	End
1	0.0	0.0	0.0	44	4.0	4.0	6.0	1	1	2	44	23	15	87	41	42
2	2.0	0.0	0.0	45	4.0	6.0	0.0	2	2	4	45	21	23	88	38	43
3	0.0	2.0	0.0	46	4.0	6.0	2.0	3	4	3	46	22	24	89	43	22
4	2.0	2.0	0.0	47	4.0	6.0	4.0	4	3	1	47	18	26	90	42	43
5	0.0	0.0	2.0	48	4.0	6.0	6.0	5	5	6	48	26	25	91	40	44
6	2.0	0.0	2.0	49	6.0	0.0	0.0	6	6	8	49	25	17	92	44	24
7	0.0	2.0	2.0	50	6.0	2.0	0.0	7	8	7	50	20	28	93	43	44
8	2.0	2.0	2.0	51	6.0	0.0	2.0	8	7	5	51	28	27	94	41	45
9	0.0	0.0	4.0	52	6.0	2.0	2.0	9	1	5	52	27	19	95	45	26
10	2.0	0.0	4.0	53	6.0	0.0	4.0	10	2	6	53	25	27	96	42	46
11	0.0	2.0	4.0	54	6.0	2.0	4.0	11	3	7	54	26	28	97	46	28
12	2.0	2.0	4.0	55	6.0	0.0	6.0	12	4	8	55	22	30	98	45	46
13	0.0	0.0	6.0	56	6.0	2.0	6.0	13	9	10	56	30	29	99	43	47
14	2.0	0.0	6.0	57	6.0	4.0	0.0	14	10	12	57	29	21	100	47	30
15	0.0	2.0	6.0	58	6.0	4.0	2.0	15	12	11	58	27	29	101	46	47
16	2.0	2.0	6.0	59	6.0	4.0	4.0	16	11	9	59	28	30	102	44	48
17	0.0	4.0	0.0	60	6.0	4.0	6.0	17	5	9	60	24	32	103	48	32
18	2.0	4.0	0.0	61	6.0	6.0	0.0	18	6	10	61	32	31	104	47	48
19	0.0	4.0	2.0	62	6.0	6.0	2.0	19	7	11	62	31	23	105	33	49
20	2.0	4.0	2.0	63	6.0	6.0	4.0	20	8	12	63	29	31	106	49	50
21	0.0	4.0	4.0	64	6.0	6.0	6.0	21	13	14	64	30	32	107	50	34
22	2.0	4.0	4.0					22	14	16	65	2	33	108	35	51
23	0.0	4.0	6.0					23	16	15	66	33	34	109	51	52
24	2.0	4.0	6.0					24	15	13	67	34	4	110	52	36
25	0.0	6.0	0.0					25	9	13	68	6	35	111	49	51
26	2.0	6.0	0.0					26	10	14	69	35	36	112	50	52
27	0.0	6.0	2.0					27	11	15	70	36	8	113	37	53
28	2.0	6.0	2.0					28	12	16	71	33	35	114	53	54
29	0.0	6.0	4.0					29	4	18	72	34	36	115	54	38
30	2.0	6.0	4.0					30	18	17	73	10	37	116	51	53
31	0.0	6.0	6.0					31	17	3	74	37	38	117	52	54
32	2.0	6.0	6.0					32	8	20	75	38	12	118	39	55
33	4.0	0.0	0.0					33	20	19	76	35	37	119	55	56
34	4.0	2.0	0.0					34	19	7	77	36	38	120	56	40
35	4.0	0.0	2.0					35	17	19	78	14	39	121	53	55
36	4.0	2.0	2.0					36	18	20	79	39	40	122	54	56
37	4.0	0.0	4.0					37	12	22	80	40	16	123	50	57
38	4.0	2.0	4.0					38	22	21	81	37	39	124	57	41
39	4.0	0.0	6.0					39	21	11	82	38	40	125	52	58
40	4.0	2.0	6.0					40	19	21	83	34	41	126	58	42
41	4.0	4.0	0.0					41	20	22	84	41	18	127	57	58
42	4.0	4.0	2.0					42	16	24	85	36	42	128	54	59
43	4.0	4.0	4.0					43	24	23	86	42	20	129	59	43

Table B.5: Scaled 3 x 3 x 3 unit cubic lattice structure with a pitch size of 2

Appendix B. Skeleton model points, lines, sections and joints lists

Points : 64				Lines : 144												
Index	X	Y	Z	Index	X	Y	Z	Index	Begin	End	Index	Begin	End	Index	Begin	End
1	0.0	0.0	0.0	44	4.0	2.0	3.0	1	1	2	44	23	15	87	41	42
2	1.0	0.0	0.0	45	4.0	3.0	0.0	2	2	4	45	21	23	88	38	43
3	0.0	1.0	0.0	46	4.0	3.0	1.0	3	4	3	46	22	24	89	43	22
4	1.0	1.0	0.0	47	4.0	3.0	2.0	4	3	1	47	18	26	90	42	43
5	0.0	0.0	1.0	48	4.0	3.0	3.0	5	5	6	48	26	25	91	40	44
6	1.0	0.0	1.0	49	9.0	0.0	0.0	6	6	8	49	25	17	92	44	24
7	0.0	1.0	1.0	50	9.0	1.0	0.0	7	8	7	50	20	28	93	43	44
8	1.0	1.0	1.0	51	9.0	0.0	1.0	8	7	5	51	28	27	94	41	45
9	0.0	0.0	2.0	52	9.0	1.0	1.0	9	1	5	52	27	19	95	45	26
10	1.0	0.0	2.0	53	9.0	0.0	2.0	10	2	6	53	25	27	96	42	46
11	0.0	1.0	2.0	54	9.0	1.0	2.0	11	3	7	54	26	28	97	46	28
12	1.0	1.0	2.0	55	9.0	0.0	3.0	12	4	8	55	22	30	98	45	46
13	0.0	0.0	3.0	56	9.0	1.0	3.0	13	9	10	56	30	29	99	43	47
14	1.0	0.0	3.0	57	9.0	2.0	0.0	14	10	12	57	29	21	100	47	30
15	0.0	1.0	3.0	58	9.0	2.0	1.0	15	12	11	58	27	29	101	46	47
16	1.0	1.0	3.0	59	9.0	2.0	2.0	16	11	9	59	28	30	102	44	48
17	0.0	2.0	0.0	60	9.0	2.0	3.0	17	5	9	60	24	32	103	48	32
18	1.0	2.0	0.0	61	9.0	3.0	0.0	18	6	10	61	32	31	104	47	48
19	0.0	2.0	1.0	62	9.0	3.0	1.0	19	7	11	62	31	23	105	33	49
20	1.0	2.0	1.0	63	9.0	3.0	2.0	20	8	12	63	29	31	106	49	50
21	0.0	2.0	2.0	64	9.0	3.0	3.0	21	13	14	64	30	32	107	50	34
22	1.0	2.0	2.0					22	14	16	65	2	33	108	35	51
23	0.0	2.0	3.0					23	16	15	66	33	34	109	51	52
24	1.0	2.0	3.0					24	15	13	67	34	4	110	52	36
25	0.0	3.0	0.0					25	9	13	68	6	35	111	49	51
26	1.0	3.0	0.0					26	10	14	69	35	36	112	50	52
27	0.0	3.0	1.0					27	11	15	70	36	8	113	37	53
28	1.0	3.0	1.0					28	12	16	71	33	35	114	53	54
29	0.0	3.0	2.0					29	4	18	72	34	36	115	54	38
30	1.0	3.0	2.0					30	18	17	73	10	37	116	51	53
31	0.0	3.0	3.0					31	17	3	74	37	38	117	52	54
32	1.0	3.0	3.0					32	8	20	75	38	12	118	39	55
33	4.0	0.0	0.0					33	20	19	76	35	37	119	55	56
34	4.0	1.0	0.0					34	19	7	77	36	38	120	56	40
35	4.0	0.0	1.0					35	17	19	78	14	39	121	53	55
36	4.0	1.0	1.0					36	18	20	79	39	40	122	54	56
37	4.0	0.0	2.0					37	12	22	80	40	16	123	50	57
38	4.0	1.0	2.0					38	22	21	81	37	39	124	57	41
39	4.0	0.0	3.0					39	21	11	82	38	40	125	52	58
40	4.0	1.0	3.0					40	19	21	83	34	41	126	58	42
41	4.0	2.0	0.0					41	20	22	84	41	18	127	57	58
42	4.0	2.0	1.0					42	16	24	85	36	42	128	54	59
43	4.0	2.0	2.0					43	24	23	86	42	20	129	59	43

Table B.6: Scaled 3 x 3 x 3 unit cubic lattice structure with gradient elementary structures

Appendix B. Skeleton model points, lines, sections and joints lists

Points: 64				Lines: 105					
Index	X	Y	Z	Index	Begin	End	Index	Begin	End
1	0	0	0	1	1	2	54	27	28
2	0.01	0.01	0	2	2	4	55	27	29
3	0	0.01	0	3	4	3	56	29	18
4	0.01	0.02	0	4	3	1	57	28	30
5	0	0	0.01	5	5	6	58	30	20
6	0.01	0.01	0.01	6	6	8	59	29	30
7	0	0.01	0.01	7	8	7	60	21	31
8	0.01	0.02	0.01	8	7	5	61	31	32
9	0	0.02	0	9	1	5	62	32	22
10	0.01	0.03	0	10	2	6	63	23	33
11	0	0.02	0.01	11	3	7	64	33	34
12	0.01	0.03	0.01	12	4	8	65	34	24
13	0	0.03	0	13	4	10	66	31	33
14	0.01	0.03	0	14	10	9	67	32	34
15	0	0.03	0.01	15	9	3	68	32	35
16	0.01	0.03	0.01	16	8	12	69	35	25
17	0	0.04	0	17	12	11	70	34	36
18	0.01	0.04	0	18	11	7	71	36	26
19	0	0.04	0.01	19	9	11	72	35	36
20	0.01	0.04	0.01	20	10	12	73	35	37
21	0.02	0.02	0	21	10	14	74	37	27
22	0.02	0.03	0	22	14	13	75	36	38
23	0.02	0.02	0.01	23	13	9	76	38	28
24	0.02	0.03	0.01	24	12	16	77	37	38
25	0.02	0.03	0	25	16	15	78	37	39
26	0.02	0.03	0.01	26	15	11	79	39	29
27	0.02	0.04	0	27	13	15	80	38	40
28	0.02	0.04	0.01	28	14	16	81	40	30
29	0.02	0.04	0	29	14	18	82	39	40
30	0.02	0.04	0.01	30	18	17	83	31	41
31	0.03	0.01	0	31	17	13	84	41	42
32	0.03	0.02	0	32	16	20	85	42	32
33	0.03	0.01	0.01	33	20	19	86	33	43
34	0.03	0.02	0.01	34	19	15	87	43	44
35	0.03	0.03	0	35	17	19	88	44	34
36	0.03	0.03	0.01	36	18	20	89	41	43
37	0.03	0.03	0	37	2	21	90	42	44
38	0.03	0.03	0.01	38	21	22	91	42	45
39	0.03	0.04	0	39	22	4	92	45	35
40	0.03	0.04	0.01	40	6	23	93	44	46
41	0.04	0	0	41	23	24	94	46	36
42	0.04	0.01	0	42	24	8	95	45	46
43	0.04	0	0.01	43	21	23	96	45	47
44	0.04	0.01	0.01	44	22	24	97	47	37
45	0.04	0.02	0	45	22	25	98	46	48
46	0.04	0.02	0.01	46	25	10	99	48	38
47	0.04	0.03	0	47	24	26	100	47	48
48	0.04	0.03	0.01	48	26	12	101	47	49
49	0.04	0.04	0	49	25	26	102	49	39
50	0.04	0.04	0.01	50	25	27	103	48	50
				51	27	14	104	50	40
				52	26	28	105	49	50
				53	28	16			

Table B.7: Conformal cubic lattice structure with non-parallel upper and lower boundaries

Appendix B. Skeleton model points, lines, sections and joints lists

Points: 54				Points: 54				Lines: 117			Lines: 117			Lines: 117		
Index	X	Y	Z	Index	X	Y	Z	Index	Begin	End	Index	Begin	End	Index	Begin	End
1	0.0	0.0	0.0	41	6.0	0.0	2.0	1	0	1	41	19	21	81	39	30
2	1.0	1.0	0.0	42	6.0	1.0	2.0	2	1	3	42	9	22	82	36	38
3	0.0	1.0	0.0	43	6.0	2.0	0.0	3	3	2	43	22	23	83	37	39
4	1.0	2.0	0.0	44	6.0	2.0	1.0	4	2	0	44	23	11	84	31	40
5	0.0	0.0	1.0	45	6.0	2.0	2.0	5	4	5	45	20	22	85	40	41
6	1.0	1.0	1.0	46	7.0	0.0	0.0	6	5	7	46	21	23	86	41	32
7	0.0	1.0	1.0	47	7.0	1.0	0.0	7	7	6	47	19	24	87	38	40
8	1.0	2.0	1.0	48	7.0	0.0	1.0	8	6	4	48	24	13	88	39	41
9	0.0	0.0	2.0	49	7.0	1.0	1.0	9	0	4	49	21	25	89	37	42
10	1.0	1.0	2.0	50	7.0	0.0	2.0	10	1	5	50	25	15	90	42	33
11	0.0	1.0	2.0	51	7.0	1.0	2.0	11	2	6	51	24	25	91	39	43
12	1.0	2.0	2.0	52	7.0	2.0	0.0	12	3	7	52	23	26	92	43	34
13	0.0	2.0	0.0	53	7.0	2.0	1.0	13	8	9	53	26	17	93	42	43
14	1.0	3.0	0.0	54	7.0	2.0	2.0	14	9	11	54	25	26	94	41	44
15	0.0	2.0	1.0					15	11	10	55	18	27	95	44	35
16	1.0	3.0	1.0					16	10	8	56	27	28	96	43	44
17	0.0	2.0	2.0					17	4	8	57	28	19	97	36	45
18	1.0	3.0	2.0					18	5	9	58	20	29	98	45	46
19	3.0	2.0	0.0					19	6	10	59	29	30	99	46	37
20	3.0	3.0	0.0					20	7	11	60	30	21	100	38	47
21	3.0	2.0	1.0					21	3	13	61	27	29	101	47	48
22	3.0	3.0	1.0					22	13	12	62	28	30	102	48	39
23	3.0	2.0	2.0					23	12	2	63	22	31	103	45	47
24	3.0	3.0	2.0					24	7	15	64	31	32	104	46	48
25	3.0	4.0	0.0					25	15	14	65	32	23	105	40	49
26	3.0	4.0	1.0					26	14	6	66	29	31	106	49	50
27	3.0	4.0	2.0					27	12	14	67	30	32	107	50	41
28	5.0	1.0	0.0					28	13	15	68	28	33	108	47	49
29	5.0	2.0	0.0					29	11	17	69	33	24	109	48	50
30	5.0	1.0	1.0					30	17	16	70	30	34	110	46	51
31	5.0	2.0	1.0					31	16	10	71	34	25	111	51	42
32	5.0	1.0	2.0					32	14	16	72	33	34	112	48	52
33	5.0	2.0	2.0					33	15	17	73	32	35	113	52	43
34	5.0	3.0	0.0					34	1	18	74	35	26	114	51	52
35	5.0	3.0	1.0					35	18	19	75	34	35	115	50	53
36	5.0	3.0	2.0					36	19	3	76	27	36	116	53	44
37	6.0	0.0	0.0					37	5	20	77	36	37	117	52	53
38	6.0	1.0	0.0					38	20	21	78	37	28			
39	6.0	0.0	1.0					39	21	7	79	29	38			
40	6.0	1.0	1.0					40	18	20	80	38	39			

Table B.8: Conformal cubic lattice structure with parallel upper and lower boundaries

Appendix B. Skeleton model points, lines, sections and joints lists

Points : 64				Lines: 144															
Index	X	Y	Z	Index	X	Y	Z	Index	Begin	End	Index	Begin	End	Index	Begin	End	Index	Begin	End
1	0.0	0.0	0.0	44	2.0	2.0	3.0	1	1	2	44	23	15	87	41	42	130	58	59
2	1.0	0.0	0.0	45	2.0	3.0	0.0	2	2	4	45	21	23	88	38	43	131	56	60
3	0.0	1.0	0.0	46	2.0	3.0	1.0	3	4	3	46	22	24	89	43	22	132	60	44
4	1.0	1.0	0.0	47	2.0	3.0	2.0	4	3	1	47	18	26	90	42	43	133	59	60
5	0.0	0.0	1.0	48	2.0	3.0	3.0	5	5	6	48	26	25	91	40	44	134	57	61
6	1.0	0.0	1.0	49	3.0	0.0	0.0	6	6	8	49	25	17	92	44	24	135	61	45
7	0.0	1.0	1.0	50	3.0	1.0	0.0	7	8	7	50	20	28	93	43	44	136	58	62
8	1.0	1.0	1.0	51	3.0	0.0	1.0	8	7	5	51	28	27	94	41	45	137	62	46
9	0.0	0.0	2.0	52	3.0	1.0	1.0	9	1	5	52	27	19	95	45	26	138	61	62
10	1.0	0.0	2.0	53	3.0	0.0	2.0	10	2	6	53	25	27	96	42	46	139	59	63
11	0.0	1.0	2.0	54	3.0	1.0	2.0	11	3	7	54	26	28	97	46	28	140	63	47
12	1.0	1.0	2.0	55	3.0	0.0	3.0	12	4	8	55	22	30	98	45	46	141	62	63
13	0.0	0.0	3.0	56	3.0	1.0	3.0	13	9	10	56	30	29	99	43	47	142	60	64
14	1.0	0.0	3.0	57	3.0	2.0	0.0	14	10	12	57	29	21	100	47	30	143	64	48
15	0.0	1.0	3.0	58	3.0	2.0	1.0	15	12	11	58	27	29	101	46	47	144	63	64
16	1.0	1.0	3.0	59	3.0	2.0	2.0	16	11	9	59	28	30	102	44	48			
17	0.0	2.0	0.0	60	3.0	2.0	3.0	17	5	9	60	24	32	103	48	32			
18	1.0	2.0	0.0	61	3.0	3.0	0.0	18	6	10	61	32	31	104	47	48			
19	0.0	2.0	1.0	62	3.0	3.0	1.0	19	7	11	62	31	23	105	33	49			
20	1.0	2.0	1.0	63	3.0	3.0	2.0	20	8	12	63	29	31	106	49	50			
21	0.0	2.0	2.0	64	3.0	3.0	3.0	21	13	14	64	30	32	107	50	34			
22	1.0	2.0	2.0					22	14	16	65	2	33	108	35	51			
23	0.0	2.0	3.0					23	16	15	66	33	34	109	51	52			
24	1.0	2.0	3.0					24	15	13	67	34	4	110	52	36			
25	0.0	3.0	0.0					25	9	13	68	6	35	111	49	51			
26	1.0	3.0	0.0					26	10	14	69	35	36	112	50	52			
27	0.0	3.0	1.0					27	11	15	70	36	8	113	37	53			
28	1.0	3.0	1.0					28	12	16	71	33	35	114	53	54			
29	0.0	3.0	2.0					29	4	18	72	34	36	115	54	38			
30	1.0	3.0	2.0					30	18	17	73	10	37	116	51	53			
31	0.0	3.0	3.0					31	17	3	74	37	38	117	52	54			
32	1.0	3.0	3.0					32	8	20	75	38	12	118	39	55			
33	2.0	0.0	0.0					33	20	19	76	35	37	119	55	56			
34	2.0	1.0	0.0					34	19	7	77	36	38	120	56	40			
35	2.0	0.0	1.0					35	17	19	78	14	39	121	53	55			
36	2.0	1.0	1.0					36	18	20	79	39	40	122	54	56			
37	2.0	0.0	2.0					37	12	22	80	40	16	123	50	57			
38	2.0	1.0	2.0					38	22	21	81	37	39	124	57	41			
39	2.0	0.0	3.0					39	21	11	82	38	40	125	52	58			
40	2.0	1.0	3.0					40	19	21	83	34	41	126	58	42			
41	2.0	2.0	0.0					41	20	22	84	41	18	127	57	58			
42	2.0	2.0	1.0					42	16	24	85	36	42	128	54	59			
43	2.0	2.0	2.0					43	24	23	86	42	20	129	59	43			

Table B.9: Output point and line list

Appendix B. Skeleton model points, lines, sections and joints lists

Sections									Connections						
Line	Begin	End	Line	Begin	End	Line	Begin	End	Line	Begin	End	Index	Type	Index	Type
1	1	1	44	1	1	1	1	1	1	1	1	Rounded	44	Rounded	
2	1	1	45	1	1	2	1	1	2	1	1	Rounded	45	Rounded	
3	1	1	46	1	1	3	1	1	3	1	1	Rounded	46	Rounded	
4	1	1	47	1	1	4	1	1	4	1	1	Rounded	47	Rounded	
5	1	1	48	1	1	5	1	1	5	1	1	Rounded	48	Rounded	
6	1	1	49	1	1	6	1	1	6	1	1	Rounded	49	Rounded	
7	1	1	50	1	1	7	1	1	7	1	1	Rounded	50	Rounded	
8	1	1	51	1	1	8	1	1	8	1	1	Rounded	51	Rounded	
9	1	1	52	1	1	9	1	1	9	1	1	Rounded	52	Rounded	
10	1	1	53	1	1	10	1	1	10	1	1	Rounded	53	Rounded	
11	1	1	54	1	1	11	1	1	11	1	1	Rounded	54	Rounded	
12	1	1	55	1	1	12	1	1	12	1	1	Rounded	55	Rounded	
13	1	1	56	1	1	13	1	1	13	1	1	Rounded	56	Rounded	
14	1	1	57	1	1	14	1	1	14	1	1	Rounded	57	Rounded	
15	1	1	58	1	1	15	1	1	15	1	1	Rounded	58	Rounded	
16	1	1	59	1	1	16	1	1	16	1	1	Rounded	59	Rounded	
17	1	1	60	1	1	17	1	1	17	1	1	Rounded	60	Rounded	
18	1	1	61	1	1	18	1	1	18	1	1	Rounded	61	Rounded	
19	1	1	62	1	1	19	1	1	19	1	1	Rounded	62	Rounded	
20	1	1	63	1	1	20	1	1	20	1	1	Rounded	63	Rounded	
21	1	1	64	1	1	21	1	1	21	1	1	Rounded	64	Rounded	
22	1	1	65	1	1	22	1	1	22	1	1	Rounded	22	Rounded	
23	1	1	66	1	1	23	1	1	23	1	1	Rounded	23	Rounded	
24	1	1	67	1	1	24	1	1	24	1	1	Rounded	24	Rounded	
25	1	1	68	1	1	25	1	1	25	1	1	Rounded	25	Rounded	
26	1	1	69	1	1	26	1	1	26	1	1	Rounded	26	Rounded	
27	1	1	70	1	1	27	1	1	27	1	1	Rounded	27	Rounded	
28	1	1	71	1	1	28	1	1	28	1	1	Rounded	28	Rounded	
29	1	1	72	1	1	3	1	1	29	1	1	Rounded	29	Rounded	
30	1	1	73	1	1	17	1	1	30	1	1	Rounded	30	Rounded	
31	1	1	74	1	1	16	1	1	31	1	1	Rounded	31	Rounded	
32	1	1	75	1	1	7	1	1	32	1	1	Rounded	32	Rounded	
33	1	1	76	1	1	19	1	1	33	1	1	Rounded	33	Rounded	
34	1	1	77	1	1	18	1	1	34	1	1	Rounded	34	Rounded	
35	1	1	78	1	1	16	1	1	35	1	1	Rounded	35	Rounded	
36	1	1	79	1	1	17	1	1	36	1	1	Rounded	36	Rounded	
37	1	1	80	1	1	11	1	1	37	1	1	Rounded	37	Rounded	
38	1	1	81	1	1	21	1	1	38	1	1	Rounded	38	Rounded	
39	1	1	82	1	1	20	1	1	39	1	1	Rounded	39	Rounded	
40	1	1	83	1	1	18	1	1	40	1	1	Rounded	40	Rounded	
41	1	1	84	1	1	19	1	1	41	1	1	Rounded	41	Rounded	
42	1	1	85	1	1	15	1	1	42	1	1	Rounded	42	Rounded	
43	1	1	86	1	1	23	1	1							

Table B.10: Output section and join shape list

Appendix B. Skeleton model points, lines, sections and joints lists

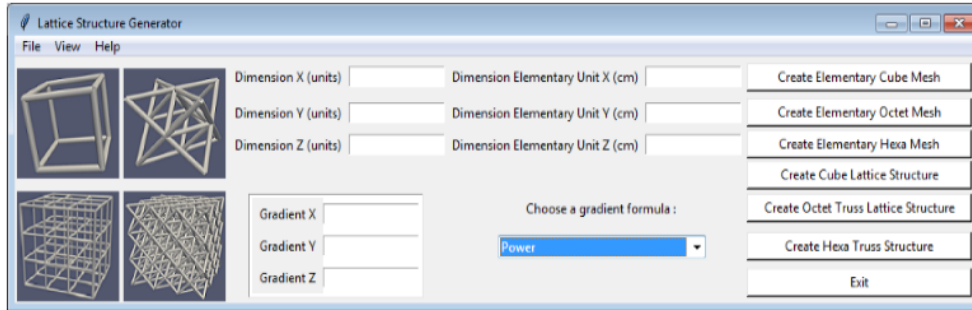


Figure B.1: Lattice structure generator user interface created to create lattice structures

Figure B.1 shows the graphic user interface of the program created. The input information is entered by the user in the user interface. For example, the dimension of the elementary and lattice units, the maths formula to create progressive lattice structure and the lattice structure pattern.

A proposal of the complete lattice structure generator user interface which contains all the input information is illustrated in figure B.2. This proposal is for future works to import the design space and create conformal lattice structures.

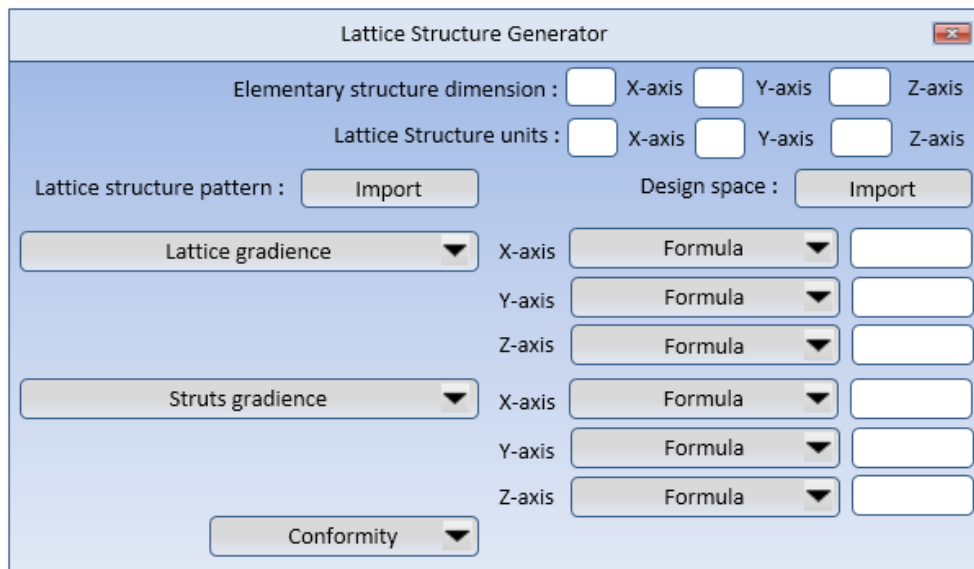


Figure B.2: Proposal of lattice structure generator user interface to create lattice structures

Abstract

It is now possible to manufacture metallic lattice structures easily with additive manufacturing. Lattice structures can be used to produce high strength low mass parts. However, it does not exist a method to design lattice structures for additive manufacturing. The thesis addressed the following research questions: Why are lattice structures so little used in part designs? What are the information necessary to help designers to design parts containing lattice structures? How can lattice structures be created quickly and easily in CAD? The main contributions are the evaluation of current CAD tools in terms of human machine interface, CAD file formats, CAE and CAM to design lattice structures, a new lattice structure design strategy, a methodology to create equivalent materials, the determination of the main lattice structure geometrical characteristics and a new skeleton model to define lattice structures with points, lines, sections and joints instead of surfaces and volumes.

Key words: Lattice structures, Design, CAD, Additive manufacturing

Résumé

Il est maintenant possible de fabriquer des structures treillis métalliques facilement avec la fabrication additive. Les structures en treillis peuvent être utilisées pour produire des pièces de faible masse et de haute résistance. Il n'existe pas de méthode de conception pour les structures treillis. La thèse a abordé les questions de recherche suivantes: Pourquoi les structures treillis sont-elles si peu utilisées dans la conception? Quelles sont les informations nécessaires pour aider les concepteurs à concevoir des pièces contenant des structures treillis? Comment les structures treillis peuvent-elles être créées rapidement et facilement dans le CAO? Les contributions principales sont l'évaluation des outils CAO actuels dans la conception des structures treillis en termes d'interface homme machine, de formats de fichiers CAO et de FAO pour la fabrication d'additive, une nouvelle stratégie de conception de structures treillis, une méthodologie pour calculer des propriétés matériau équivalent, détermination des caractéristiques géométriques principales des structures treillis à partir de points, de lignes, de sections et de connexions au lieu des surfaces et des volumes et une méthode pour visualiser et découper les structures treillis à partir du modèle squelette.

Mots clés: Structure treillis, Conception, CAO, Fabrication Additive